OCTOBER 2020 Ph.D. in Mechanical Engineering BEGÜM KÜTÜK

REPUBLIC OF TURKEY

GAZİANTEP UNIVERSITY

GRADUATE SCHOOL OF NATURAL & APPLIED SCIENCES

3D TRANSIENT THERMOELASTIC ANALYSIS OF VVER-1200 NUCLEAR REACTOR VESSEL DURING A LOSS – OF – COOLANT ACCIDENT (LOCA) SCENARIO

Ph.D. THESIS

IN

MECHANICAL ENGINEERING

BY

BEGÜM KÜTÜK

OCTOBER 2020

3D TRANSIENT THERMOELASTIC ANALYSIS OF VVER-1200 NUCLEAR REACTOR VESSEL DURING A LOSS – OF – COOLANT ACCIDENT (LOCA) SCENARIO

Ph.D. Thesis

in

Mechanical Engineering

Gaziantep University

Supervisor

Prof. Dr. İbrahim Halil GÜZELBEY

by

Begüm KÜTÜK

October 2020

REPUBLIC OF TURKEY
GAZİANTEP UNIVERSITY
GRADUATE SCHOOL OF NATURAL & APPLIED SCIENCES
MECHANICAL ENGINEERING

Name of the Thesis	: 3D Transient Thermoelastic Analysis of VVER-1200 Nuclear Reactor Vessel during a Loss – of – Coolant Accident (LOCA) Scenario
Name of the Student	: Begüm KÜTÜK
Exam Date	: 23.10.2020

Approval of the Graduate School of Natural and Applied Sciences

Prof. Dr. A. Necmeddin YAZICI
Director

I certify that this thesis satisfies all the requirements as a thesis for the degree of Doctor of Philosophy.

Prof. Dr. Melda ÇARPINLIOĞLU
Head of Department

This is to certify that we have read this thesis and that in our consensus opinion it is fully adequate, in scope and quality, as a thesis for the degree of Doctor of Philosophy.

Prof. Dr. İbrahim Halil GÜZELBEY
Supervisor

Examining Committee Members:	Signature
Prof. Dr. İbrahim Halil GÜZELBEY	…………………..
Prof. Dr. Bülent GÖNÜL	…………………..
Prof. Dr. Ayşegül ABUŞOĞLU	…………………..
Prof. Dr. Emrah ÖZAHİ	…………………..
Assoc. Prof. Dr. Şule ERGÜN	…………………..

I hereby declare that all information in this document has been obtained and presented in accordance with academic rules and ethical conduct. I also declare that, as required by these rules and conduct, I have fully cited and referenced all material and results that are not original to this work.

Begüm KÜTÜK

ABSTRACT

3D TRANSIENT THERMOELASTIC ANALYSIS OF VVER-1200 NUCLEAR REACTOR VESSEL DURING A LOSS – OF – COOLANT ACCIDENT (LOCA) SCENARIO

KÜTÜK, Begüm
Ph.D. in Mechanical Engineering
Supervisor: Prof. Dr. İbrahim Halil GÜZELBEY
October 2020
108 pages

In order to evaluate the structural integrity of a reactor pressure vessel (RPV), a comprehensive mechanical analysis is necessary to be performed for the transients during several operating conditions. For RPVs, because there is a sudden change in the temperature gradient across the vessel wall, it adds to the complexities while calculating the stress field there. Reactor vessels are required to be supplemented with a comprehensive thermal stress analysis. This thesis discusses the comprehensive thermoelastic stress analysis performed for RPV of a VVER-1200 by means of a numerical model. The results were utilized for structural integrity evaluation of reactor vessels. Three dimensional comprehensive simulations of fluid flow in currently operating nuclear reactors are an integral part of modern scientific research throughout the world. The highly dramatic improvements in computer-based programming capabilities recently made the detailed three-dimensional simulations of huge structures feasible and made the complex turbulence models in CFD codes relatively simple. The PWR with multiple loops might possess asymmetric operating conditions with reactor coolant pumps (RCPs) out of running in one or more loops. In this thesis, a CFD numerical analysis of the 4-loop VVER-1200 RPV is presented. Both symmetric (full-loop) and asymmetric (three-loop) inlet conditions, velocity, pressure and temperature distributions are obtained. The results match with the experimental reference values of the VVER-1200. This thesis also represents the loss-of-coolant accident (LOCA) simulation of the RPV using CFD code FLUENT 17.2 and FAVOR analysis for reflooding phase after LOCA occurred.

Key Words: FLUENT, Turbulent Model, Fluid Dynamics, Nuclear Reactor, CFD.

ÖZET

VVER-1200 NÜKLEER REAKTÖR KABININ SOĞUTUCU KAYBI KAZA SENARYOSU ESNASINDA 3 BOYUTLU ZAMANA BAĞLI TERMOELASTİK ANALİZİ

KÜTÜK, Begüm
Doktora Tezi, Makine Mühendisliği
Danışman: Prof. Dr. İbrahim Halil GÜZELBEY
Ekim 2020
108 sayfa

Reaktör Basınç Kabı (RPV)'nın yapısal bütünlüğünü değerlendirmek için, farklı çalışma koşullarında zamana bağlı durumlar için kapsamlı bir mekanik analiz yapılması gerekir. RPV'lerde duvar boyunca ani sıcaklık değişimi olduğu için bu durum duvardaki gerilim dağılımını hesaplarken karmaşıklıklara sebep olur. RPV duvarının kapsamlı bir termal gerilim analizi ile desteklenmesi gerekir. Bu tez, bir VVER-1200'ün RPV için sayısal model kullanılarak yapılan kapsamlı termoelastik gerilim analizini tartışmaktadır. İşletimde olan nükleer reaktörlerde 3 boyutlu kapsamlı akışkan simülasyonu dünyadaki bilimsel araştırmanın ayrılmaz bir parçasıdır. Bilgisayar kapasitelerindeki artış nedeniyle, büyük yapıların 3 boyutlu simülasyonları mümkün olmuş ve CFD kodlarındaki karmaşık türbülans modellerine giriş yapılabilmiştir. Çok döngülü bir basınçlı su reaktörü, bir veya daha fazla döngüde devre dışı kalmış reaktör soğutucu pompaları ile asimetrik çalışma koşullarına sahip olabilir. Bu tez çalışmasında, 4 döngülü VVER-1200 RPV'sinin CFD sayısal analizi sunulmuştur. Hem simetrik hem de asimetrik giriş koşullarında, tüm hacim için hız, basınç ve sıcaklık dağılımları elde edilmiştir. Sonuçlar VVER-1200'ün deneysel referans değerleri ile eşleşmiştir. Bu tez ayrıca, CFD kodu FLUENT 17.2 kullanılarak bir basınç kabının Soğutucu Kaybı Kazası simülasyonunu ve kaza sonrası reaktör kabı yeniden dolumu (reflooding) için FAVOR analizi sonuçlarını içerir.

Anahtar Kelimeler: FLUENT, Türbülans Modeli, Akışkanlar Dinamiği, Nükleer Reaktör, CFD.

"Dedicated to my lovely daughter, Berrak"

ACKNOWLEDGEMENTS

Firstly, I would like to thank my supervisor, Prof. Dr. İbrahim Halil Güzelbey for his continuous guidance and encouragement throughout my years of study at Gaziantep University. I would also like to appreciate Prof. Dr. Ayşegül Abuşoğlu, Assoc. Prof. Dr. Şule Ergün for serving on my dissertation monitoring committee and Prof. Dr. Emrah Özahi and Prof. Dr. Bülent Gönül for being committee members during my dissertation defense.

I would like to thank my husband, Erkan, for the support and encouragement during the hardest years. I want to thank my lovely daughter, Berrak, for the inspiration and bringing so much joy into my life each and every single day. I would also like to express my gratitude to my family for their support, always best wishes.

TABLE OF CONTENTS

Page

LIST OF TABLES

LIST OF FIGURES

Page

LIST OF SYMBOLS

ρ	Density, kg/m^3
μ	Dynamic Viscosity, $Pa.s$
α	Permeability
u	Velocity, m/s
C_2	Square Resistance Coefficient
C	Coefficient Matrix
D	Coefficient Matrix
D_e	Subchannel Equivalent Diameter, m
E	Total Energy
Δp	Pressure Drop, Pa
p_{in}	Inlet Pressure, Pa
p_{out}	Outlet Pressure, Pa
f	Friction Factor
G_m	Mass Flux, $kg/s.m^2$
Z_{in}	Height of the Inlet, m
Z_{out}	Height of the Outlet, m
A_z	Flow Cross-sectional Area, m^2
Re	Reynolds number
Δn	Medium Thickness, m
k	Thermal Conductivity, $W/m.K$

LIST OF ABBREVIATIONS

BC	Boundary Condition
BWR	Boiling Water Reactor
CFD	Computational Fluid Dynamics
CL	Cold Leg
ECCS	Emergency Core Cooling System
FE	Finite Element
FEM	Finite Elements Method
HL	Hot Leg
LBLOCA	Large-Break Loss-of-Coolant Accident
LOCA	Loss-of-Coolant Accident
LWR	Light Water Reactor
MBLOCA	Medium-Break Loss-of-Coolant Accident
NOC	Normal Operating Condition
NPP	Nuclear Power Plant
PTS	Pressurized Thermal Shock
PWR	Pressurized Water Reactor
RCP	Reactor Coolant Pump
RPV	Reactor Pressure Vessel
SBLOCA	Small-Break Loss-of-Coolant Accident
VOF	Volume-of-Fluid

CHAPTER I

INTRODUCTION

1.1 Background Information

Nuclear energy is known as an indispensable and reliable energy source. In several countries like the United States, France, and Japan, nuclear reactor industry is used as a main source of electricity. Despite its use in high demand, RPV integrity is of vital importance since they are considered as non-replaceable components during the lifetime of the nuclear reactor and since they keep the radioactive materials inside. One of the potential risks that may result in fracture of RPV is accidental condition. This condition may be caused by several accidents in nuclear reactors, such as break in the main pipeline and loss-of-coolant accident (LOCA). Thus, for a nuclear reactor having multiple loops, transients during the asymmetric flow such as the loss of power for one of the main circulating pumps, may become important. There is no doubt that the asymmetric operating conditions of a nuclear reactor having multiple loops will raise the probability of an accident. Therefore, thermoelastic structural analysis of reactor components is necessary for accurate safety evaluation. Additionally, because there are plans to increase the lifetime of current nuclear reactors from 40 years to 80 years, structural integrity of nuclear reactor components is becoming more interesting to investigate (IAEA, 2009).

1.1.1 Thermoelastic Analysis

The reactor pressure vessel (RPV) is addressed as the most reliable nuclear reactor structure of pressurized water reactors (PWRs) (IAEA, 2009). The main goal of current corresponding research is the increase of lifetime of the nuclear reactors and its internals. The status of the reactor vessel is a governing limiting factor for the lifetime of a nuclear reactor (Gálik et al., 2019). After the emergency core cooling system (ECCS) injection occurs, PWRs are exposed to some severe thermohydraulic transients consequent to the quick cooling of the inner wall of the RPV. Analyses of thermal shock events show that as a result of great tensile stresses developed from pressurized thermal shock (PTS) together with fast neutron radiation induced embrittlement during normal operating conditions (NOC) may cause quick propagation of flaws. The coupled load of these factors raises the possibility of mechanical harm to the integrity of RPV in case of pressurized thermal shock events. When PTS affects the solid structures in a bad way, this leads to a great possibility of mechanical damage or even total failure in severe accidents.

The reactor vessel may be exposed to LOCA scenario with the injection of cold water by the ECCS. Such an accident scenario develops very large tensile thermal stresses near the internal wall of the RPV as depicted in Figure 1.1. Whether an axial crack is present near the internal wall of the vessel, this large tensile thermal stress combined with the tensile stress due to inner pressure can develop large opening hoop stresses as a risk to the reactor vessel integrity.

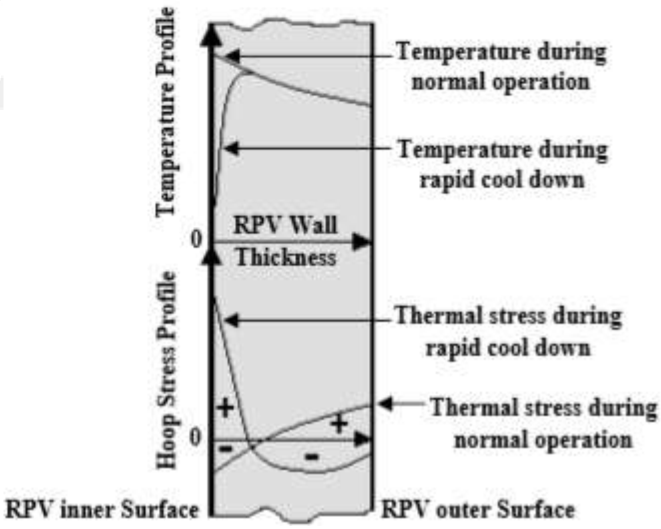

Figure 1.1 Temperature and thermal stress distributions across the thickness of RPV during NOC and cool down transient (Shrivastav et al., 2012).

1.1.2 CFD Analysis

The enhancement of the new nuclear reactors increases the simulation requirements to a higher level. Numerical design tools for multiphase and multidimensional analyses are desirable. The demand for intact and economically more reliable designs of new nuclear power plants creates many challenges for the nuclear engineers when developing design tools for reactors' structural integrity and optimization analyses. Nowadays, capabilities of thermal-hydraulic analyses have been developed greatly to satisfy the latter requirements. Dramatic development has been performed in both hardware and software. Meanwhile, Computational Fluid Dynamics is earning acceptance by the nuclear reactor industry. The improvement of new nuclear reactors must benefit from the large-scale CFD analysis in the design of the advanced nuclear reactor designs.

In order to determine the resulting stresses during PTS condition, an accurate prediction of the temperature distributions is required. Nowadays, 1D models are often utilized in thermohydraulic analysis during PTS condition. But, the complicated mixing phenomena in the downcomer region cannot be defined exactly by the 1D models. On the other hand, the 3D CFD simulation is able to compute the temperature distribution developed by mixing phenomena between the hot water mixture in the downcomer and the cold ECCS water (Ruan et al., 2017).

For safety of nuclear reactors, thermohydraulics is a very important subject. Computational fluid dynamics are developed as a helpful tool in the last decade to simulate thermohydraulics, in which a realtime three-dimensional geometry can be investigated. New technology simulation techniques with computers, such as FEM or CFD, may be very useful since one is able to change initial and boundary conditions easily (Kutiš et al., 2016). The mixing phenomena in nuclear power plants are inherently 3D, hence this phenomena can be truly simulated with numerical tools having three-dimensional capabilities, particularly the CFD codes (Moretti et al., 2008). Therefore, it is the main goal of CFD research to simulate three-dimensional flow phenomena in highly complicated systems (Ayhan and Ergün, 2013).

1.1.3 Loss-of-Coolant Accident (LOCA)

The LOCA is the design-basis accident of most nuclear reactor types. LOCA has two different versions according to the size of the break; small-break LOCA (SBLOCA) and large-break LOCA (LBLOCA). The hypothetical LBLOCA is the classical design-basis accident for the PWR reactor concept. The following sequence of events is envisioned to happen in this case; blowdown phase (0-20 seconds), bypass phase (20-30 seconds), refill phase (30-40 seconds), reflooding phase (40-250 seconds) and long term cooling (>250 seconds) (Ragheb, 2016).

In blowdown phase, the large break in one of the inlet nozzles causes a rapid depressurization in the system. A two-phase water and steam mixture is formed by the flashing of the water into steam when the coolant pressure is decreased to the saturation pressure. After 10 seconds from the initiation of the break, the flow from the ECCS line injects in the cold leg (Ragheb, 2016). In bypass phase, the coolant water bypasses the upper part of the inlet plenum and flows out through the break. In refill phase, after the steam pressure is decreased enough, the ECCS water may now ingress into the lower plenum of the core.

In this thesis study, FLUENT was used in order to study a break in one of the hot legs in a VVER-1200. Due to the LBLOCA situation considered here, the RPV depressurizes rapidly and all water evaporates quickly. When the ECCS injection is engaged, they are injecting liquid water into the cold legs and into the downcomer that contains just steam. In this thesis study, the refill phase of the LOCA was investigated during the cold leg injection.

1.2 Motivation of Study

PWRs are the most common type of nuclear power plants that are under operation throughout the world today. The VVER-1200 is a Russian-design nuclear reactor and can be classified as Pressurized Water Reactor.

For a VVER-1200 having multiple loops, asymmetric operation conditions can occur. Under asymmetric operating conditions of nuclear power plants having multiple loops, there may be a fail in a reactor coolant pump. Once it switches between normal and asymmetric operating conditions, the water inside the core is going to be distributed again. Hence, velocity, temperature and pressure distributions are going to be time-dependent in the reactor vessel. Surely, the asymmetric operating conditions of a VVER-1200 with multiple loops will raise the possibility of an accident. Hence, it is rather important to know about velocity, temperature, mass flow rate, and pressure distributions in reactor vessel under asymmetric operating conditions.

For the LOCA case, a quick break in one of the four main circulation pipes is assumed and a following depressurization in the primary loop of the nuclear power plant. The depressurization propagates at the sound speed, goes into the RPV, and leads to some pressure difference affecting the RPV internal components. It then comes to asymmetrical impacts of the core barrel according to gradual spread of pressure wave in the gap between the vessel and core barrel walls. Those asymmetrical impacts are vital only in the very beginning of a LOCA – within a time interval of tenths of second after accident occurred. After that time interval, the pressure balances everywhere in the RPV. Such a case can be addressed by two approaches given below:

1. The two-step approach: In the initial step, the time distribution of pressure difference for the RPV components is obtained. Then, in the next step, the structural simulations are carried out by means of the pressure loads obtained in the initial step. For those analyses, two calculation models are generated, one for the thermal analysis, one for the mechanical one.

2. The integrated approach: Structural and CFD analyses are solved together and the fluid-solid interaction is obtained.

For this thesis, asymmetric (three-loop) inlet condition for a VVER-1200 RPV was assumed including the loss-of-power in one reactor coolant pump. The asymmetric (three-loop) inlet conditions in a nuclear power plant, even if NOC exists, will raise the possibility of an accident. Therefore, it is very important to have the numerical knowledge of the characteristics like temperature, pressure and velocity distributions at the reactor core entrance and exit, RPV hot legs and cold legs for asymmetric operating conditions. Especially for safety concerns of nuclear power plants, specification of a coolant flow behavior helps nuclear engineers to prevent and predict the transient of a LOCA (Cartland Glover et al., 2007).

Accurate simulation for those large-scale nuclear power plants is complex and hard to deal with for the coolant flow in the RPV. In addition, the overall simulation takes a long computational time to solve and cannot solve further under real-time operating conditions. Fortunately, a comprehensive view of coolant motion and heat transfer in the RPV of nuclear power plants with techniques like CFD is possible and of a wide margin. Computational Fluid Dynamics techniques are powerful tools since the 3D effects of the coolant flow cannot be predicted well by 1D nuclear engineering system codes.

A 32-core Intel Xeon CPU cluster with 2.10 GHz and 128 GB RAM running with Windows 10 Pro was used for the Computational Fluid Dynamics analyses and enough for dealing with the single-phase flow with standard k-Ɛ turbulence model with an element number of 4.8 million structured mesh. This thesis begins with establishing the whole coolant flow domain in the RPV of VVER-1200. For grid generation ANSYS Meshing Platform was used allowing the treatment of that number of cells. Then, Computational Fluid Dynamics simulations of the complicated 3D turbulent flow for both symmetric and asymmetric inlet boundary conditions have been performed. The behaviors of distributions of the pressure, the velocity and the temperature at the several cross-sections in the reactor vessel have then been found at symmetric and asymmetric inlet BCs due to a fail because of loss-of-power in an RCP out of four. According to the results of the Computational Fluid Dynamics simulations, it is conceiving to create a more comprehensive method while simulating the RPV of a VVER-1200 operating at asymmetric conditions. As a result of the analyses, several parameters such as temperature, velocity, and pressure distributions have been obtained for the whole RPV. The obtained results for pressure losses through the reactor core matches with the analytical values of the VVER and the temperature results matched well with the design values. The obtained results show that it is possible to perform a transient analysis for both normal operating condition (NOC) and LOCA conditions utilizing the CFD simulation knowledge obtained. In these analyses detailed calculations have been performed separately for the downcomer and for the upper part of the downcomer too.

In this thesis, three different detailed CFD analyses have been performed to investigate the temperature, pressure, velocity and mass flow rate behaviors in a VVER-1200 whole RPV with both symmetric (full-loop) and asymmetric (three-loop) inlet boundary and LOCA conditions by means of ANSYS FLUENT 17.2. After three different CFD analyses, a structural analysis using FAVOR code for the RPV integrity following LOCA has been performed. The geometry of VVER-1200 model will be given at first. Then, the grid generation strategy will be explained. Setup of the CFD analyses will be given next, with the selection of turbulent models, wall functions, and heat source applied. The comparison of the pressure drop through the reactor core with the analytical values will prove to match with the numerical results. The boundary conditions are of special focus to be applied truly. Finally, the thermal, pressure, velocity and mass flow rate results will be shown and discussed in detail.

The detailed results will be given from the thermoelastic stress analysis of a reactor vessel following a loss-of-coolant accident (LOCA). The aim of the mechanical part of this dissertation is to evaluate the Pressurized Water Reactor (PWR) pressure vessel, which has already been exposed to neutron flow and the material in the reactor beltline region has become brittle, with Fracture Analysis of Vessels Oak Ridge (FAVOR) code, which makes probabilistic analysis of the fracture mechanisms that may occur as a result of the LOCA.

1.3 Organization of Thesis

This thesis includes 7 chapters, beginning with an introduction consisting of some background information about safety of reactor pressure vessels. The second chapter gives a comprehensive literature survey including the relevant research on the thermoelastic, CFD and FAVOR analyses of several types of reactor pressure vessels under several different boundary and initial conditions including accidental scenarios with different geometrical details.

In Chapter 3, general design and operational characteristics of VVER-1200 type of nuclear reactors are introduced. Chapter 4 presents the methodology for computational fluid dynamics and heat transfer simulation of reactor pressure vessel of VVER-1200 with its internal components, and also the general methodology of FAVOR code. Chapter 5 includes the analyses performed using codes of FLUENT and FAVOR. The details on selection and application of boundary conditions and porous medium approach are given in this chapter.

Corresponding results and discussion of computational fluid dynamics simulations including symmetric (full-loop), asymmetric (three-loop) operational condition scenarios as well as LOCA scenario and FAVOR results are presented in Chapter 6. Finally, the outcomes of this study with concluding remarks are summarized in the last chapter. Recommendations on potential future works are also included.

CHAPTER II

LITERATURE SURVEY

2.1 Studies on Thermal and Mechanical Analyses

Most of the researchers have only studied about computing the thermal or mechanical stresses in cylindrical bodies for steady-state. Zhang et al. (2012) derived an analytical solution in order to specify the stress field of a multilayered composite pressure vessel. The pressure vessel was exposed to an inner pressure due to fluid flow and temperature load. Authors constructed only a quarter of the geometric model because of the axisymmetric condition of the composite pressure vessel (Figure 2.1(a)). A horizontal cross-section at A-A of the multilayered composite vessel is depicted in Figure 2.1(b).

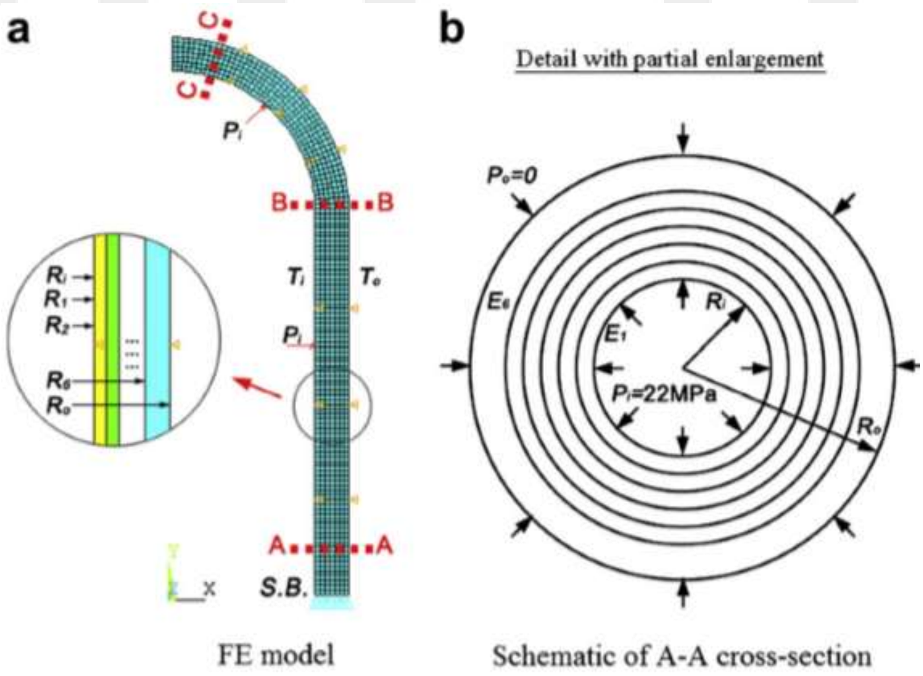

Figure 2.1 The finite element model and boundary conditions (Zhang et al., 2012)

Kanlıkama et al. (2013) carried out a coupled thermoelastic analysis in order to obtain the temperature, radial displacement, radial stress and tangential stress behaviors of a cylinder. Then, an RPV was subjected to an internal pressure and temperature loads due to coolant. For the solution, a severe location is investigated in order to analyze the effect of the hot leg connections of the RPV. To verify their own computer code, the temperature, radial displacement, radial and tangential stress behaviors were computed utilizing FEM. Results showed that the analytical results matched well with the numerical ones for the typical cylinder.

Chaudhry et al. (2014) performed the detailed thermomechanical analysis for RPV of Tarapur Atomic Power Station. Authors obtained a comprehensive temperature and structural stress behavior among the reactor vessel thickness utilizing a numerical model. In their model, the temperature of the inner wall changes according to several transients such as reactor start-up, shut-down and emergency situation. The results of simulation show that the most critical location in terms of stress in the vessel wall is vessel wall-clad interface. The corresponding transient is the emergent shut-down case. Authors used the results for structural integrity evaluation of RPV.

Mohanty et al. (2016) represented thermomechanical stress analysis of a PWR RPV with its inlet and outlet nozzles. Authors established FE models for both heat transfer and following thermomechanical stress analysis. But, the details of the support structures and BCs were not taken into account for simplicity as given in Figure 2.2. For instance, the hot leg and the cold leg connections displacement BCs were modeled as that situation would let thermal expansion in all directions. The results were given from heat transfer and thermomechanical stress analysis for different conditions such as heat-up, cool-down, and load-following conditions.

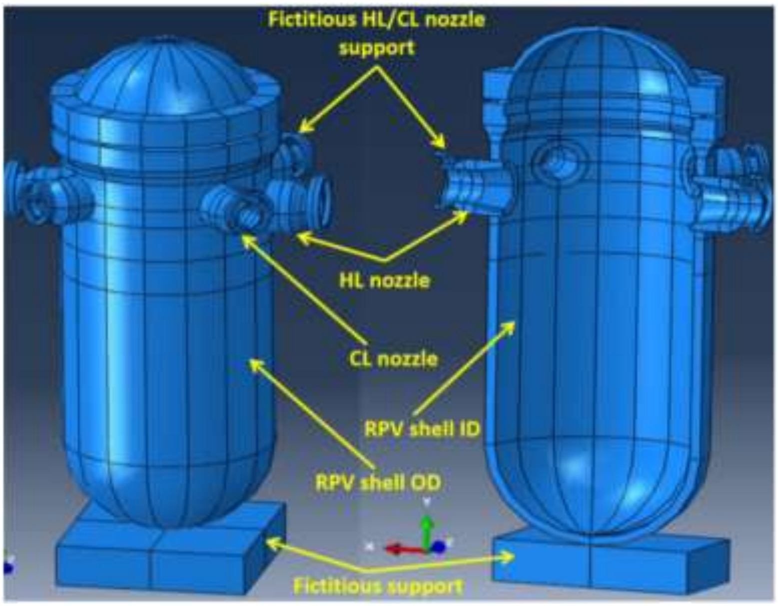

Figure 2.2 Solid model of the reactor pressure vessel, cold leg and hot leg nozzles (Mohanty et al., 2016)

2.2 Studies on CFD Analyses

The analysis results by some common time-dependent thermo-hydraulic nuclear engineering system codes like RELAP5 are commonly being used. Comprehensive knowledge concerning complicated 3D flow mixing phenomena, temperature and pressure behaviors in reactor vessel cannot be calculated. The reason is that 1D system codes are not capable of predicting well the three-dimensional properties in the flow mixing (Espinoza et al., 2006). With the advance of new numerical techniques such as Computational Fluid Dynamics, it is now possible to give a comprehensive view of the coolant motion and heat transfer in an RPV (Khanbabaei et al., 2008). Until now, numerous researches have been performed and reported in the literature concerning the three-dimensional Computational Fluid Dynamics analyses of the complicated coolant motion and heat transfer in several components of existing LWRs with different level of complexities.

2.2.1 Studies on Asymmetric Analyses

Prosický and Zácha (2003) presented justification of ANSYS FLUENT 6.0 against experimental data from the experimental database. As a result, the transient fluid flow greatly affects the flow field in the lower plenum and downcomer in the beginning of the simulation. As the time proceeds, the fluid flow was gradually divided as nearly symmetrically into two flow streams. This can be seen in Figure 2.3 at 21.2 sec after start up.

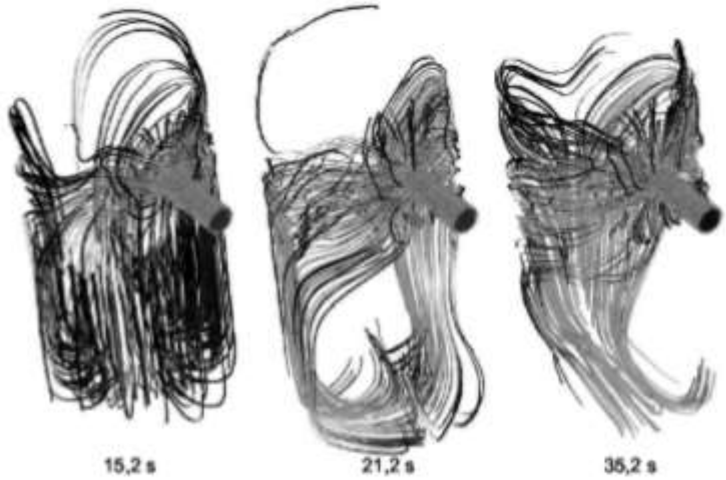

Figure 2.3 The streamlines in the downcomer and lower plenum at 15.2 sec, 21.2 sec and 35.2 sec after start up, respectively (Prosický and Zácha, 2003)

Höhne and Bezrukov (2005) studied the mixing of a slug during start-up of the RCP scenario in VVER-1000 nuclear power plant utilizing the computational fluid dynamics package CFX-5.7. The computational mesh model involved the inlet (cold leg) nozzles, the downcomer and lower plenum with the elliptical core support plate and internal components. Parts of the complicated lower plenum elements were modeled with the porous medium approach for providing simplification. In Figure 2.4 given below, fluid flow velocity pathlines are illustrated showing the velocity field in the lower plenum and downcomer regions during reactor coolant pump start up obtained using computational fluid dynamics package CFX-5.

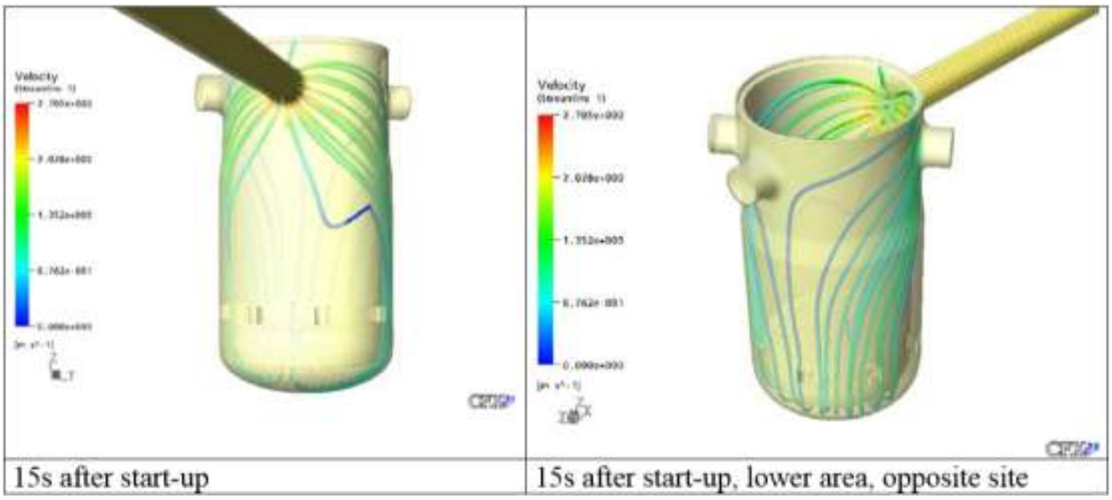

Figure 2.4 Flow velocity streamlines at the RCP start-up scenario (Höhne and Bezrukov, 2005).

The asymmetric coolant motion behavior in reactor vessel of VVER-1000 using a CFD code was analyzed by Bieder et al. (2007). The results were helpful to develop the mixing matrices for the lower plenum that are usually used in system codes.

Computational fluid dynamics validation research was carried out by analyzing the flow mixing in a primary loop of a PWR by Rohde et al. (2007). Authors accomplished CFD calculations with two different CFD programs, FLUENT and CFX. Authors could not achieve a completely grid-independent numerical solution. However, the results of the study told about the suitability of applying CFD techniques in turbulence mixing applications in nuclear systems. Figure 2.5 depicts flow pathlines showing the velocity field in the lower plenum and downcomer regions during the start-up scenario calculated with CFX-4. Because of the strong momentum-driven coolant flow at the cold leg connection, the horizontal component of the coolant flow is dominant in the downcomer compared to the vertical component. The injection is propagated into two main streams forming the so-called butterfly distribution.

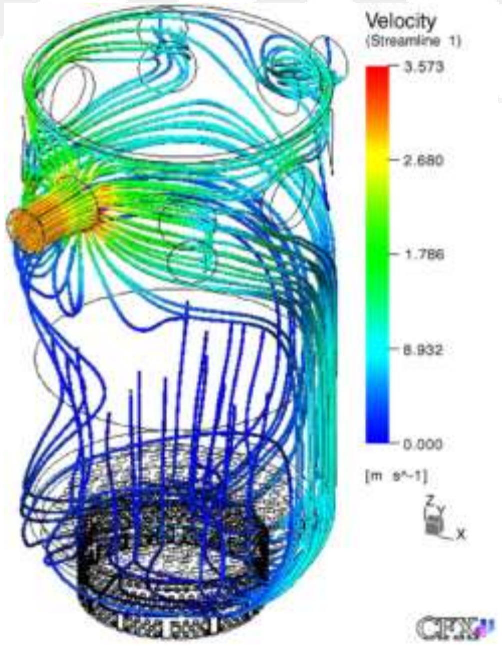

Figure 2.5 Fluid streamlines at 15 sec after the start-up (Rohde et al., 2007).

Böttcher (2008) studied an ANSYS CFX model of the reactor vessel of VVER-1000 in Kozloduy nuclear reactor. The geometry included all important components of the reactor vessel, although some of the small geometrical details had been simplified and perforated core barrel bottom was modeled with porous medium. The reliable results of the simulation about temperature at each loop and coolant mixing coefficients proved the method and approaches were rather useful to deal with complex problems. Figure 2.6 shows the upper plenum of the nuclear reactor more precisely.

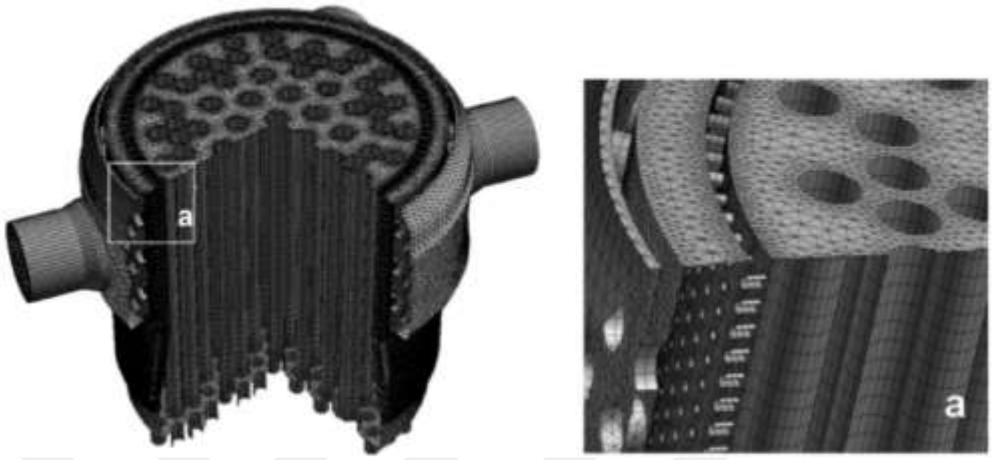

Figure 2.6 Meshing of the upper plenum containing 9.6 million of meshes (Böttcher, 2008).

Khanbabaei et al. (2008) described the fluid flow and heat transfer with a mathematical model which was associated with the VVER-1000. Utilizing a CFD code, CFX, a 3D fluid flow in the downcomer and the lower plenum were introduced assuming some simplifications which include some reduction in the total number of fuel assemblies. However, the model was validated by the outlet temperature. As a result, fluid pathlines that directly flow into the downcomer region after passing through the cold legs also moved around the circumference of the vessel and there was obviously no fluid flow down the downcomer in the region vertically below cold legs. Figure 2.7 illustrates the fluid pathlines in the lower plenum and the downcomer.

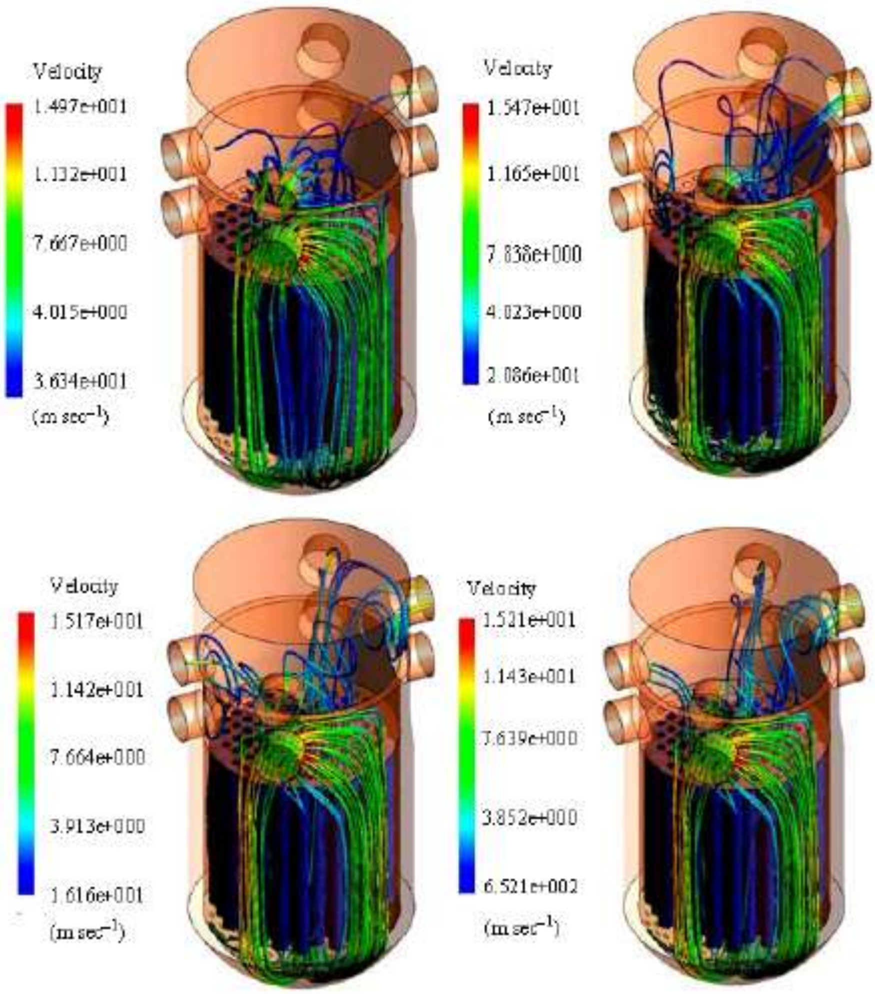

Figure 2.7 The velocity streamlines in the downcomer and lower plenum by ANSYS CFX 1 sec, 10 sec, 40 sec and 80 sec after start up, respectively (Khanbabaei et al., 2008)

Moretti et al. (2008) modeled a VVER-1000 reactor and purposed studying the coolant mixing in the RPV. The studied experiment includes the start-up of a RCP while remaining other three RCPs loss-of-power, and the presence of a tracer slug on the working loop, which is therefore transferred into the RPV where it mixes with the clear water. Authors carried out CFD simulations of the abovementioned experiment.

In further studies, Höhne (2009) searched several turbulent models in analyses and the results of Large Eddy Simulation turbulent model showed a better match with Kozloduy experimental data. Böttcher and Krumann (2010) improved a detailed VVER-1000 reactor vessel model and simplified primary loop components models by their external shapes and additional source terms for energy and momentum transfer. Authors simulated the swirl of flow patterns at the core entrance. But due to the lack of technical details, the swirl was overestimated.

Ayhan and Ergün (2013) modeled a 3D reactor vessel of the VVER-1200. Authors observed the thermo-hydraulic distribution of coolant flow ignoring some console elements and assuming porous media approach for perforated parts to reduce the computational time. The temperature behaviors and pressure losses were calculated. This study is important because it includes a new type of VVERs, on which there is not much study addressed in the open literature.

Cheng et al. (2016) performed numerical analysis of the thermohydrodynamic characteristics in the reactor vessel for different inlet conditions for both three and four RCPs under operation. Different characteristics of temperature, pressure losses, velocity and mass flow rates in the RPV were studied. The results were justified the practical distributions. It may be more obviously seen from the temperature distribution in a horizontal cross-section of the hot legs' elevation in Figure 2.8. The temperature contours at the two hot legs closer to the failed loop were also affected, particularly the closer exit.

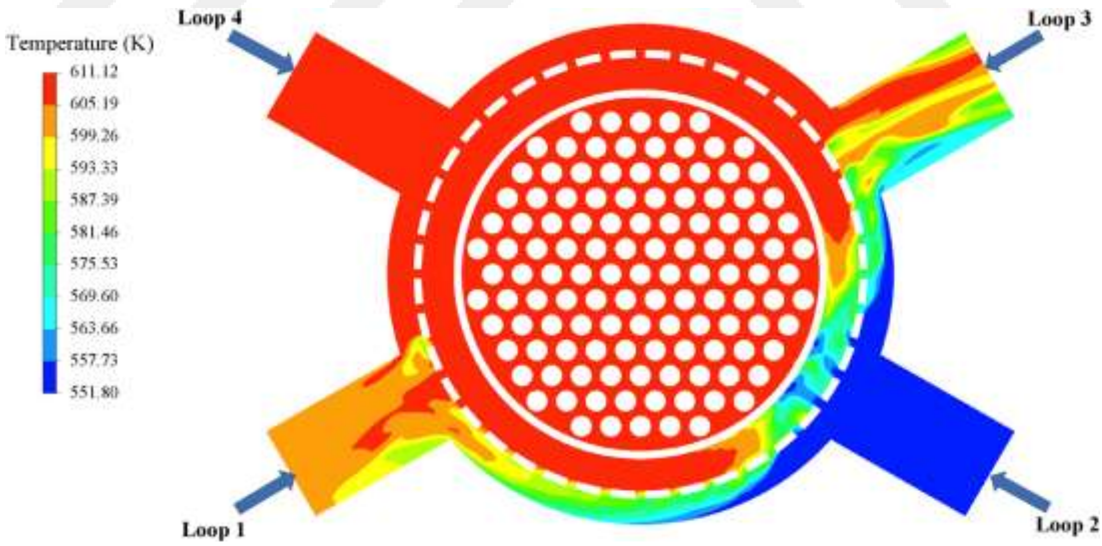

Figure 2.8 The temperature contours in a horizontal cross-section of the hot legs' elevation (Cheng et al., 2016).

Kutiš et al. (2016) focused on CFD analyses of the flow in the VVER-440 type of reactor. The purpose of the analyses was to investigate the effect of the diameter of orifice on the massflow through fuel assemblies located in the core. Applied boundary conditions in the corresponding region of the water coolant were based on nominal coolant flow conditions in the VVER-440. Figure 2.9 below depicts a huge vortex in the water coolant. It is formed in the perforated elliptic bottom of the core barrel.

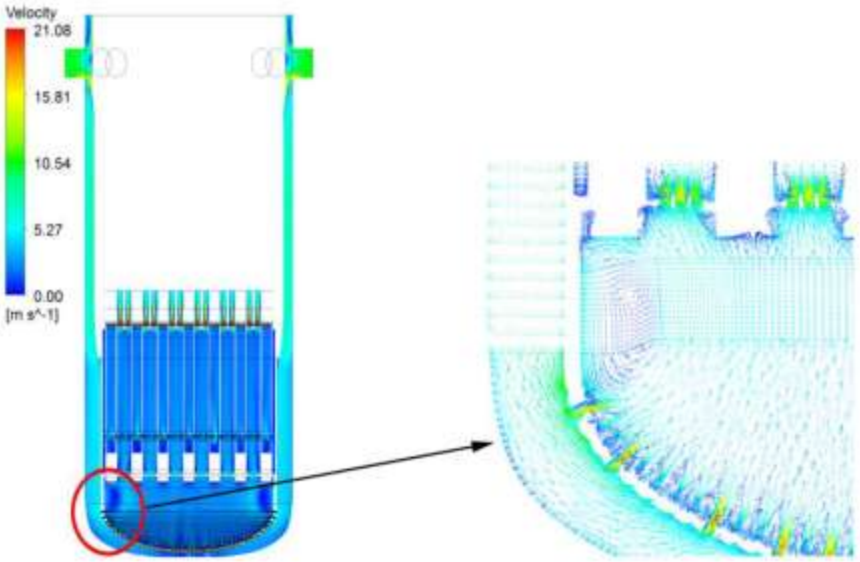

Figure 2.9 Greatly magnified vortex in the water coolant over the perforated core barrel bottom (Kutiš et al., 2016).

Chen et al. (2017) simulated the three-dimensional thermo-hydraulic parameters of nuclear reactor core based on porous medium approach. Authors utilized porous medium model to simplify the core and upper plenum of the RPV. ANSYS CFX was used in order to obtain 3D temperature, velocity, and pressure distributions.

Farkas et al. (2017) validated the applicability of Computational Fluid Dynamics to investigate the thermo-hydraulic results of a Main Steam Line Break. From 9 to 12 million hexahedral grids was established in order to capture all details in the system. The simulation was a transient one. CFD and experimental results were compared. Mixing in the inlet nozzle connections with ECCS was overestimated. The temperature behavior in the reactor core entrance plane matched well with the measurement results. Figure 2.10 gives the temperature behavior in the downcomer of RPV under specified analysis.

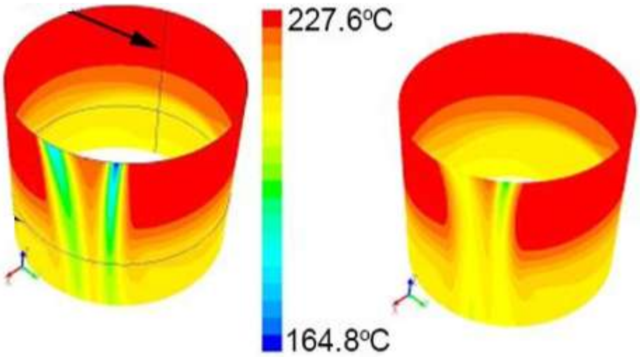

Figure 2.10 Temperature distribution in the downcomer region for at external (left) and internal (right) surface of RPV (Farkas et al., 2017).

Liu et al. (2018) aimed to research the critical heat flux characteristics of AP1000 type of nuclear reactor based on both numerical and experimental analyses under NOC and loop fail conditions. Once two RCPs of one loop fail suddenly, the coolant flow of that loop decreases gradually until it is completely lost. In order to analyze the loop fail accident scenario, which means the coolant flow of one loop is completely lost, two inlets of the failed loop were applied as massflow inlet BC with 0 kg/s mass flow rate and the other two inlets were applied as massflow inlet with 3761 kg/s at 280.7 °C, which denotes the average magnitude of inlet temperature. Besides, two outlets were applied as pressure outlet and the reference pressure was set to 15.4 MPa. All walls were set as nonslip BC. The differences of flow characteristics were investigated and given in Figures 2.11 and 2.12 below.

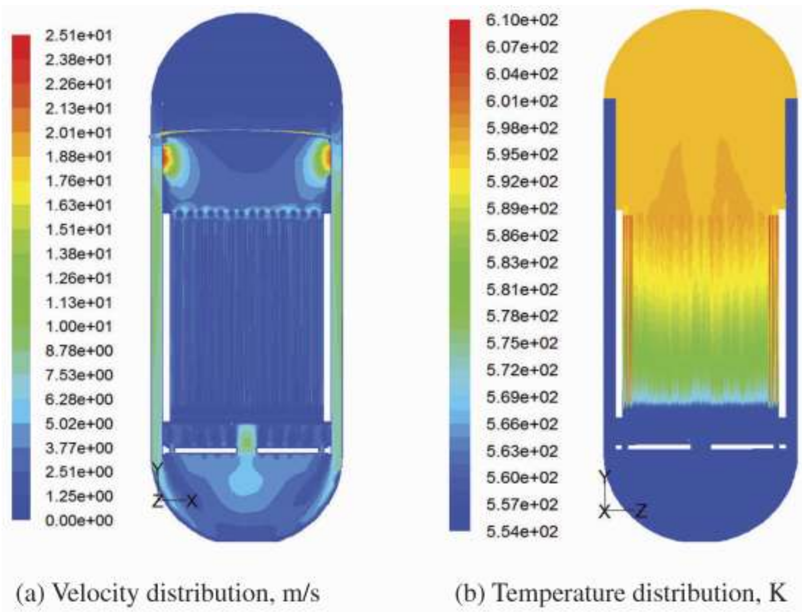

Figure 2.11 Coolant flow behaviors on RPV vertical cross-section (a) Velocity, m/s (b) Temperature, K (Liu et al., 2018).

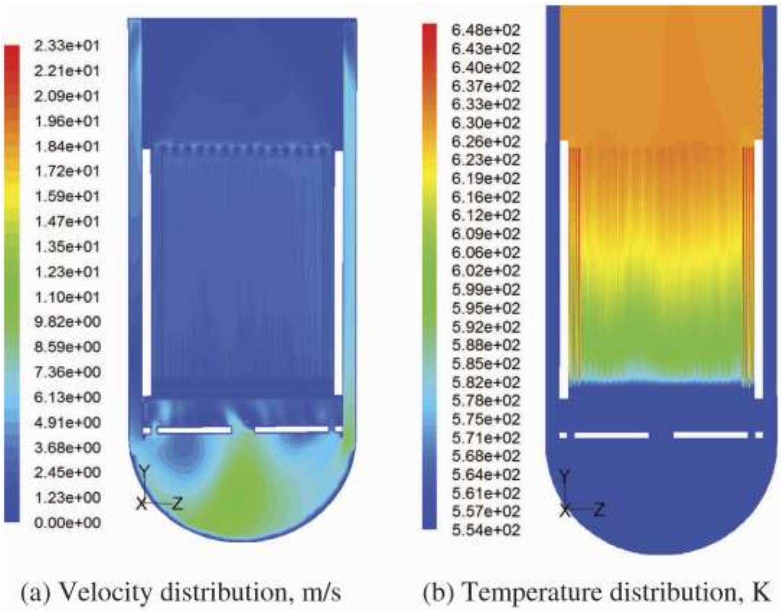

Figure 2.12 Coolant flow behaviors on RPV vertical cross-section for loop fail accident (a) Velocity, m/s (b) Temperature, K (Liu et al., 2018).

2.2.2 Studies on LOCA Analyses

A loss-of-coolant accident was the postulated transient selected as the most challenging for VVER type of nuclear reactors. In fact, the accident evolution is the fastest and the decay heat of the reactor core is the greatest in this accident scenario.

Cai and Watanabe (2011) analyzed actuation of emergency core cooling system during a small-break loss-of-coolant accident (SBLOCA) in pressurized water reactors and cold water was injected into cold legs. Authors used an open source CFD program, OpenFOAM in order to analyze mixing in the cold leg. One of the cold legs was simulated starting from the RCP exit to the downcomer inlet. The temperature distribution in the cold leg was compared with both experimental and ANSYS FLUENT results.

Hermanský and Krajčovič (2012) gave numerical simulation results of RPV internals of a VVER440/V213 to hypothetical large-break loss-of-coolant accident (LBLOCA). Their aim was to obtain the RPV internals response after the quick depressurization of RPV and to verify that no deformations that would prevent timely and proper activation of the emergency control system occur. According to the results, the greatest value of the pressure difference of 5.5MPa was observed at the time of 5ms. However, the greatest value of the pressure difference for loss-of-coolant accident (LOCA) in a hot leg was found to be 3.3MPa at the time of 10ms. The pressure contours for several time steps are given for the LOCA occurred in a cold leg in Figure 2.13 and in a hot leg in Figure 2.14.

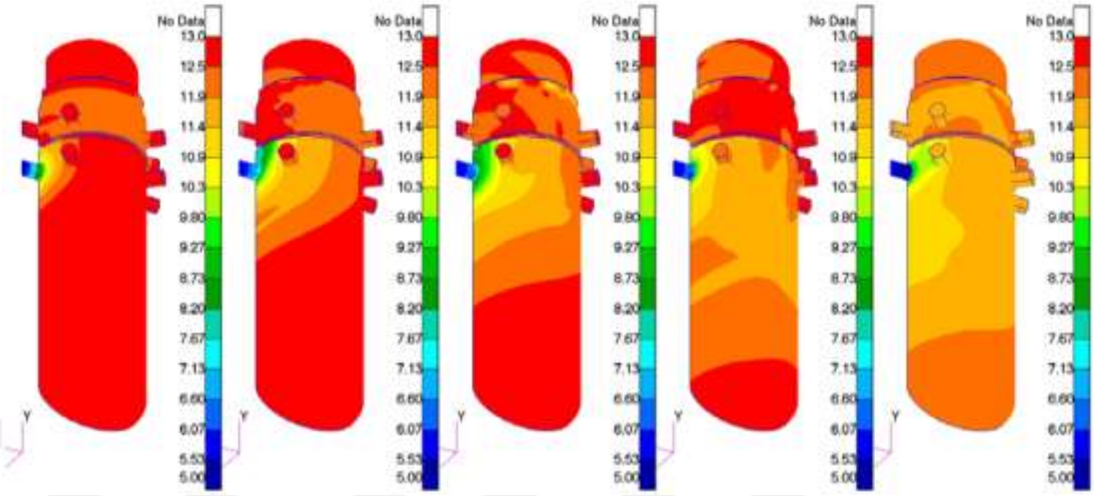

Figure 2.13 The pressure contours in unit of MPa at time steps of 2 ms, 4 ms, 6 ms, 10 ms and 30 ms, respectively for a LOCA occurred in a cold leg (Hermanský and Krajčovič, 2012)

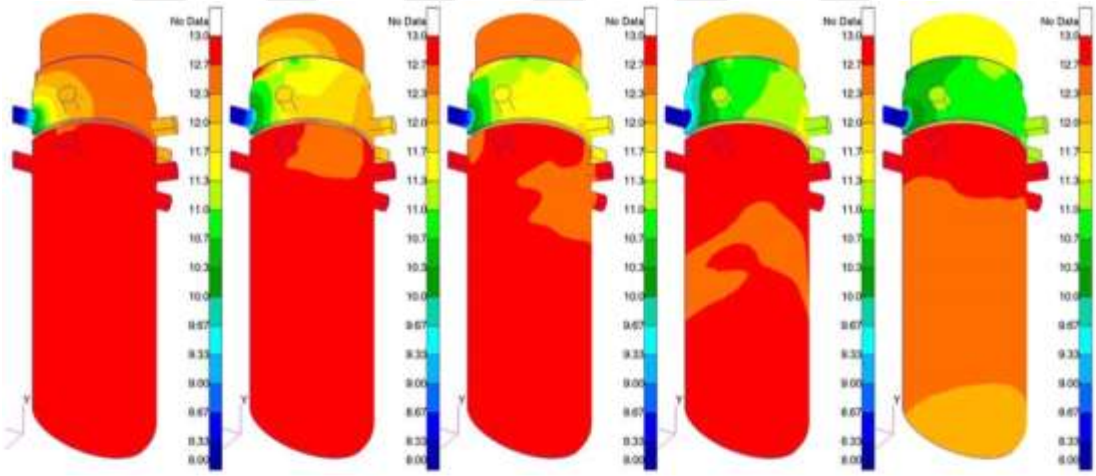

Figure 2.14 The pressure contours in unit of MPa at time steps of 2 ms, 4 ms, 6 ms, 10 ms and 20 ms, respectively for a LOCA occurred in a hot leg (Hermanský and Krajčovič, 2012)

Duspiva (2015) performed analyses for the accident scenario initiated with the large-break loss-of-coolant accident with a break size of 200 mm with the loss of all active systems. Author assumed primary system depressurization, reflooding and continuous water injection for the VVER-1000. Analyses performed with the

MELCOR 1.8.6 YV version showed successful cooling of the RPV for sufficiently long period of time by the heat removal from the vessel wall.

González-Albuixech et al. (2015) presented a medium-break loss-of-coolant accident which was assumed in one of the outlets of the reactor vessel for a two-loop PWR. The BCs obtained from RELAP5 were utilized as input for the 3D CFD analysis to obtain temperature contours for the mechanical analysis. Figure 2.15 depicts the temperature behavior at the inside wall of the reactor vessel according to their study.

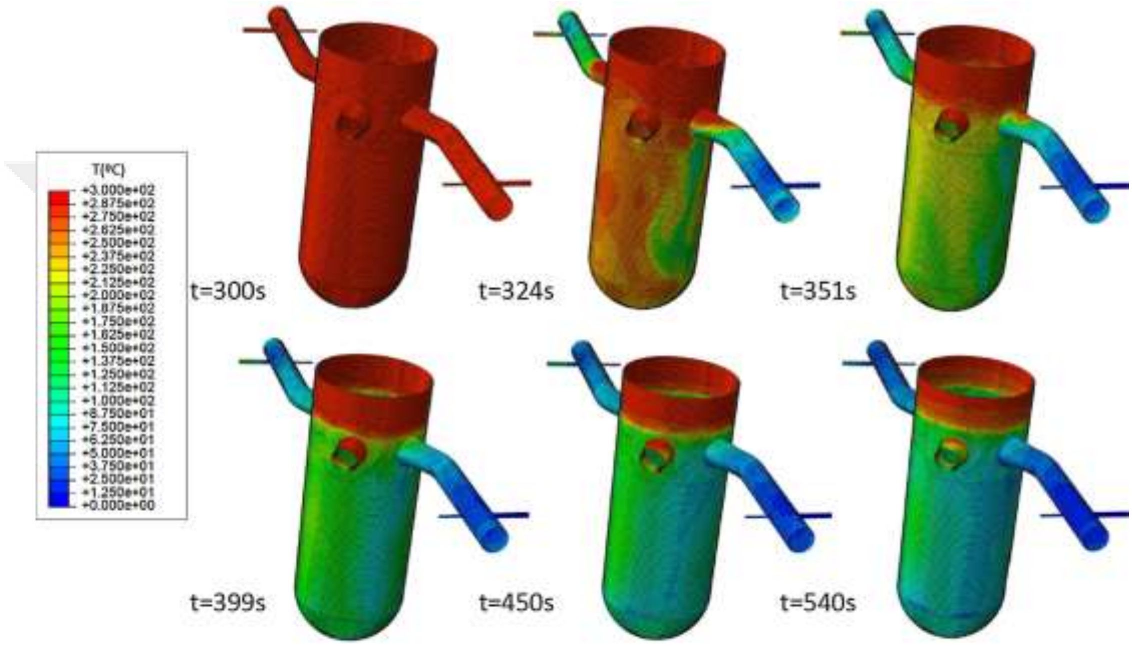

Figure 2.15 The temperature distributions on the inside wall of the reactor vessel (González-Albuixech et al., 2015).

Jaros et al. (2017) used FLUENT in order to study a break in an outlet nozzle connection within a two-loop PWR. Authors assumed a large break LOCA situation and resolved the interface between steam and liquid water with the volume of fluid method. The final goal was to obtain the stresses resulting from thermal gradients. In the beginning of ECCS, once the amount of water in the vessel was low, the injected cold water flowed while touching the inner wall of the vessel. Consequently, just a slightly change in temperature for the top region of the downcomer was obvious, as seen in Figure 2.16. After a few seconds passed, detachment from inner wall of RPV occurs because of the increased mass flow rate of the injection.

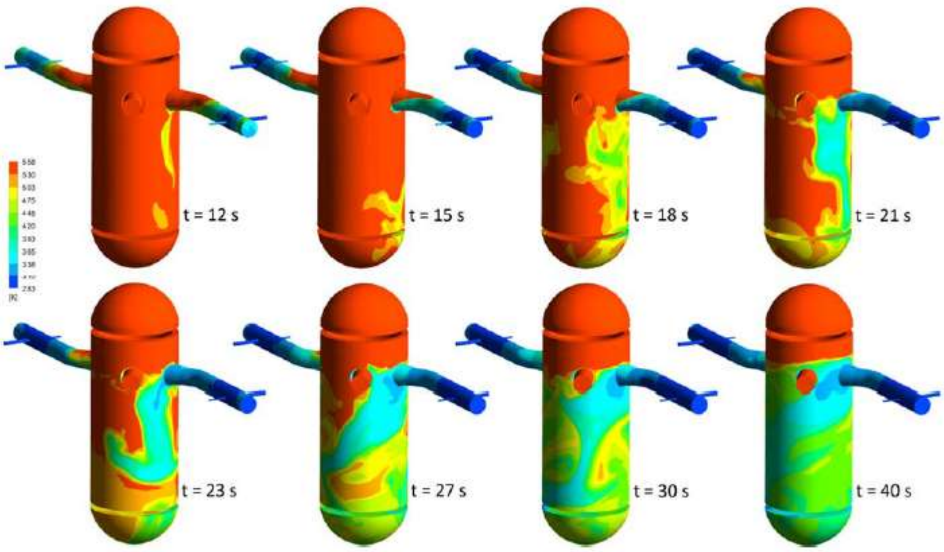

Figure 2.16 The temperature distributions in the inner wall of the reactor vessel (Jaros et al., 2017).

Ruan et al. (2017) carried out a 3D CFD analysis and a structural analysis. A 4-loop reactor vessel was used. Three cases of different amounts of mass flow rates were assumed in the simulations. The structural analysis was performed in order to investigate the integrity of reactor vessel according to the temperature behavior obtained by computational fluid dynamics. Their results are helpful for structural integrity of RPVs.

Gálik et al. (2019) described a PTS simulation within an RPV resulting from a SBLOCA. The accident transient is modeled by using a transient thermo-hydraulic CFD simulation. The transient pressure and temperature results were then transferred into a mechanical analysis. The effect of ECCS-injected coolant temperature variation was investigated. Figure 2.17 depicts the transient of the temperature behavior of the internal face of the RPV wall. The RPV is seemed to be cooled in a long thin strip under the cold leg.

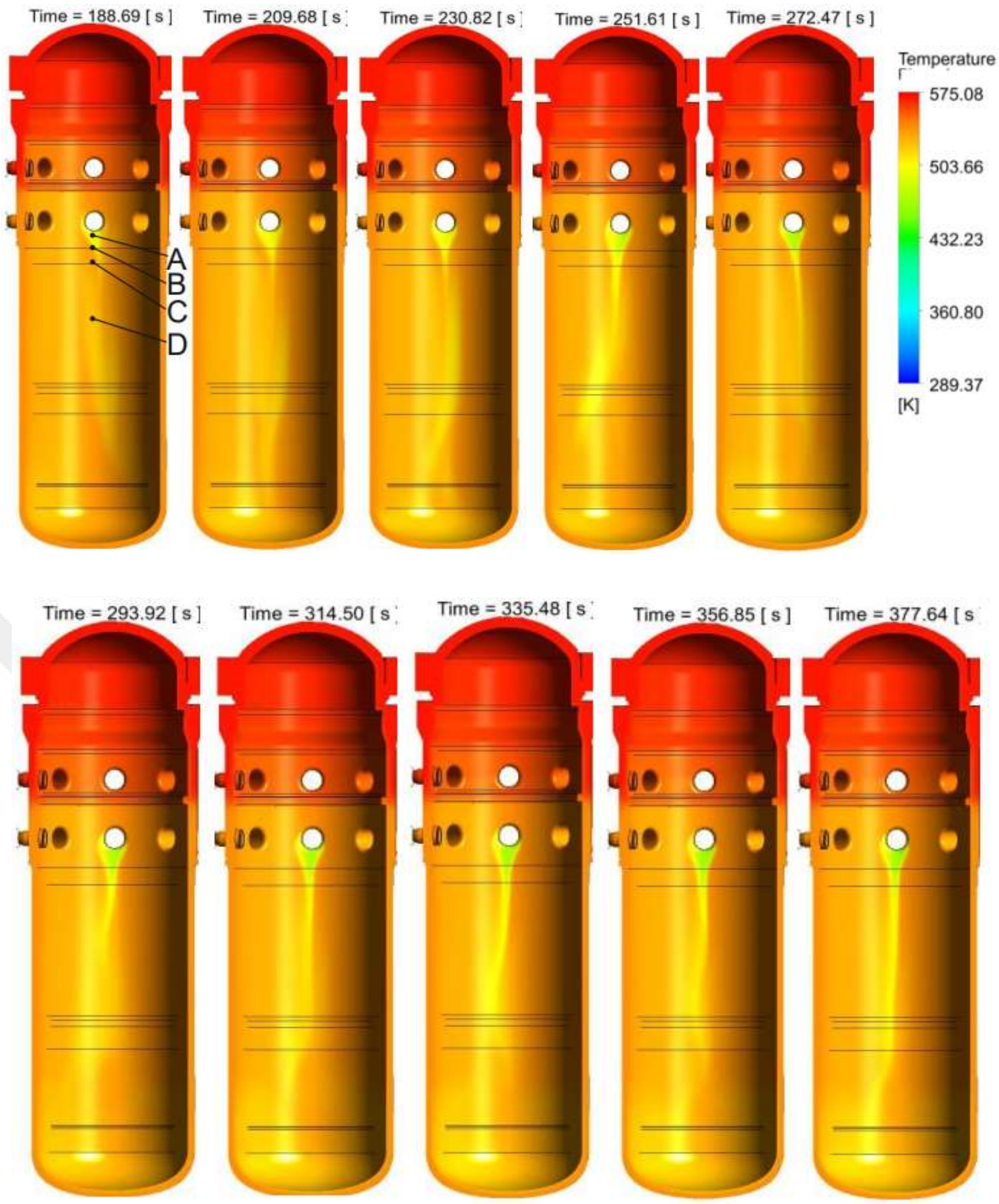

Figure 2.17 Temperature transient on the internal face of the reactor vessel for several instants (Gálik et al., 2019).

Fyza et al. (2019) studied to analyze a critical scenario in VVER-1200. The specific type of loss-of-coolant accident includes solely cold and solely hot leg break in the primary side, respectively. For the simulation of break in hot and cold leg, a 500 cm^2 of break is assumed in the system. A LOOP is assumed starting from 500th second of transient. The corresponding temperature, pressure, void fraction etc. were investigated in their study. The results provided helpful knowledge concerning safety of such type of nuclear reactors in case of loss-of-coolant accident occurring simultaneously with LOOP.

Kütük and Güzelbey (2020) presented computational fluid dynamics simulation for a VVER-1200 nuclear reactor vessel. Analyses of the RPV were carried out for symmetric and asymmetric inlet boundary conditions, and also for loss-of-coolant accident conditions. As a result of the analyses, several parameters such as temperature, velocity, and pressure distributions were obtained for the whole reactor vessel.

More three-dimensional turbulent fluid flow simulations are being performed by Computational Fluid Dynamics techniques. The Computational Fluid Dynamics tools have been very reliable in order to deal with the three-dimensional complicated fluid flow in reactor pressure vessel.

2.3 Studies on FAVOR Analyses

There are many studies investigating the safety analysis of nuclear reactor pressure vessels. In United States, Nuclear Regulatory Commission (NRC) has eased the code development to examine the consequences of Pressurized Thermal Shock in Pressurized Water Reactors (PWR). The problems of Pressurized Thermal Shock condition have been analyzed with codes such as OCA-P in PWR pressure vessels. FAVOR, upon the request of the NRC, is the latest code developed. Improvements are still being made to the code.

In this part of the thesis, the studies in the literature on events such as Pressurized Thermal Shock which are the basis of FAVOR have been mentioned in general.

Pressurized Thermal Shock condition is a condition that increases the probability of losing pressure vessel's integrity due to thermal stress, pressure load, exposure to radiation for a long time and presence of crack-like defects on its inner surface. Thermal shock condition is the most critical factor for a reactor pressure vessel. When temperature drops excessively, high stresses occur.

Huang et al. (2012) supposedly analyzed the low temperature and high pressure conditions that will force the reactor pressure vessel in Taiwan Boiling Water Reactor (BWR). Since Boiling Water Reactors (BWR) operate at half the pressure values compared to Pressurized Water Reactors (PWR), they showed a less critical situation in terms of thermal shock. The probability of fracture in circumferential welds in the beltline region of the pressure vessel of Boiling Water Reactors is less than half the probability of possible fracture in the axial direction. So, it was stated that in-service inspection was not required while operating Boiling Water Reactors. While this inspection has been abolished in the USA, it is still being applied in Taiwan. This study is a work done to show that this inspection is not necessary in Taiwan. All flaws were considered as surface flaws, embedded flaws were not considered. Low temperature, high pressure was hypothetically considered to be a constant temperature of 85 °F and a pressure of 1150 psi.

Qian and Niffenegger (2014) examined the 3-dimensional fracture analysis of SBLOCA and MBLOCA in terms of rupture mechanism in the reactor pressure vessel, which was designed hypothetically with the thermal hydraulic data with ABAQUS code. The analysis showed that in cases of Pressurized Thermal Shock, the cracks in the shallow places in the reactor pressure vessel are more taken into account.

Qian et al. (2014) identified certain cracks in the Shoreham and PVRUF nuclear reactors that had been decommissioned in the USA. Both Shoreham and PVRUF reactors were manufactured by Combustion Engineering. Shoreham was a Boiling Water Reactor (BWR) type, while PVRUF was a Pressurized Water Reactor (PWR) type of nuclear reactor. For these reactors, a probabilistic safety analysis was performed with FAVOR by modeling the Small-Break Loss-of-Coolant Accident (SBLOCA) and the Medium-Break Loss-of-Coolant Accident (MBLOCA). The probability of failure was higher for SBLOCA than that for MBLOCA. This is due to the different distributions of fracture toughness values. Among the cracks, the crack dimensions that cause the deformation most was the surface crack with a depth of 5.13 mm and the embedded crack with a depth of 6.83 mm. The time interval with the greatest deformation was between 0-9 minutes for MBLOCA and 150-170 minutes for SBLOCA.

Chen et al. (2015) applied the FAVOR code Version 6.1 in order to depict both the methodology and the results of the PFM in their study. The effects of the fracture depth and fast neutron current on the safety margin of the reactor pressure vessel were investigated. It has been seen that the defect distribution seriously affects the results. The maximum fracture-initiating frequency has been seen in the embedded flaws. These defects are more common in the reactor vessel. In this study, the shortcomings of the FAVOR code are also addressed. To investigate the constraint effect, modeling was performed by using ABAQUS code, which uses Finite Elements Method in three-dimensions for fracture analysis. It has been observed that it produces different results for the constraint effect depending on the type of the load applied, pressure load or temperature load. The temperature load was found to be the dominant load type in constraint effect.

Huang et al. (2016) investigated the probabilistic fracture mechanics analysis for Taiwan domestic Pressurized Water Reactor with FAVOR code. Pressure thermal shock was specified in the comparative evaluations of the loss-of-off site power condition, large-brake loss-of-coolant accident condition, main steamline brake and SGTR. Error files for Taiwan Nuclear Power Plant were created with the VFLAW code. In all specified accident situations, it was determined that the defects did not spread in the beltline region. Table 2.1 specifies parameters such as coolant temperature and cooling rate in the RPV during such accidents.

Table 2.1 Parameters during pressurized thermal shock and steam generator tube rupture for Taiwan domestic nuclear power reactor

Values Specified for Pressurized Thermal Shock		**Values Specified for Steam Generator Tube Rupture**	
Inlet temp. of water (°F)	550.40	**Inlet temp. of water (°F)**	550.40
Final temp. of water (°F)	150.08	**Final temp. of water (°F)**	199.94
Cooling rate (1/min)	0.15	**Cooling rate (1/min)**	0.04
Internal pressure (ksi)	0.9998	**Internal pressure (ksi)**	0.9998

2.4 Remarks on the Literature Survey

There is no doubt of really high quality of all previous studies by numerous researchers, however the calculation strategy will be deficient without several comprehensive and highly representative accident scenarios of different types.

Since the coolant flow in the downcomer region is a complete 3D flow, 1D system codes are not enough to accurately solve several flow characteristics in case of a loss-of-coolant accident. Up to now, numerous researchers have performed three-dimensional computational fluid dynamics analyses for coolant flow in several different components of pressurized water reactors and VVER-1000s. However, there are not many studies concerning the new design of VVER nuclear reactors, namely VVER-1200. This thesis includes three-dimensional CFD analyses of the overall fluid flow domain in reactor vessel of VVER-1200. Numerical analyses of the complicated turbulence and heat transfer in reactor vessel at several operating conditions are processed.

The system codes alone are not sufficient to obtain all of the flow characteristics. Therefore, calculating only the thermal loads is not conservative for the thermoelastic analysis; thereby the results from CFD are then used in FAVOR analysis for the last part of the thermoelastic study.

2.5 Conclusion

Numerous researchers have performed three-dimensional CFD analyses for coolant flow in different components of pressurized water reactors (PWRs) and VVER-1000s. But there are not many studies about VVER-1200. A total of 22,457 papers in the SCOPUS database include the denomination of the nuclear reactor types (data collected in April 2020). Among this criterion, 11,762 (around 52%) of the total published papers include PWR. The total number of 971 papers in the SCOPUS database includes the denomination of the most important nuclear reactor designs. Among this criterion, VVER-1200 only covers up 25 of the published research papers (around 2.5%) (Fernández-Arias et al., 2020).

There are several abovementioned studies which deal with the coupling of CFD codes and nuclear engineering system codes such as RELAP5. However, there is not any study concerning the CFD - FAVOR coupling in the open literature. Thus, by means of this thesis study, various thermoelastic cases can be investigated thoroughly as the solid models of each RPV component are available.

CHAPTER III

A GLOBAL REVIEW OF VVER-1200 NUCLEAR REACTORS

3.1 Introduction

Today, nuclear energy has regained its position that it played throughout the past 20th century as an alternative to CO_2 emitting energy generation systems due to the increasing demand for energy throughout the world (Fernández-Arias et al., 2020). For the last 80 years, several nuclear power plant designs have been developed worldwide, which can be classified according to their working principle and their generation stage. According to their working principle, nuclear reactors include two different designs; fast reactors and thermal reactors. Fast reactors can generate more fissile material than they have consumed, while thermal reactors use slow or thermal neutrons by means of a neutron moderator. Most nuclear reactors are thermal reactors. Figure 3.1 shows the past and next generations of nuclear power plants.

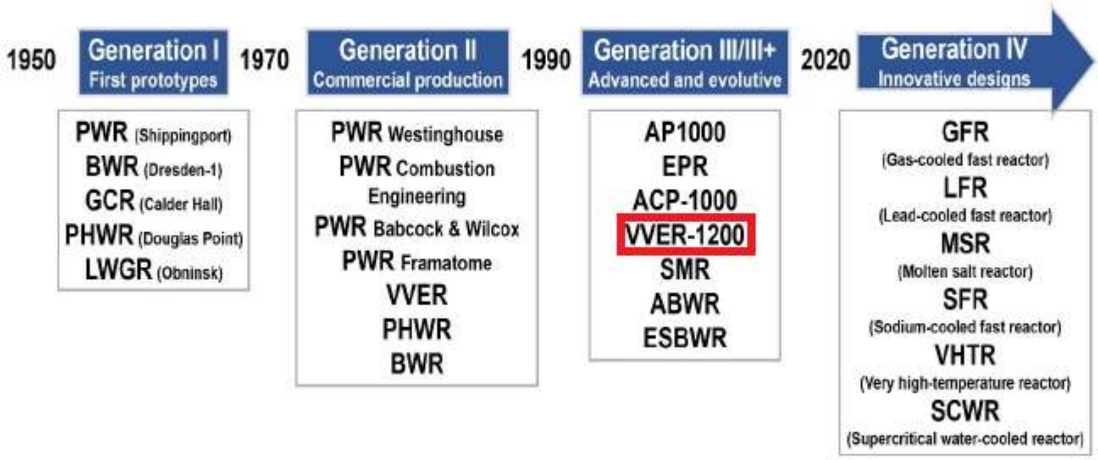

Figure 3.1 Generations of nuclear power plants throughout the past 70 years (Fernández-Arias et al., 2020).

Among the 440 nuclear power plants under operation worldwide as of August 2020, 297 of them are pressurized water reactors, representing 67.5 percent of the operating nuclear power plants and a power generation capacity of 281 GWe (IAEA, 2020).

3.2 VVER-1200 Nuclear Power Plants

As for the PWR design, the different members of the Soviet variant, so called VVER, was named Water-Water Energetic Reactor (WWER) from the Russian Vodo-Vodyanoi Energetichesky Reaktor (VVER) by the company known as Rosatom. VVER is a thermal reactor with pressurized water utilized both as moderator and coolant. The VVER-1200 nuclear reactor design is the latest evolution in the long history of VVER nuclear power plants. The new Russian reactor meets all the required international safety standards for Generation III+ nuclear reactors. The VVER-1200 units under operation in Russia are two units in Novovoronezh and one unit in Leningrad II. The first VVER-1200 was constructed at Novovoronezh II Unit 6 brought online in August 2016. The VVER-1200 units under construction are another Leningrad II unit in Russia, two units in Belarus, two units in Akkuyu, Turkey, and two units in Bangladesh (IAEA, 2020). In addition, construction contracts have been signed and site preparation is ongoing for another two units in Turkey. It is also proposed for two units (Temelin 3-4) in Czech Republic and one unit (Hanhikivi 1) in Finland.

There are 2 versions of VVER-1200 reactor designs. First of them, V-392M design, was developed by Moscow Atomenergoproekt. The reactor Novovoronezh II which is under operation in Russia is of this type. In addition, V-392M is the design which is under construction in the Akkuyu nuclear power plant in Turkey. The last version of VVER-1200 design is the V-491. It was developed by St. Petersburg Atomenergoproekt for China, as successfully deployed at Tianwan.

Figure 3.2 shows the schematic diagram and the locations of the active emergency core cooling system injection in a VVER-1200 nuclear reactor.

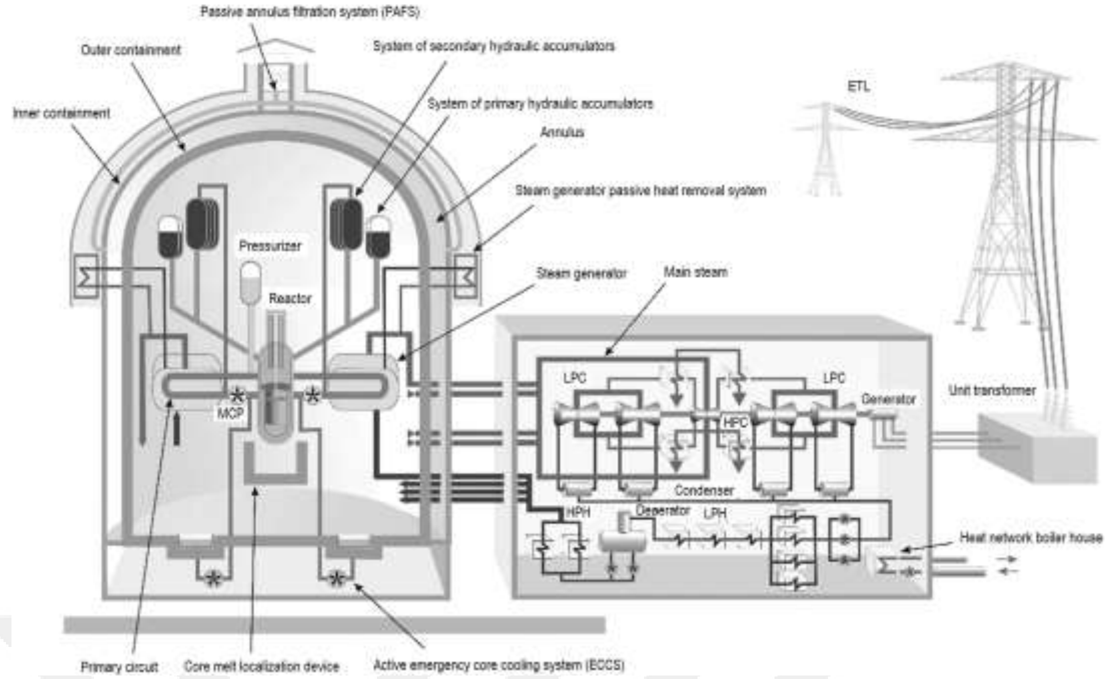

Figure 3.2 Schematic diagram and the locations of ECCS injection of the VVER-1200 Power Plant (Asmolov et al., 2017).

3.3 VVER-1200 Primary Circuit

The primary circuit of VVER-1200 type of nuclear reactors includes the reactor pressure vessel, four loops between the vessel and four steam generators, pressurizer, reactor coolant pump, accumulator tanks of the ECCS and the main pipelines which provide a connection. The RPV includes the core, core barrel and control rods located in it. The RCS transfers the heat from the reactor core by water circulation in a closed loop. It contributes to the heat transfer from the primary side to the secondary side by steam generator. The steam generator operates as the heat exchanger between two sides by linking them. The heat-exchange tubes in the steam generator serve as a wall between the primary side and secondary side water. They restrict the radioactive materials transfer from the primary circuit to the secondary one. The pressurizer is a component of the primary circuit. It carries out the pressurization in primary circuit, pressure control for several conditions such as steady-state, heat-up and cool-down, and also the control of pressure fluctuations under sudden events and accident conditions. The reactor coolant pump loops the water through primary coolant side. The main coolant pipeline connects all those components mentioned above of the primary circuit. The main components of the primary coolant side are shown in Figure 3.3.

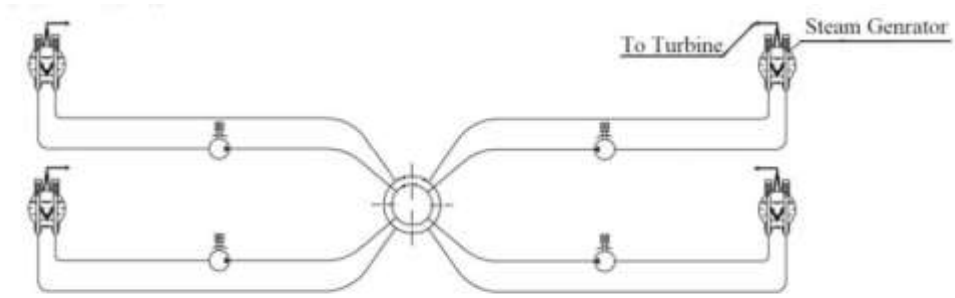

Figure 3.3 Components of primary side of VVER-1200 nuclear reactor (Fyza et al., 2019).

The RPV, SG and RCP are connected by the main coolant pipeline. The main coolant pipeline has four loops, in which every loop contains two different paths. The paths are named as cold and hot legs. The inner diameter of the hot and cold legs is 850 mm each. Figure 3.4 shows the primary circuit flow of VVER- 1200 type of nuclear reactors, while Figure 3.5 depicts the layout of the VVER-1200 primary circuit equipment. In NOC, the coolant goes into the RPV with a temperature of 298.2 °C and leaves the vessel with 328.9 °C of temperature. The mean fuel temperature in the core is 800 °C.

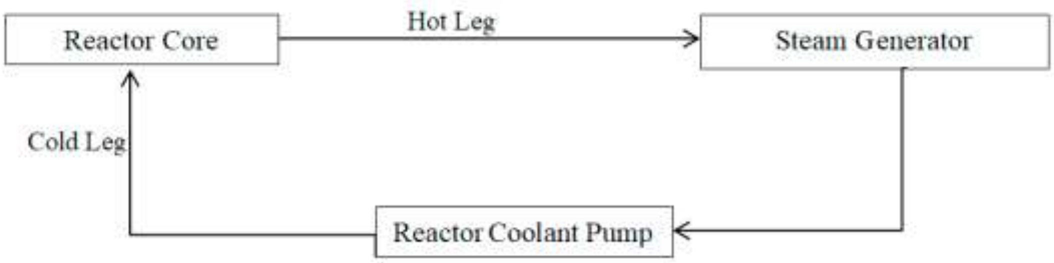

Figure 3.4 Primary side flow of VVER-1200 nuclear reactor (Fyza et al., 2019).

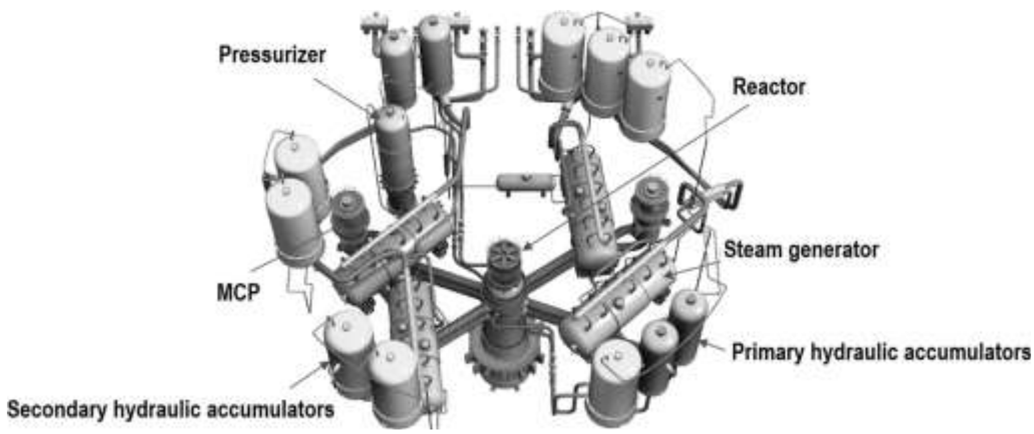

Figure 3.5 Layout of the VVER-1200 primary circuit equipment (Asmolov et al., 2017)

The basic design data for VVER-1200 is given in Table 3.1 below.

Table 3.1 VVER-1200 basic data

Service life, years	**60**
Rated electric power, MW	**1198**
Rated thermal power, MW	**3212**
Capacity for heat supply, MWt	**300**
Availability, %	**>90**
Efficiency, %	**37.0 gross, 34.5 net**
Unplanned automatic scram per year	**< 1**
Number of operating personnel, person/MW	**0.37**
Fuel lifetime in the reactor core, years	**4**
Frequency for refuelling, months	**12**
RPV and core inlet temp., °C	**298.2**
RPV and core outlet temp., °C	**328.9**
Coolant flow rate through RPV, m^3 / hour	**86000**
Nominal primary pressure, MPa	**16.2**
Primary side design parameters: - gauge pressure, MPa; - temperature, °C	 **17.64** **350**
Pressure of the primary side hydraulic tests, MPa: - for tightness; - for strength	 **17.64** **24.5**
Feed water temp. at steam generator inlet, °C	**225**

3.4 Reactor Core and Fuel Assemblies

The core of VVERs is characterized by hexagonal layout. The fuel assemblies have hexagonal geometry and the control rods are located according to hexagonal symmetry. The fuel rods in a fuel assembly are distributed on triangular lattice. There is a bypass coolant flow between the outer walls of the fuel assemblies. The VVER-1200 core includes 163 standard fuel assemblies. The fuel assemblies serve for the heat production in the core and heat transfer from rod surface to water during the reactor life preventing the fuel rods from exceeding the permissible limits in order to eliminate any probability of corruption. The fuel assemblies have 4570 mm of length. The active fuel length which means the length of the heat generating part of the fuel rod once the reactor is in the hot state is 3750 mm high. Each fuel assembly includes 312 fuel rods, thus total number of fuel rods are 50856 for the VVER-1200.

The fuel assembly is assembled of 13 spacer grids, 18 guide tubes, 1 instrumentation tube and a support grid. The fuel rod cladding material is zirconium alloy. Sintered UO_2 fuel pellets with a 5% maximum enrichment are stacked inside the cladding. The average linear heat rate of a fuel rod is 167.8 W/cm. Reactor output is controlled by using 121 control rods as they are intended for rapid chain reaction suppression, by burnable neutron absorber in the fuel rods, and by changing the boric acid concentration in the primary circuit coolant. During NOC, most of the control assemblies are in the top position. In the case of a scram, each control rod moves down. The control rods are twice as long as the fuel assemblies.

The control rod drive mechanisms are installed on the reactor top head. Annually, 42 new fuel assemblies are loaded into the reactor core.

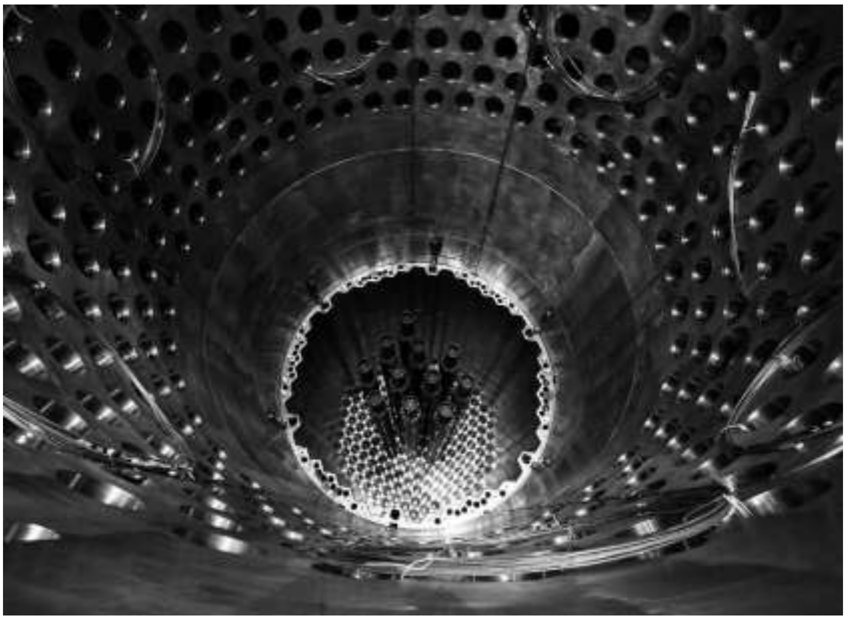

Figure 3.6 Inside the core barrel looking from top (Rosatom, 2020)

Table 3.2 VVER-1200 reactor core basic data

Active fuel height	3.75 m
Equivalent reactor core diameter	3.16 m
Avg. linear heat rate	16.78 KW/m
Avg. fuel power density	36.8 KW/KgU
Avg. core power density	108.5 MW/m3
Fuel material	UO2 and UO2 + Gd2O3
Fuel element type	Fuel rod
Cladding material	Alloy E-110
Outside diameter of fuel rods	9.10 mm
Rod array of a fuel assembly	hexahedral

3.5 The Reactor Pressure Vessel

The reactor is a vertically-positioned RPV comprises a vessel and a reactor top head that houses the internal components of the core, core barrel, core baffle, protective tube unit, control rods and in-core instrumentation system equipment located in the upper plenum. The RPV and the downcomer are cylindrical. The RPV head is integrated with the upper assembly. The core barrel, core baffle and protective tube unit are prevented from lifting under NOC by their weight. The reactor is located in the concrete cavity with a thermal and biological shield and a cooling system. The RPV is supported and fastened by the thrust ring fixed in the support truss. The thrust ring prevents RPV from transverse displacements. Reactor fastening inside the concrete cavity at two different elevations safely prevents it from displacements during seismic impacts or pipeline breaks. The VVER-1200 RPV design is provided in Figure 3.7.

Figure 3.7 VVER-1200 RPV (Rosatom, 2020).

In VVERs, the inlet and outlet nozzles are positioned at different elevations on the RPV. The outlet (hot leg) nozzles are higher than the cold leg nozzles as can be seen in Figure 3.8 below. The hot legs do not penetrate the downcomer as in Western-type PWRs. However, they have connections to the upper plenum. Hence, as a consequence of this design, there is more coolant above the reactor core, which can cause a little delay on core uncovery.

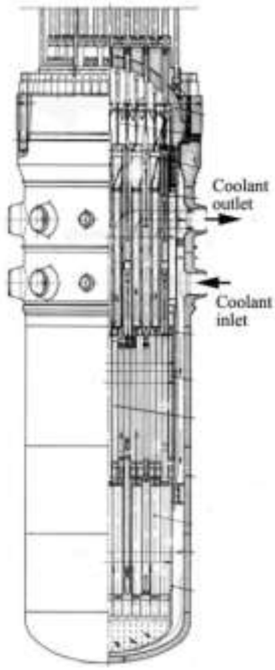

Figure 3.8 Typical geometry of RPV (Gottlasz et al., 2013).

VVER-1200 reactor vessel is the result of evolutionary development and enhancement of nuclear reactor vessels of VVER reactors. The distinction of the RPV used in the VVER-1200 reactor design is as follows:

- The RPV diameter is increased by 100 mm;
- The RPV length is increased by 300 mm due to some increase in the length of the supporting shell;

The increase in the RPV diameter makes it possible to decrease the probability of the fast neutron fluence to the vessel wall while ensuring the reactor design life of 60 years, and to reduce neutron fluxes near the reactor nozzle region. The elongated RPV helps to reduce the fast neutron fluence by approximately 10% on the welded joint of the shell to the nozzle region shell and to enhance the core cooling conditions in LOCA cases. The main design parameters of the reactor vessel are given in Table 3.3 below.

Table 3.3 RPV basic data

Inside diameter	4232 mm
Wall thickness	197.5 mm
Design temperature	350 °C
Design pressure	17.64 MPa(a)
Material	Steel 15H2NMFA
Inner total height	3855 mm
Weight	330 t

3.6 Active and Passive Safety Systems

Finally, VVER-1200 combines engineering solutions with a set of passive and active safety systems compliant with requirements after Fukushima nuclear accident in Japan. The active safety systems that are incorporated into the VVER-1200 design are as follows (Niwemuhwezi and Lee, 2018):

- High-pressure emergency injection system: boric acid solution supply into the RCS in case of LOCAs that exceed the self compensatory capability of the system at the pressure below 7.9 MPa;

- Low-pressure emergency injection system: boric acid solution supply into the RCS in case of LOCAs when the pressure in the system reduces below the working parameters of the corresponding safety system;

- Emergency gas removal system: decreases the pressure in the primary circuit by removing steam-gas mixture out of the primary circuit.

- Emergency boron injection system: boric acid supply into the pressurizer in case of a leak in order to decrease the pressure in the primary system and provide the necessary boric acid concentration in the primary system coolant.

- Main steamline isolation system: rapid and reliable steam generator isolation from a leakage region of feedwater or steam.

The passive systems which are incorporated into the VVER-1200 are as following:

- Emergency core cooling system, passive part: reactor cooling process if heat removal by steam generators becomes unavailable or insufficient.

- System of passive heat removal: residual heat removal and power plant cooling in case of an anticipated normal shut down of reactor.

- Double-envelope containment and core catcher: retaining of radioactive materials and nuclear radiation within design limits and protection against containment damage resulting from core meltdown.

CHAPTER IV

METHODOLOGIES OF CFD AND FAVOR CODES

4.1 Numerical Background

The computational fluid dynamics (CFD) has several advantages compared to the analytical experiments. The numerical simulations are more effortless and less time-consuming than analytical experiments because of the software packages on clusters. It is possible to perform different flow analysis with one calculation that makes CFD rather effective. In addition to the effectiveness, boundary conditions are easily applied for computational fluid dynamics applications compared to the experimental effort. CFD method utilizes detailed solutions of the Navier-Stokes equations for complicated 3d geometries and flows, for which the basic flow analysis fails.

Turbulence is an important issue and it has to be modeled mathematically in most cases. The use of mathematical models to reduce the computing effort is required because the exact equations are not available, so, using them is not feasible. The mathematical models depend on the simplification of exact conservation laws; however, they need to be modified into the specific case for consistency. Governing equations in CFD mathematically express three basic physical principles which define the flow of any fluid. These governing equations are given in the following:

• Continuity equation / mass conservation equation

Equation (4.1) is the time-dependent equation of mass conservation for both incompressible and compressible flows,

$$\frac{\partial \rho}{\partial t} + \nabla.(\rho \vec{u}) = S_m \tag{4.1}$$

where S_m denotes for the mass source term in the fluid domain.

• Newton's 2nd law / momentum equation

The Newton's 2nd law is the momentum equation. Equation (4.2) is the principle of momentum conservation or the equations of Navier-Stokes, utilized in ANSYS FLUENT,

$$\frac{\partial}{\partial t}(\rho\vec{u})+\nabla.(\rho\vec{u}.\vec{u})=-\nabla p+\nabla.(\overline{\overline{\tau}})+\rho\vec{g}+\vec{F} \tag{4.2}$$

where p denotes for the static pressure, $\overline{\overline{\tau}}$ denotes for the stress tensor defined in Equation (4.3), $\rho\vec{g}$ denotes for the gravitational body force term, while $\vec{F}$ denotes for the external body force term, respectively. The stress tensor $\overline{\overline{\tau}}$ is described as

$$\overline{\overline{\tau}}=\mu\left[(\nabla\vec{u}+\nabla\vec{u}^{T})-\frac{2}{3}\nabla.\vec{u}.\overline{\overline{I}}\right] \tag{4.3}$$

in which μ denotes for the molecular viscosity and $\overline{\overline{I}}$ is the unit tensor. The external body force can also include other model-dependent source terms such as porous medium approach source term and other user defined source terms. Many application-dependent CFD models are incorporated using $\vec{F}$.

• The 1st law of thermodynamics / energy conservation equation

Principle of energy conservation in ANSYS FLUENT can be given as

$$\frac{\partial}{\partial t}(\rho E)+\nabla.(\vec{u}(\rho E+p))=\nabla.\left(k_{eff}\nabla T-\sum_{j}h_{j}\vec{J}_{j}+(\overline{\overline{\tau}}_{eff}.\vec{u})\right)+S_{h} \tag{4.4}$$

in which k_{eff} denotes for the effective thermal conductivity, h_j denotes for the specific enthalpy of the species j and $\vec{J}_j$ denotes for the diffusion flux of species j. Three terms in brackets on the right-hand side of Equation (4.4) represent energy transfer due to conduction, diffusion and viscous dissipation, respectively. S_h includes all volumetric heat sources described according to the problem solved. The effective thermal conductivity is

$$k_{eff}=k+k_{t} \tag{4.5}$$

in which k_t denotes for the turbulence thermal conductivity described according to the turbulent model used. In Equation (4.4), E can be written as

$$E = h - \frac{p}{\rho} + \frac{u^2}{2} \tag{4.6}$$

in which h denotes for the specific enthalpy. For the standard $k-\varepsilon$ model, the effective conductivity can be written as

$$k_{eff} = k + \frac{c_p \mu_t}{\Pr_t} \tag{4.7}$$

in which k, in this case, is the fluid thermal conductivity, while the very last term in Equation (4.7) is the turbulence thermal conductivity.

A fluid is a substance which does not show a specified form, but adapts into the form of the vessel that contains it, because of its molecular distances. Thus, it is hard to handle a fluid from the universal approach used for solid substances. Generally, a fluid can be described as a substance which deforms continuously under the effect of some shear stress. If a fluid flows, its velocity can be different at different locations in the domain, and its particles can deform and rotate.

For non-complex geometries, the mesh can be structured. On the other hand, for complex geometries and flows, unstructured mesh is utilized because of their flexibility. The disadvantage comes from the irregularity of the data structure that leads the solver to be much slower compared to the regular mesh.

4.2 Turbulence Models

Turbulence means the flow of fluids that are not stable or controlled. Turbulence occurs once there are weak stabilizing viscous forces. Once the Re is high, the fluid flow seems in the shape of eddies of different dimensions. Hence, turbulence cannot be neglected in fluid flow simulations because of its vitality. There are several turbulence models. However, some of them are more commonly used. These are zero-equation, one-equation and two-equation models.

In order to define the effects of velocity fluctuations for turbulence in a single-phase flow, FLUENT utilizes several types of closure models. However, for multi-phase, the number of terms within the momentum equation is high. So, the simulation of turbulent flow for multi-phase flows is really complicated. FLUENT includes 3 techniques in order to model the turbulent multi-phase flow within the context of the $k-\varepsilon$ models. These $k-\varepsilon$ model options are mixture turbulence model as the default model, dispersed turbulence model and turbulence model for each phase. The multi-phase modifications of standard $k-\varepsilon$, RNG and realizable $k-\varepsilon$ models are similar. FLUENT also includes 2 turbulent flow options within the context of the Reynolds Stress Models (RSM), the options for which are mixture turbulence model as the default one and dispersed turbulence model.

4.3 Software ANSYS FLUENT and Boundary Conditions

The program FLUENT is one of the most common tools to discretely solve the governing equations including the continuity, momentum conservation and heat conservation equations. It is very useful to give the behavior of a wide range of flows including laminar, turbulent, compressible, incompressible, steady and unsteady. FLUENT also has a wide range of mathematical models for transport phenomena which can be applied to both simple and complicated geometries. It can be applied to laminar or turbulent flows within devices such as vessels, nozzles, heat exchangers, compressors, pumps, turbomachinery, heat engine components, external flows and etc.

This code relies on the finite volume method, in which the fluid region is divided into finite set of control volumes such as tetrahedrons, pentahedrons, and hexahedrons. FLUENT utilizes a control-volume method in order to convert the governing equations into algebraic equations, which can be solved numerically. FLUENT includes several turbulence models. These turbulent models possess some advantages and disadvantages. Simulations are carried out by means of a CFD code Fluent.

Table 4.1 gives some equivalencies associated to the general variable in FLUENT.

Figure 4.1 gives a diagram of coupled solver mode’s performance.

Table 4.1 Different variables used in the general equation.

Equation	Variable
Continuity	1
Momentum X	u
Momentum Y	v
Momentum Z	w
Turbulent kinetic energy transport	k
Turbulent kinetic energy dissipation	ϵ

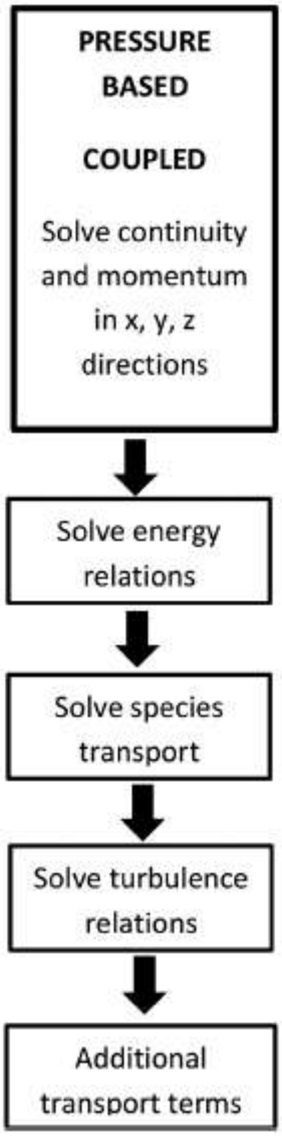

Figure 4.1 The pressure-based coupled solver diagram (Alonzo-García et al., 2016).

Before the simulations, the FLUENT needs to describe the number of dimensions utilized in order to obtain the solution; two-dimensional or three-dimensional. The program has a choice to select double-precision. This choice is suggested once high gradients in the variables are anticipated, cells with high aspect ratio or once solution is desired to converge better.

Other essential feature of the software is to set the number of parallel processors to be utilized within. This feature is particularly useful for multiphase problems, problems which need large number of iterations to be solved, very high mesh sizes, and complicated geometries. Multiphase flow can also be modeled by ANSYS FLUENT. These capabilities are very useful in the simulations of liquid-vapor flows in the nuclear reactors that utilize water as coolant material. For multiphase analysis, ANSYS FLUENT also possess the VOF, mixture and Eulerian models. The applications of multiphase flows include condensation, boiling, spraying, and etc. Multiphase flow modeling by computational fluid dynamics has great potential in nuclear engineering field because most reactors under operation are LWRs that could have two-phase flow in normal operational conditions for boiling water reactors or in accident conditions for pressurized water reactors. But multiphase flow requires a great computational effort due to the limitations of the models in the commercial computational fluid dynamics programs. Multiphase flow problems in nuclear reactors will also be addressed in this thesis for a LOCA case.

In a computational fluid dynamics model, BCs must show exactly the real-time conditions at the boundaries. Due to the algebraic features of the differential equations, BCs can be classified given in the following:

- Dirichlet BC: The value of the flow variable is represented at the boundary. Dirichlet BC is typically related to cases including inlets and isothermal walls.

- Neumann BC: The value of the gradient normal to the flow variable is specified. Neumann BC is often linked to symmetry at the boundaries and adiabatic walls.

- Mixed BC: These conditions result from a combination of the first two types of BCs (Dirichlet and Neumann).

4.3.1 Velocity Inlet Boundary Condition

This boundary condition prescribes a homogeneous velocity condition in the inlet of a flow domain. It is created in order to simulate incompressible flows, such as internal flows in pipes or machinery and external flows over complicated geometries. It is not suggested to be used for compressible flows. This boundary condition allows the user to input both the magnitude and the direction of a homogeneous velocity profile. Other velocity profiles, i.e. sinusoidal, parabolic, and logarithm can be specified by a UDF. For turbulence, FLUENT allows to define the turbulence levels in the fluid domain with different options. For example, a turbulence intensity and hydraulic diameter can be used for this occasion for internal flows.

The turbulence intensity represents a percentage of the fluctuating magnitudes of velocity compared to the average magnitude. For instance, if the coolant velocity is 5 m/s and a turbulence intensity of 10% is chosen, the inlet velocity would represent velocities from 4.5 to 5.5 m/s. In addition to these, different parameters such as fluid temperature or heat flux can be specified in the fluid domain, which required for heat and mass transfer analysis.

4.3.2 Pressure Outlet Boundary Condition

This BC needs to prescribe the static or gauge pressure at the exit. The value of static pressure is important for subsonic fluid flows (M < 1). In order to utilize “pressure outlet” truly, it is needed to construct a set of backflow relations to reverse fluid flow at the exit. Backflow relations are important since wrong values of them can lead to convergence problems during the solution process.

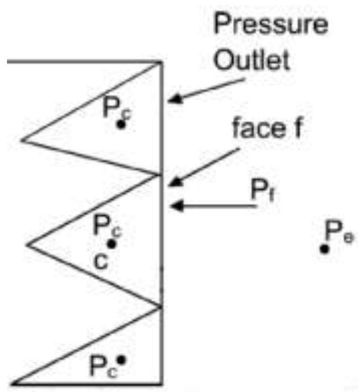

Figure 4.2 Components of the “pressure outlet” BC (Alonzo-García et al., 2016).

For incompressible flows, the outlet face pressure is computed as a mean between the exit pressure and the mean pressure value (Figure 4.2).

$$P_f = \frac{1}{2}(P_c + P_e) \tag{4.8}$$

This BC does not certainly mean a constant pressure value throughout the exit of the fluid domain. But, when the solution reaches the criterion of convergence, the mean pressure at the exit will probably reach a pressure which is close to the gauge pressure at the outlet.

4.3.3 Mass Flow Inlet Boundary Condition

Mass flow inlet BC can be utilized in order to supply a specified mass flow rate or mass flux at an entrance. As with a velocity inlet BC given in Section 4.2.1, specifying the mass flux allows the total pressure to vary according to the interior solution. This is in contrast to the "pressure inlet" BC, where the total pressure is constant while the mass flux varies. But the mass flow inlet is equally applicable to both compressible and incompressible fluid flows, unlike a "velocity inlet" BC.

A "mass flow inlet" boundary condition is often utilized once exact value of mass flow rate is more vital than the exact value of the total pressure of the fluid flow. In addition, a mass flow inlet BC can be utilized as an outflow by prescribing the flow direction going out from the solution domain.

4.3.4 Walls

For viscous flows, the no slip condition has to be applied on the walls. This can be achieved by specifying u = v = w = 0 at the walls to reproduce the formation of the dynamic boundary layer. Shear stress values, temperature values (Dirichlet-type) or normal heat flux values (Neumann-type) can be applied and they are especially helpful for thermal analysis. One can also describe values of wall roughness, which are particularly helpful in turbulent flows.

4.4 FAVOR

Since the 1980s, a number of codes have been created in order to carry out the probabilistic analysis of reactor vessels, such as OCA-P, VISA-II, PROFMACII, OPERA, VIPER, FAVOR and PASCAL. Among them, FAVOR and PASCAL have been commonly utilized nowadays. FAVOR code was developed by Oak Ridge National Laboratory (ORNL). The motivation for the development of the FAVOR code is PTS condition that may occur in the reactor pressure vessels. In case the coolant which is in contact with reactor pressure vessel wall is overcooled over time, temperature gradients occur along the reactor pressure vessel wall. It creates variable two-dimensional stress situations along the reactor pressure vessel wall. If the internal pressure is also high enough, Pressurized Thermal Shock (PTS) occurs as a result of thermal and mechanical loading.

Knowledge and models that have undergone change and development until today (material interaction, fracture mechanisms, computational technology, probabilistic methods) have participated in the FAVOR code developed at the request of the Nuclear Regulatory Commission (NRC).

FAVOR code can perform scenarios such as Pressurized Thermal Shock (PTS), cool-down, heat-up and also reactor pressure vessel integrity analysis for other situations such as loss-of-coolant accidents. Analyzes can be done for PWR and BWR. This code has been prepared for reactors of USA origin. A configuration is available in databases according to material properties created as a result of tests and measurements for reactor pressure vessels in the USA. These data files have been attached to the FAVOR code and the analyses are made accordingly.

4.4.1 Features and Working Principles of FAVOR Code

The FAVOR code consists of 3 modules:

1. FAVLOAD module that calculates the stress and temperature distribution along the reactor pressure vessel using the Finite Element method
2. FAVPFM module calculating CPI and CPF values for events with Monte Carlo method
3. FAVPOST module that calculates crack initiation and propagation frequencies per reactor year for reactor pressure vessel as a result of accident and event frequencies

In Figure 4.3, FAVOR's working principle is shown.

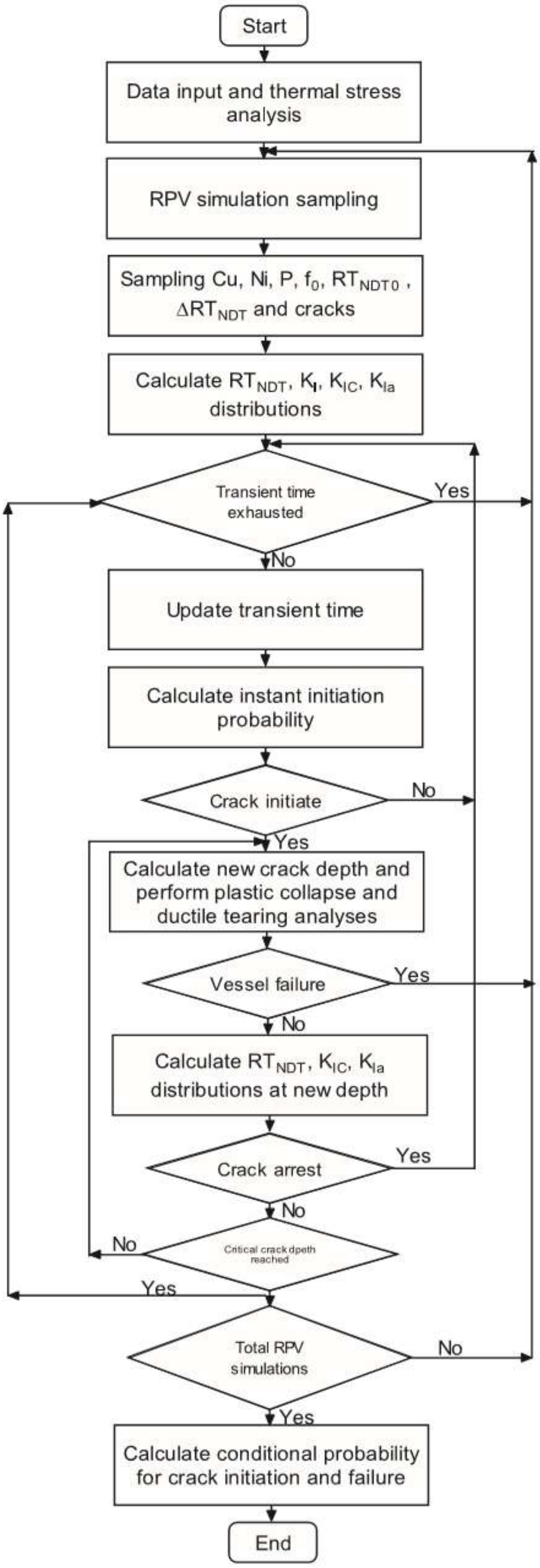

Figure 4.3 FAVOR's working principle (Qian et al., 2014).

4.4.1.1 Features of FAVLOAD Module

FAVLOAD module calculates the axial stress, tangential stress, temperature and stress intensity factor for thermally and mechanically loaded reactor pressure vessel wall by finite element method. Thermal hydraulic data, reactor pressure vessel geometry, thermo-elastic properties are entered as input to the FAVLOAD module. Thermal hydraulic data are the values of coolant temperature, coolant pressure and heat-transfer coefficient of coolant over time on the downcomer around the beltline region of reactor pressure vessel. These values can also be entered for more than one state depending on the computer memory.

Reactor pressure vessel geometry data includes reactor inner radius value, reactor pressure vessel thickness and cladding thickness. The thermoelastic property values are entered separately for the reactor pressure vessel base material and the stainless steel cladding material in its inner wall. These values are those such as thermal conductivity, specific heat, density, Young's modulus of elasticity, thermal expansion coefficient, Poisson's ratio.

4.4.1.2 Features of FAVPFM Module

FAVPFM module working principle is based on Monte Carlo calculation technique. This technique allows deterministic fracture analysis to be performed with probabilistic RPV trials. In Monte Carlo method, many flaw geometries and Reactor Pressure Vessel (RPV) material values are selected with appropriate probability distributions. For the specified event, the stress, temperature, geometry, stress intensity factors calculated by FAVLOAD module and fracture toughness value of RPV calculated by probabilistic analysis are compared. Then, fracture initiation and RPV decay matrices are created.

4.4.1.3 Features of FAVPOST Module

The frequency and distribution of events per reactor year of the event specified as input for the FAVPOST module is required.

4.4.2 Stress Analysis

The geometry of the reactor vessel, thermoelastic properties of the base metal and the cladding, the time-dependent temperature of coolant and convection coefficients between the coolant and reactor vessel wall are utilized in order to compute the thermal stress and temperature behaviors through the RPV wall during the pressurized thermal shock accident. Heat flux at the external wall of the RPV is assumed as zero for adiabatic BCs and the RPV wall is assumed to be at uniform initial temperature.

In order to calculate the stresses along the vessel wall, the thermal stresses or secondary stresses are superimposed with pressure stresses or primary stresses. To calculate precise thermal stresses, the transient average linear coefficients of thermal expansion are utilized. Note that the average linear coefficients of thermal expansion need to be input for the reference temperature. The correct utilization of different coefficients of thermal expansion on the vessel integrity is given in Niffenegger and Reichlin (2012). The reactor vessel is basically assumed as stress-free at the initial temperature value. Tangential and longitudinal stresses are computed at different instants during the whole transient by the elastic FEM under plain-strain condition. In the structural analysis, the vessel is supposed as having no crack. The tangential and longitudinal stresses at different points through the RPV wall are fitted by the third-order polynomial given below.

$$\sigma_\theta, \sigma_z = b_0 + b_1 \frac{a'}{a} + b_2 \left(\frac{a'}{a}\right)^2 + b_3 \left(\frac{a'}{a}\right)^3 \tag{4.9}$$

where a is the distance of the crack tip to the internal wall of the RPV in unit of mm. a' is the distance from the internal wall of the RPV to the investigated point on the solid structure in unit of mm. σ_r is not taken into account in the study.

4.4.3 Analysis of K_I, K_{Ic} and K_{Ia}

There are two techniques in order to compute stress intensity factor of the reactor vessel exposed to Pressurized Thermal Shock events. The first method is the FEM, in which a two-dimensional or three-dimensional model of the crack is utilized in order to compute the J-integral. Hence, the stress intensity factor, K_I, can be obtained by,

$$K_I = \sqrt{\frac{JE}{1-\nu^2}} \tag{4.10}$$

The last method is the influence function method which is an analytical one and can be given as below.

$$K_I = \sqrt{\frac{\pi a}{Q}}\left[b_0 i_0 + b_1 i_1 a + b_2 i_2 a^2 + b_3 i_3 a^3\right] \tag{4.11}$$

The fitted coefficients, i_0, i_1, i_2 and i_3, are computed by the finite element method and included in FAVOR system code. To explain the circumferential and axial stress discontinuity at the clad-base metal interface, initially K_I is computed with a continuous stress distribution obtained by a linear extrapolation of stress distribution in the base metal to the clad–base metal interface (Marie et al., 2005). Later on, K_I is computed for the stress in the clad by removing the linearly extrapolated stress value from the actual stress value in the clad region. The sum of these two parts gives the stress intensity factor of the corresponding crack in the surface of the RPV wall. For surface cracks, the pressure load on the crack face is also taken into account. For an embedded crack, the stress intensity factor is computed by the EPRI model in the ASME procedure and can be written as below.

$$K_I = \sqrt{\frac{\pi a}{Q}}\left(M_m \sigma_m + M_b \sigma_b\right) \tag{4.12}$$

M_m stands for the free-surface correction for membrane stress, M_b stands for the free-surface correction for bending stress, σ_m is the membrane stress (MPa), and σ_b is the bending stress (MPa). In order to obtain the fracture toughness, there are several different techniques. These are ASME, FAVOR and Master Curve methods. According to ASME method, the fracture toughness can be found by,

$$K_{IC} = 36.5 + 22.78\exp\left[0.0636(T - RT_{NDT})\right] \tag{4.13}$$

in which

$$RT_{NDT} = RT_{NDT0} + \Delta RT_{NDT} + \text{Margin} \tag{4.14}$$

in which RT_{NDT0} is the initial nil-ductility transition reference temperature.

$$\Delta \mathrm{RT}_{NDT} = [CF]\, f^{\,0.28-0.1\log f} \tag{4.15}$$

and the safety margin can be written as

$$\text{Margin} = 2\sqrt{\sigma_I^2 + \sigma_\Delta^2} \tag{4.16}$$

The neutron fluence f at the distance a* from the clad-base metal interface can be expressed as

$$f = f_0 \exp(-0.00945a^*) \tag{4.17}$$

where f_0 is the moderated neutron fluence at the internal wall of the RPV.

4.4.4 Probabilistic Method

A limit state function L can be described as the difference between K_{Ic} and K_I, can be written as below.

$$L = K_{Ic} - K_I \tag{4.18}$$

Once L is greater than 0, that means the reactor vessel remains intact. However, if L is smaller than and equal to 0, fracture takes place and a crack extension analysis is going to be initiated. Therefore, the expression for the probability of fracture may be given as below.

$$P_f = P(L \leq 0) \tag{4.19}$$

4.5 Conclusion

A comprehensive thermoelastic analysis of reactor vessel should present the integrity analyses of a model RPV exposed to PTS. The analyses must be performed by a one-way multi-step solving strategy that includes the thermal hydraulics, thermomechanical and fracture mechanics analyses in order to simulate three LOCA. The thermal hydraulics analyses can be carried out by the CFD code FLUENT and a three-dimensional model of the RPV, providing the input for the mechanical analyses by the system code FAVOR.

CHAPTER V

CFD AND FAVOR ANALYSES OF REACTOR VESSEL

This chapter includes the generation of the solid models and the fluid domain for CFD, meshing and grid sensitivity analysis results, thermal material properties of coolant in the RPV, heat transfer correlations in turbulent flow, single-phase pressure drop calculation for VVER-1200 nuclear reactor, the porous medium model applied, all boundary conditions applied for three different analyses (symmetric flow, asymmetric flow and LOCA situation) and finally the input deck of FAVOR for structural analysis.

5.1 Solid Models of RPV Components

The VVER-1200 nuclear reactor is a Russian-design 4-loop PWR with horizontal steam generators. The core contains 163 hexagonal fuel assemblies. VVER-1200 has a thermal power of 3200 MWt at NOC. The operating pressure amounts to 16.2 MPa while the inlet temperature of water at the RPV inlet nozzles equals 298.2 °C. The total vertical length of the RPV is 11185 mm. The fuel rod cladding has a diameter of 9.1 mm. Four cold legs and four hot legs of the RPV, each has a diameter of 0.85 m, are located in a nonuniform and asymmetric layout with respect to reactor core symmetry axes. Some acceptable simplifications have to be added into the analysis, but one should note that those simplifications must guarantee the coolant flow will not be affected. There is not any solid in the domain, the whole domain contains fluid. Since the bypass flow does not have important effect on the coolant mixing and only have minor effect on the additional pressure loss, the upper plenum and its corresponding components such as steam separators and steam driers are not considered. Then, the complex geometries of 163 fuel assemblies are ignored. The fuel assemblies are modeled as a whole using the porous media model. The reactor core has hexagonal-shaped fuel assemblies and each fuel assembly consists 312 fuel rods. Hence, a total number of 50856 fuel rods are there in the reactor core. The element number in the meshed structure must be sufficiently high in order to simulate all details in the reactor core comprehensively. The simplified model is depicted below in Figure 5.1.

Using the model discussed above, a heat transfer analysis for VVER-1200 reactor vessel was carried out. This analysis was carried out in order to determine temperature distribution across the reactor vessel, core barrel, and hot and cold leg thicknesses. This thermal output can then be utilized for the thermomechanical stress analysis. The related thermal properties and results of the simulations are given below.

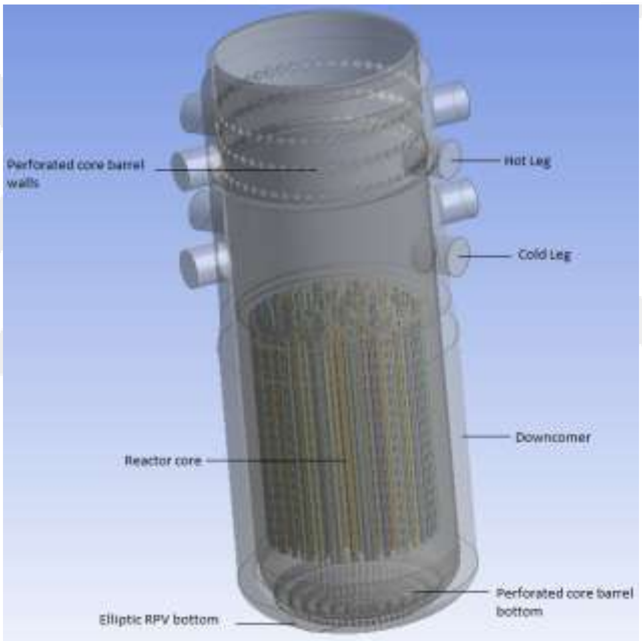

Figure 5.1 Three-dimensional image of the reactor vessel of a VVER-1200.

Figure 5.2 depicts the horizontal cross-section of the reactor pressure vessel with four hot or cold legs. Azimuthal arrangement of inlet and outlet nozzles in the RPV is nonuniform in tangential direction and has a layout having asymmetry with respect to the reactor core symmetry axes, seen in Figure 5.2 below.

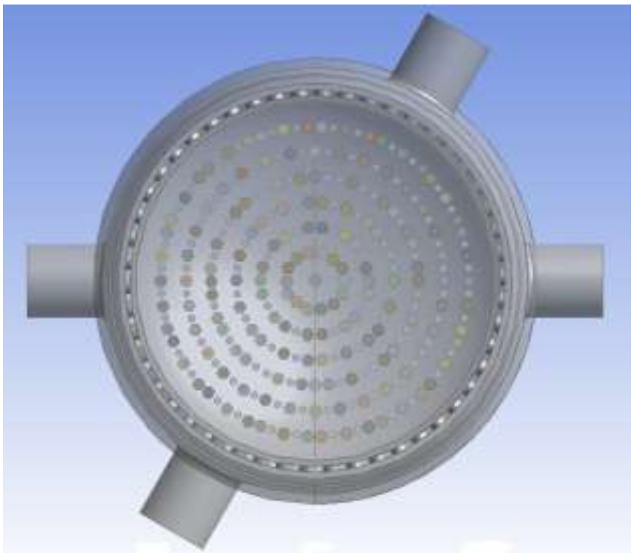

Figure 5.2 Cross-sectional positions for both hot and cold legs.

In VVER-1200 design, outlet nozzles are placed higher compared to the inlet nozzles. The whole fluid domain was modeled with SolidWorks to generate the external boundary of the model which is the wall of the reactor vessel. Later on, ANSYS Space Claim was utilized to perform the volume extract operation. The aim of the volume extraction operation is to evolve the outer shell into the internal volume. After selecting all the openings that the reactor vessel has and also selecting the internal surface of the shell (which also denotes the external surface of the flow domain), Space Claim simply generates the internal volume to be analyzed. As depicted in Figure 5.1, the fluid domain includes cold legs, hot legs, downcomer, lower plenum, bottom holes of core barrel, core itself, upper plenum and holes located on the side wall of the core barrel. But the spacer grids and the lower plenum structures were subtracted from the geometrical model. The fluid comes into the reactor vessel from the cold legs and then continues to the downcomer vertically. Then, it passes to the elliptic reactor vessel bottom plate after it reached to the lower plenum. Later on, it flows among lower small holes of the core barrel. When the water flows up among the core, it is heated and its temperature increases. The water passes through the holes located at the core barrel wall before it leaves the reactor pressure vessel through the hot legs.

Figure 5.3 depicts a preliminary design of the reactor pressure vessel for VVER-1200. The main components of this vessel consist of upper head, RPV side shell, and bottom head as a lower shell. Upper head is a closure head with ellipsoidal shape.

RPV shell components are the upper and bottom cylindrical shells and lower closure head with hemispherical shape. The upper part of the vessel is cover that is connected to lower part with bolts. The lower part of the vessel is a cylindrical shell with hemispherical-shaped bottom head. Geometrical models of the main components for nuclear reactor vessel can be shown in Figures 5.3 - 5.7.

Figure 5.3 RPV for the VVER-1200 including the upper part and the lower part.

Figure 5.4 Geometrical model of the upper head.

Figure 5.5 Geometrical model of the top cylindrical shell.

Figure 5.6 Solid model of the bottom cylindrical shell and head.

Most of the reactor internals are located in the core barrel that is inserted in the reactor vessel. Core barrel is one of the main internals of the reactor vessel. Core barrel includes six shells and an elliptical bottom. The component height is approximately 11 meters and weight is 63 tons. On the top part of the core barrel, there are 238 holes with diameter of 196 mm. The holes are located in a specific order that represents six rows along the perimeter of the shell and intended for the water coolant exit. In addition to these, there are 1344 holes having different diameters on the lower head of the structure. These holes at the bottom are intended for supports installation and keep the fuel assemblies from being injected with small mechanical particles.

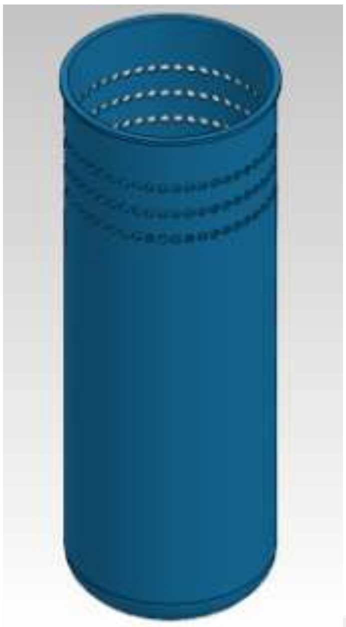

Figure 5.7 Core barrel model generated for simulations of RPV.

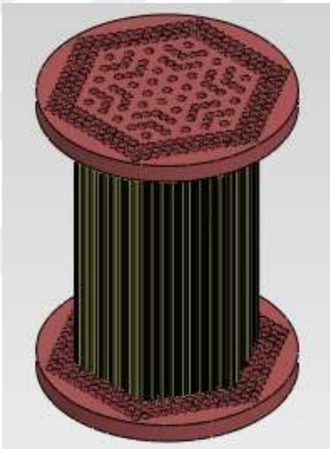

Figure 5.8 Fuel assemblies and core support plates models generated for simulations of RPV.

After the outer volume was generated by using SolidWorks, that assembly consisting of solids should be simulating the flow in the flow region loosely defined by these solids. Hence, after preparing the geometry, the fluid volume is extracted by using SpaceClaim.

The primary side water coolant flows into the lower plenum of the vessel through the perforated core barrel bottom via 1344 holes. After passing lower plenum, the water passes into the fuel support columns which are intended to be flow distributors. The fuel support columns are inserted into aligned holes of the lower support plate.

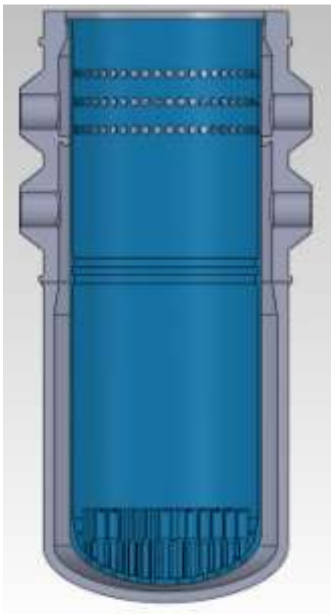

Figure 5.9 Assembly of RPV and core barrel.

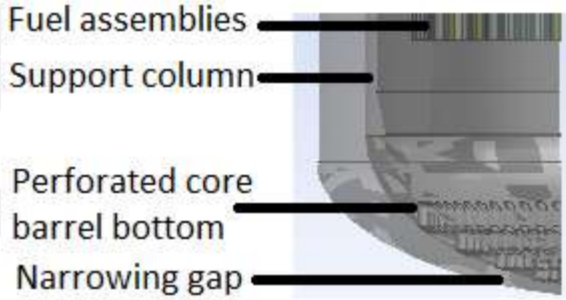

Figure 5.10 Main components in the lower plenum of a VVER-1200 NPP.

Figure 5.11 Fluid domain after converting the external volume into the internal one.

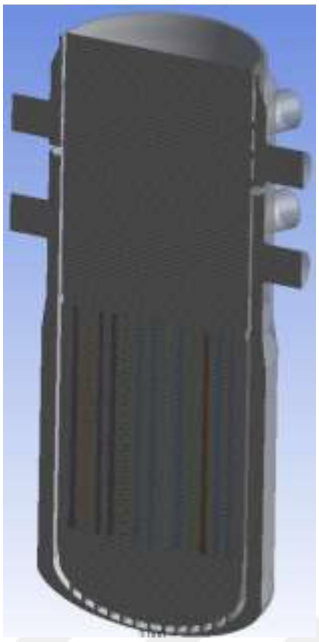

Figure 5.12 Vertical cross-section of the fluid domain showing all internals.

5.2 Meshing and Grid Sensitivity

In order to solve a Computational Fluid Dynamics problem truly, a group of best practices is required to provide better convergence in the analyses. The first of them is the skewness that needs to be verified in most of the grid elements and should be between 0 and 0.5. Being closest to zero is the best situation.

The structured grid system details of several zones in the RPV of the fluid domain and the fuel assemblies with ANSYS Meshing Platform are depicted in Figure 5.13. The whole mesh structure of the model is renewed several times. The model consists of nearly 4.8 million elements. Hence, the mesh quality is greatly increased, while skewness value is decreased. For the latter form of grid, value of average skewness is 0.23874. Figures 5.13a-5.13e show the structured hexahedral grid of the fuel assemblies and the tetrahedral meshes of the overall coolant domain of the RPV. The perforated side wall of the core barrel is modeled with holes as it has in real. The overall coolant domain is separated into two zones in order to apply the best meshes. These zones are the reactor core and the rest of the domain. The mesh elements near the contact regions are highly skewed, which could lead to some convergence issues and influence computational accuracy (Niu and Wang, 2019). The total element number amounts to $4.8x10^6$. The total node number equals 950000. However, sadly, the element numbers are limited by computer capabilities from time to time in Computational Fluid Dynamics studies.

A mesh independency should be performed in computational fluid dynamics analysis of complicated flows within complex geometries. However, from time to time it is limited by several reasons like the computer capabilities. For this study, nearly $1.7x10^6$, $1.9x10^6$, $2.6x10^6$ and $4.8x10^6$ numbers of elements are established, respectively, for the purpose of carrying out a complete mesh sensitivity analysis. The numerical values of the outlet nozzle temperatures as depicted in Figure 5.14 below are sharply raises between $1.7x10^6$ and $1.9x10^6$ number of elements. However, just a small increase is observed after $2.6x10^6$. It proves that more-refined meshes after $4.8x10^6$ numbers of elements have not any remarkable effect on the exit temperature. Therefore, taking the computational time and computer capabilities into account, $4.8x10^6$ elements is accepted for the all remaining parts of the simulations.

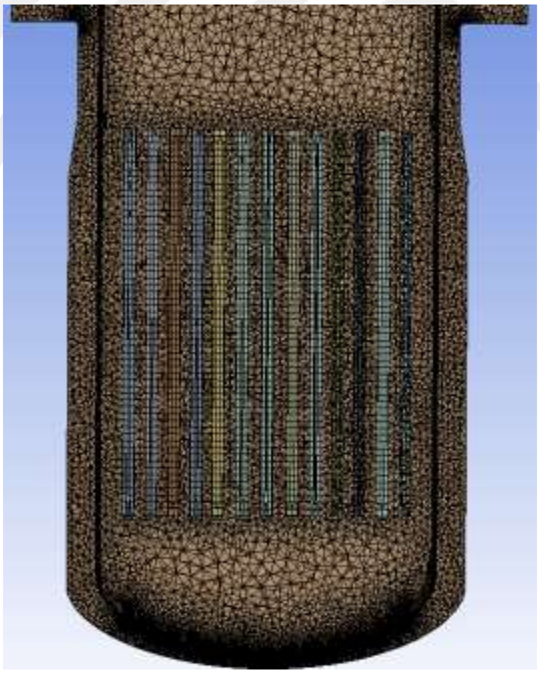

(a) Downcomer, lower plenum, and reactor core

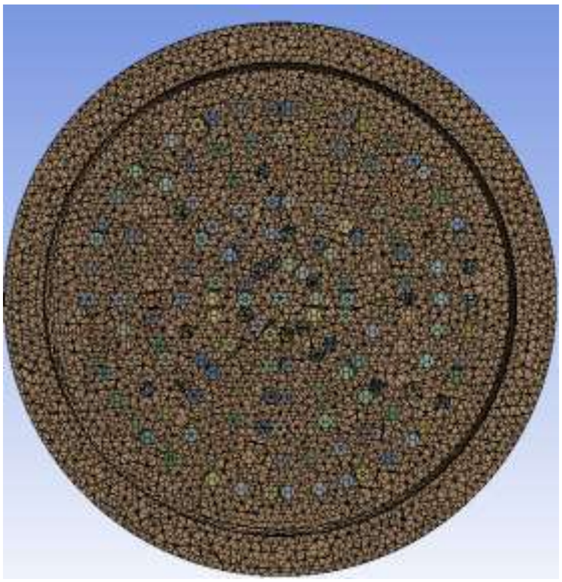

(b) Reactor core from horizontal cross-section

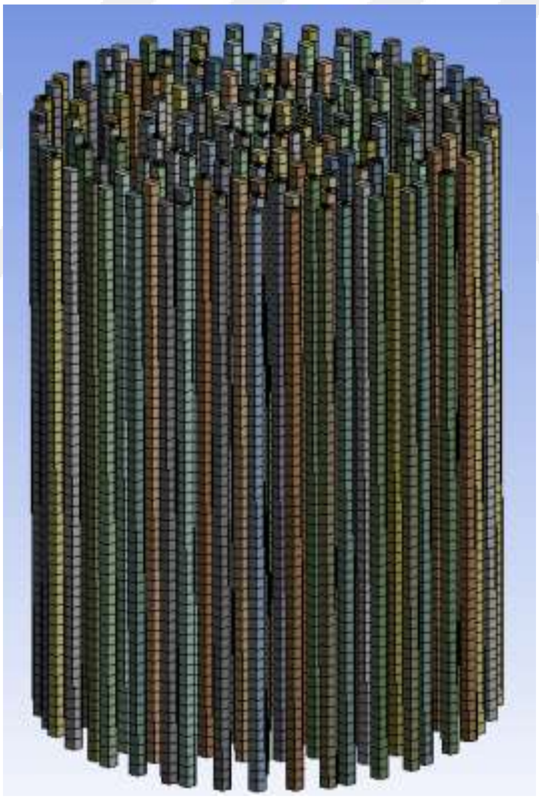

(c) Fuel assemblies

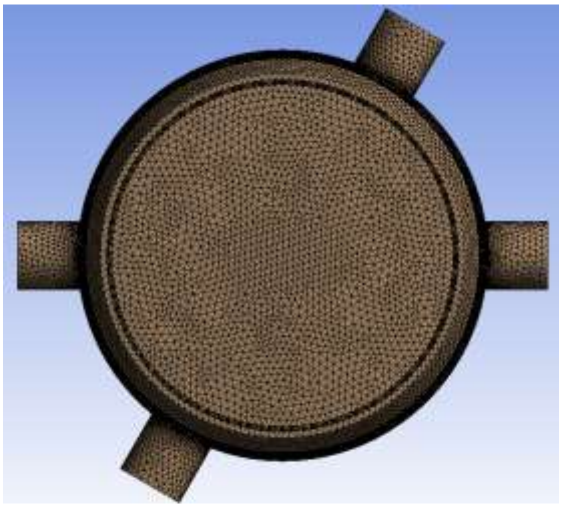

(d) Top view of the vessel including four hot legs and perforated side walls of the core barrel

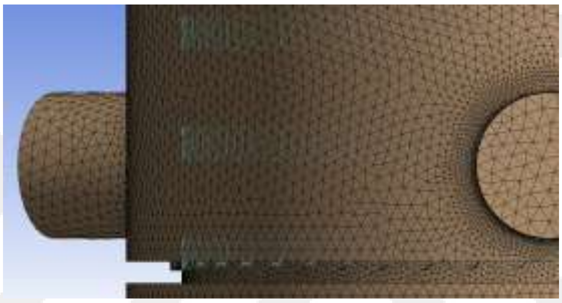

(e) Perforated side walls of the core barrel

Figure 5.13 Structured mesh of the fuel assemblies and unstructured mesh of the fluid domain of the reactor vessel.

In general, it might be better to use hexahedral mesh when calculating the two-phase situation. The reason of using tetrahedral mesh instead of hexahedral mesh for the fluid domain is that pressure solvers are generally better at giving good accuracy on tetrahedral meshes today than they were a couple of years ago. In a complicated geometry, it is harder to generate a conforming hexahedral mesh leading to worse mesh quality and difficulties in making the solver converge. But, if the geometry allows for it, utilizing hexahedral mesh has some advantages as has been addressed above. Required mesh refinements studies are carried out and mesh quality is greatly increased and skewness value is decreased. Now, average skewness of the mesh is 0.23874. The use of hexahedral mesh will be taken into account and investigated in future studies.

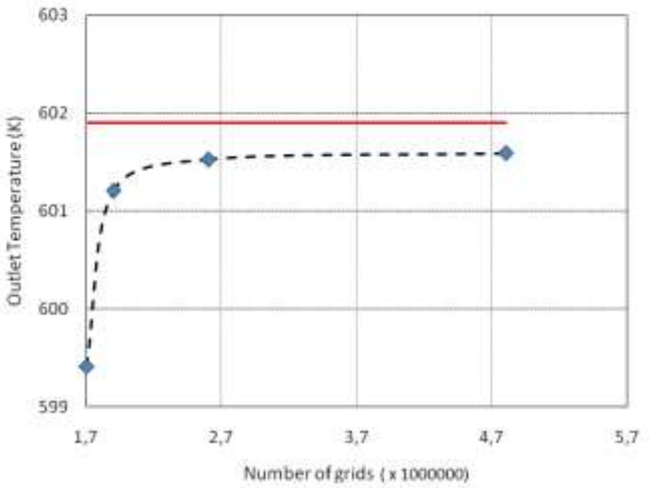

Figure 5.14 Mesh independence test at hot leg locations for different numbers of grid cell, red line indicating the design value of the outlet temperature for VVER-1200.

5.3 Thermal Material Properties

The commercial CFD package ANSYS FLUENT 17.2 (ANSYS Inc., 2011) is used to solve the equation of the heat transfer between the RPV wall and the coolant, with the momentum and heat conservation and the continuity equations. The physical properties of water as coolant for prescribed temperature and pressure of 298.2 °C and 16.2 MPa, respectively, are given below:

(a) density amounts to 731.48 kg/m^3,

(b) coefficient of thermal conduction equals to 0.5672 W/m-K,

(c) dynamic viscosity amounts to 8.946×10^{-5} Pa-s,

(d) specific isobar heat capacity equals to 5.393 kJ/kg-K.

In order to solve a CFD problem truly, a group of best practices is required to provide better convergence in the analyses. One of them is to provide better convergence values in the simulation is to obtain solutions utilizing single-precision and first-order discretization models at first. Then, changing the discretization models from first-order to second-order helps to improve the convergence in the CFD problem. This must be performed due to the fact that second-order discretization models cause lower error. Hence, it is suggested that the energy equation or any multi-phase fluid flow must be activated in order to provide sufficient convergence values.

Based on the aforementioned solutions, the first-order upwind resolution discretization schemes are used for turbulent kinetic energy and dissipation rate equations. On the other hand, second-order upwind schemes are utilized for energy and momentum expressions. The most widely used two-eqn. turbulence models in FLUENT are k–ε and k–ω. The analyses performed in this dissertation are performed using the standard k–ε. RNG k–ε supplies derived formula for effective viscosity which requires smaller Re (Yakhot et al., 1992). The corresponding Re for the hydraulic diameter of the case is 252,339 and is well inside the turbulent flow regime. Hence, the value of Re for the coolant through the lower core plate is too high, which means the results obtained using RNG k–ε may be overestimated.

The turbulence flows are greatly affected by the wall surfaces. The wall treatment option used significantly influences the reliability of the results. Standard wall functions are suitable for grids coarser than y+>11. It has no differences than other advanced near-wall treatment options. The second one is the scalable wall functions which provide persistent results for grids having any level of refining. Hence, based on the aforementioned knowledge, the standard k–ε and the standard wall functions are applied for the CFD analyses in this dissertation. More sensible results are attained comparing to other turbulent models according to computational capabilities allow. If another turbulent model or finer grid system is used for future studies, the near-wall treatment options will be addressed again in order to obtain adequately consistent results.

FLUENT computes the superficial velocities according to the volumetric flow rate of fluid in porous media. The negative momentum source term tends to create more pressure loss which is also proportional to the fluid velocity. For geometries having a region with holes, the viscous effect may be ignored. So, just the inertial effects are taken into account. The holes are vertical and restricted in the radial direction. The radial velocity of coolant is very low; therefore, the flow could be considered as laminar. It is adopted from the open literature that the pressure loss can be evaluated accurately when the ratio of directional coefficients of radial to longitudinal amounts to 100. The cross-sectional area of the core equals to 7.86×10^6 mm². The total cross-sectional area of the fuel assemblies is nearly 3.3×10^6 mm². Therefore, the porosity amounts to 0.58. The value of permeability is adopted from open literature in a research paper by Cheng et al. (2016) for a VVER-1000 nuclear reactor, which equals to 6.56×10^{-9} m². The square resistance coefficient is also evaluated in the same study mentioned as 11. But the coolant velocity around the core inlet and exit dramatically raises because of the narrower cross-sectional areas of these regions, particularly at the core exit.

The cross-sectional velocity distribution is addressed starting from the reactor core inlet height to the reactor core exit height. Then, the axial velocity distribution is calculated from x=0.97 to x=-3.6. The definitions of these x coordinates are the core inlet and outlet elevations, respectively. When these two coordinate values are summed up, total active fuel rod height whose magnitude is 4.57 m will be obtained. The root mean square of the velocity was computed as 3.15 m/s. The square resistance coefficient was found by Cheng et al. (2016) as 9.02 for a VVER-1000. Thus, the axial resistance coefficient is applied as 9.02, while the radial one is set accordingly as 902 in the simulation. The reactor parameters that affect the square resistance coefficient are the primary pressure, density of the fluid, axial direction length of core, and the velocity component in the axial direction. The pressure value is only 3.1% in deviation between the primary pressure values of VVER-1000 reactor and VVER-1200 reactor. The fuel assemblies of VVER-1000 and VVER-1200 are actually identical in design. They only differ a small amount in the fuel column height. Moreover, symmetric (full-loop) mass flow rates in Table 4.1 are for VVER-1200, because VVER-1200 is a 4-loop reactor design and it has 19000 kg/s, which specifies 4750 kg/s mass flow rates entering in each loop.

The internal heat source was assumed to be uniform and steady. For a VVER-1200 nuclear reactor, the heat power of the core amounts to 3000 MWt under normal operating conditions. The average core power density for VVER-1200 is 10.85×10^{7} W/m³ for symmetric case and 72.7×10^{7} for the asymmetric case. The power density values must be calculated according to the equation below.

$$\omega = W/Al \tag{5.1}$$

where W, A, and l stand for heat power, flow cross-sectional area, and active fuel height (Cheng et al., 2016).

The main reason of this drop is the decrease in the heat power of the core from 3000 MW for full-power to 2010 MW for asymmetric case. Therefore, there is a directly proportional relationship in average power density per unit volume.

5.4 Heat Transfer Correlations in Turbulent Flow

Several theoretical and experimental studies have been carried out in order to evaluate the effects of heat transfer coefficient for simple geometries. Such studies have proved the following.

1. The heat transfer coefficient varies significantly in the entrance region where the temperature and velocity fields are still developing. In typical Light Water Reactor cores, the entrance region is a small percentage of the whole channel, so it can be ignored. The heat transfer capability of a channel can be represented by the overall heat transfer coefficient of the channel by averaging for the whole height of the core. Thus, the heat transfer coefficient in the analysis was taken as 40000 $W/m^2{}^{\circ}C$ averaged approximately according to the coolant velocity values along the rod bundles in the literature and by the values obtained from Presser and Weisman correlations.

2. The laminar layer is quite thin compared to the turbulent layer, which dominates the flow and the heat transfer coefficient is not very sensitive to boundary conditions for the nonmetallic fluids such as light water, where Prandtl number ≥ 1.

Coolant velocity throughout the fuel assemblies is constraint to a maximum of 10 m/s to avoid cavitation. Data in need for the VVER-1200 is given in Section 5.3. The heat transfer coefficient of coolant at 10 m/s and 1 m/s velocities, and at mean temperature which is approximately 315°C for a VVER-1200 was calculated as following.

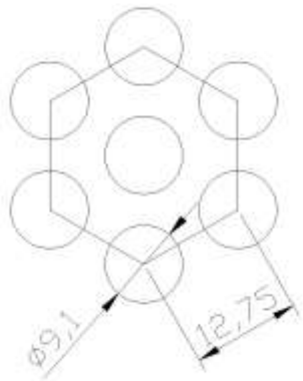

Figure 5.15 Dimensions of the pitch between fuel rods and outer diameter of cladding in mm.

For light water at 10 m/s velocity

The common way in order to represent the relevant correlation is expressing the Nu for a fully developed flow (Nu_∞) as a product of $(Nu_\infty)_{c.t.}$ for a circular tube multiplied by a correction factor:

$$Nu_\infty = \psi (Nu_\infty)_{c.t.} \tag{5.2}$$

where $(Nu_\infty)_{c.t.}$ is generally found by the Dittus-Boelter correlation unless otherwise stated.

Dittus-Boelter equation For cases $\mu \approx \mu_w$ the Dittus-Boelter equations are the most well-known used equations:

$$Nu_\infty = 0.023 \mathrm{Re}^{0.8} \mathrm{Pr}^{0.4} \text{ when the fluid is heated} \tag{5.3}$$

for $0.7 < \mathrm{Pr} < 100$, $\mathrm{Re} > 10000$, and $L / D > 60$. All fluid properties are at the average temperature.

$$(Nu_\infty)_{c.t.} \mathrm{Presser} = 0.023 \left(\frac{\rho V D_e}{\mu} \right)^{0.8} \left(\frac{c_p \mu}{k} \right)^{0.4}$$

The concept of the hydraulic diameter is:

$$D_e \equiv \frac{4A_f}{P_w} \tag{5.4}$$

for the Re. A_f denotes the flow cross-sectional area and P_w denotes the wetted-perimeter.

$$D_e = \frac{4\left(6\frac{P^2\sqrt{3}}{4} - \frac{\pi D^2}{2} - \frac{\pi D^2}{4}\right)}{6\frac{\pi D}{3} + \pi D} = 10.6mm$$

where P is the pitch between fuel rods (across the triangular grid) with a value of 12.75 mm, and D is the outer diameter of the cladding which is 9.1 mm.

$$(Nu_\infty)_{c.t.}\text{Presser} = 0.023\left[\frac{(704)(10)(10.6\times10^{-3})}{8.69\times10^{-5}}\right]^{0.8}\left[\frac{(6270)8.69\times10^{-5}}{0.5}\right]^{0.4} = 1330$$

For the specific case of light water, Weisman gave:

$$(Nu_\infty)_{c.t.} = 0.023\,\text{Re}^{0.8}\,\text{Pr}^{0.333} \tag{5.5}$$

and

$$\psi = 1.130P/D - 0.2609 \tag{5.6}$$

$$(Nu_\infty)_{c.t.}Weisman = 1322$$

Then, the case is formulated as the evaluation of ψ. Presser proposed, for infinite arrays:

$$\psi = 0.9090 + 0.0783P/D - 0.1283e^{-2.4(P/D-1)} \tag{5.7}$$

for triangular array and $1.05 \le P/D \le 2.2$.

$$\psi\text{Presser} = 0.97$$

$$\psi\text{Weisman [Eqn. (5.6)]} = 1.32$$

$$Nu_\infty\text{Presser} = 0.97\times1330 = 1290$$

$$Nu_\infty\text{Weisman} = 1.32\times1322 = 1749$$

But,

$$Nu = \frac{hD_H}{k} \tag{5.8}$$

in which D_H and k stand for the hydraulic diameter and thermal conductivity, respectively.

$$D_H = \frac{4Af}{P_h} = D_e \tag{5.9}$$

$$\therefore h\text{Presser} = \frac{kNu}{D_H} = \frac{0.5(1290)}{10.6\times10^{-3}} = 60.8kW/m^2{}^\circ C$$

$$h\text{Weisman} = \frac{0.5(1749)}{10.6\times10^{-3}} = 82.5kW/m^2{}^\circ C$$

For light water at 1 m/s velocity

The Reynolds number is still in the turbulent region.

$$h\text{Presser} = (0.1)^{0.8}(60.8) = 9.6$$

$$h\text{Weisman} = (0.1)^{0.8}(82.5) = 13.1$$

In order to study the effect of velocity on thermohydraulic parameters such as heat transfer coefficient, two different liquid flow velocities were input which are 1 m/s and 10 m/s, respectively. Most realistic liquid flow velocities along rod bundles of similar reactor types are within this range (Zsíros et al., 2012; Böttcher, 2008; Rautaheimo et al., 1999). Fluid flow velocity along rod bundles is constraint to a maximum of 10 m/s in order to avoid cavitation. At that liquid flow velocity, the heat transfer coefficient of water was compared at mean coolant temperature of a VVER-1200 to the heat transfer coefficient of water at 1 m/s velocity by using two different correlations.

While comparing the effect of liquid flow velocity along rod bundles on heat transfer coefficient of water, both Presser and Weisman correlations were used. To sum up, at velocities from 1 to 10 m/s, the heat transfer coefficient values are given below in Table 5.1. In Figure 5.16, the values of heat transfer coefficient computed by Eqn. (5.7) with that by well-known correlations for heat transfer coefficients in rod bundles are compared (Presser, 1967; Weisman, 1959). It can be seen for hexagonal lattices. Figure 5.16 depicts that the coolant velocity profile starts from 1 m/s to 10 m/s. The coolant velocity goes up along the reactor core by means of the viscous effects on the flow. The mean hot leg velocity equals the cold leg velocity which is 3.25 m/s in the literature (Abdi et al., 2012). The curve obtained by the Weisman method is graphically easily distinguishable from the curve obtained by Presser method for Nu for a hexagonal lattice as seen in Figure 5.17.

Table 5.1 Heat transfer coefficient values for both Presser and Weisman correlations.

Velocity (m/s)	Presser	Weisman
10	60.8	82.5
9	55.9	75.8
8	50.9	69.0
7	45.7	62.0
6	40.4	54.8
5	34.9	47.4
4	29.2	39.6
3	23.2	31.5
2	16.8	22.8
1	9.6	13.1

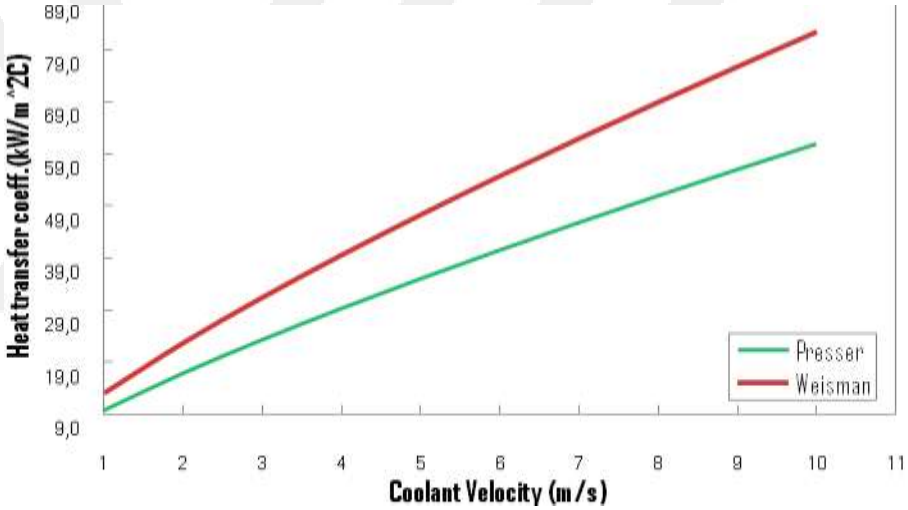

Figure 5.16 Heat-transfer coefficients at velocities from 1 to 10 m/s.

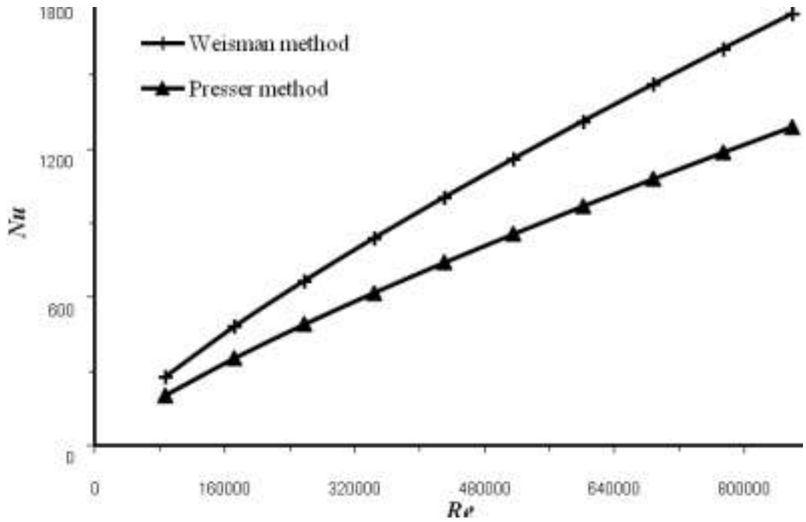

Figure 5.17 Nu number for hexagonal array of VVER, P/D=1.4 and Pr=1.1.

5.5 Single-Phase Pressure Drop

Based on the single-phase phenomena, the change in the physical characteristic of the fluid along the channel can be assumed as negligible. When the cross-sectional area of the fluid does not change vertically, the mass flux will be constant. Moreover, when density is constant, the acceleration pressure loss will be negligible. Therefore, the momentum equation can be given as below (Todreas and Kazimi, 2011).

$$p_{in} - p_{out} = +\frac{fG_m|G_m|}{2D_e\rho_l}(Z_{out} - Z_{in}) + \Delta p_{form} + \rho_l g(Z_{out} - Z_{in}) \qquad (5.10)$$

where p_{in} is the inlet pressure, p_{out} stands for the pressure at the exit, f stands for the friction factor, G_m stands for the mass flux, Z_{out} stands for the exit elevation and Z_{in} stands for the inlet elevation. For the VVER-1200, the pressure drop along the reactor core is calculated for the validation of results. Spacer grids, exit and inlet losses are ignored, thereby a bare rod fuel assembly is considered. The coolant is assumed to be spread uniformly throughout the core. Subcooled boiling is also ignored. Some of the dimensions for fuel assemblies are the rod pitch of 12.75 mm, fuel rod height of 4.57 m and the active fuel height of 3.75 m. Firstly in order to obtain the mass flux in unit of kg/m^2s (G_m), the cross-sectional area of the fluid (A_z) in each subchannel must be calculated.

$$A_z = 6\frac{P^2\sqrt{3}}{4} - \frac{\pi D^2}{2} - \frac{\pi D^2}{4} \tag{5.11}$$

$$G_m = \frac{\text{mass flow per subchannel}}{\text{flow area}} \tag{5.12}$$

The Reynolds number depends on the subchannel equivalent diameter (D_e) and it must be determined to obtain the friction factor, f. Thus,

$$\mathrm{Re} = \frac{G_m D_e}{\mu} \tag{5.13}$$

Using the friction factor correlations (Todreas and Kazimi, 2011);

$$f = 0.184(\mathrm{Re})^{-0.20} \tag{5.14}$$

The pressure drop through the reactor core is calculated accordingly as 51566 Pa. Transcendental equation of Eqn. (5.13) is utilized numerically to obtain f dependent on the Reynolds number and the pitch-to-diameter ratio for turbulent flow. A typical curve is depicted in Figure 5.18. We can observe that f decreases considerably with the Re.

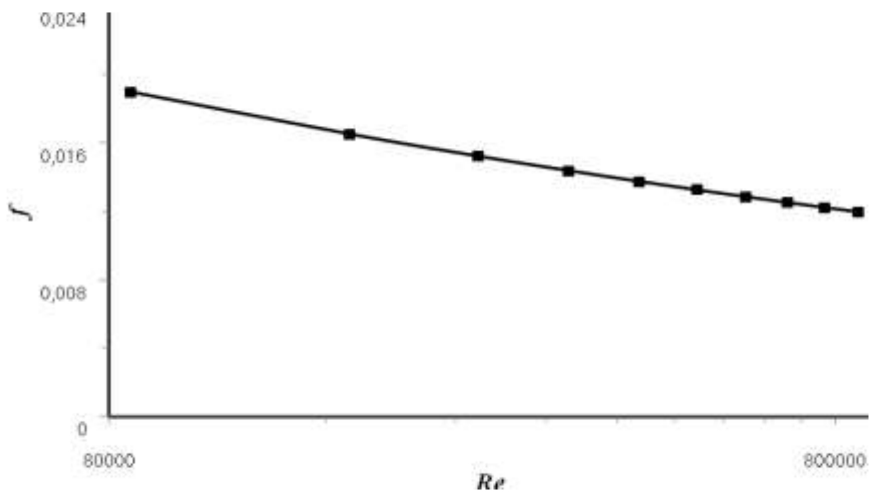

Figure 5.18 Friction factor, f for a hexagonal lattice, P/D=1.4.

5.6 Applied Model of Porous Medium

The porous medium model is an approximate technique as described in the FLUENT 17.2 User's Manual (2011). The fluid flow in porous media model is laminar in many cases. This is basically because of the fact that many fluid flows in porous media model have small velocities and hydraulic diameters. As a result, the standard k−ϵ or k−ω turbulent models are not suitable to be applied in porous media approach without modification. In porous medium approach, the computational domain containing both fluid and solid regions is assumed fluid region as a whole. To express the losses due to the porous media approach, a momentum source term is joined to the momentum equation. This momentum source term is;

$$S_i = -\sum_{j=1}^{3} D_{ij}\mu u_j - \sum_{j=1}^{3} C_{ij}\frac{\rho}{2}|u|u_j \tag{5.15}$$

The source term consists of 2 different parts. The first term is a viscous loss term, on the other hand the second term is an inertial loss term. For simple homogeneous porous media, the momentum source term may be decreased to

$$S_i = -\frac{\mu}{\alpha}u_i - C_2\frac{\rho}{2}|u|u_j \tag{5.16}$$

where C_2 stands for the square resistance coefficient and α denotes the permeability. The two coefficients are the diagonal elements of C and D when they are decreased to matrices. The negative momentum contributes to the pressure drop that is proportional to the inlet velocity of the flow. The relationship between the pressure drop and the momentum source term is utilized in order to compute the inertial and viscous loss coefficients for the fuel assemblies:

$$\Delta p = -S_i \Delta n \tag{5.17}$$

where Δn denotes the thickness of the medium. The channels have small cross-sectional area as Figure 4.3c depicts, which permit only limited motion in the radial direction compared to the longitudinal direction. Thereby, the radial resistance coefficient is set as 100 times greater than the longitudinal resistance coefficient to block the radial flow.

5.7 Inlet and Outlet Boundary Conditions

5.7.1 Boundary Conditions for Symmetric and Asymmetric Inlet Cases

The water coolant is considered as incompressible. The BCs are set as mass flow inlet and pressure outlet. For the asymmetric case in which a reactor coolant pump stops working, one of the inlet nozzles is set to be mass flow inlet in the outlet boundary and negative velocity inlet in the inlet boundary. The reason is that the flow in the failed loop will come back inside from the hot leg when the RCP in the corresponding loop fails. There is no prescribed velocity profile. The temperature BC for all of the inlets for the symmetric (full-loop) case is 298.2 °C, while for the asymmetric case they are 295.2 °C. The flow rate BC for all of the inlets for the symmetric case is 4750 kg/s. However, for the asymmetric (one RCP fails) analysis, the failed loop possesses a flow rate BC of -1833 kg/s and the rest of the loops possess 4861.4 kg/s (Cheng et al., 2016). The pressure BC for all of the exits are set to be 16.2 MPa for symmetric analysis, only with an exceptional case of the failed loop is assumed to have velocity inlet BC of 4.5 m/s for the asymmetric (three-loop) analysis.

Turbulent viscosity ratio is defined as the ratio of turbulent viscosity to dynamic viscosity and is directly proportional to the turbulent Reynolds number. For internal flows, the turbulent intensity at the inlets is totally dependent on the upstream history of the flow. If the flow is fully developed as in the analysis, the turbulent intensity can be as high as a few percent. The turbulent intensity may be estimated from an empirical correlation for pipe flows:

$$I = 0.16\,\mathrm{Re}^{-1/8} \tag{5.18}$$

At a Reynolds number of 252,339 in the analysis, the turbulent intensity will be 3.4%, according to this formula. The inlet turbulence parameters are applied to be the nearest turbulence intensity value of 5% and a viscosity ratio value of 10. FLUENT uses these constant estimated magnitudes for the inlet BCs for turbulent intensity and viscosity ratio. All structures and wall surfaces are applied as adiabatic and with no-slip condition. Those BCs are written below in Table 5.2.

Table 5.2 Boundary conditions for symmetric and asymmetric inlet cases

Inlet mass flow rate (kg/s)		
Three loops	Four loops	Loop number
-1833.0	4750	1
4861.4	4750	2
4861.4	4750	3
4861.4	4750	4
Inlet temperature (K)		
Three loops	Four loops	Loop number
568.2	571.2	1
568.2	571.2	2
568.2	571.2	3
568.2	571.2	4
Outlet pressure (MPa)		
Three loops	Four loops	Loop number
V = 4.5 m/s	16.2	1
16.2	16.2	2
16.2	16.2	3
16.2	16.2	4

5.7.2 Boundary Conditions for LOCA Case

Computational fluid dynamics analyses are performed with a 2-phase volume-of-fluid model having formulation of sharp interface. Turbulence flow is modeled using standard k-ε. Large-break loss-of-coolant accident in one of the four hot legs of a VVER-1200 is simulated. In the LOCA scenario studied, one of four reactor coolant pumps trip off at start and an emergency shutdown of the nuclear reactor occurs because of the low-pressure signal in the RPV. According to the LBLOCA case considered here, the RPV depressurizes rapidly and the overall water inventory in the RPV evaporates suddenly. Thereby, at the beginning of the analysis, the RPV contains only steam. When the safety injection pumps are initiated, they inject cold water into all cold legs with high mass flow rates. ECCS initiates the safety injection pumps to inject water into all cold legs at 20°C. The mass flow rates of ECCS injection are assumed to be 1000 kg/s through the inlets.

When the pressure in the primary side is remarkably low, the thermal stresses are more severe than the pressure stresses. The volume-of-fluid model is applied for the interface between steam and liquid water. During the simulation, main steam valves are assumed to keep closed, thereby isolating the steam generators from the domain. Simulations for the LOCA part are performed with a two-phase volume-of-fluid (VOF) model with sharp interface formulation.

The initial and BCs for LOCA are tabulated in Table 5.3. The simulation initiates with the RPV occupied by steam at saturation temperature of 558 K.

Table 5.3 Boundary conditions for LOCA case

Initial pressure [MPa]	6.9
Initial temperature [K]	558
Vapor volume fraction [dimensionless]	1
Cold legs, inlet boundary condition	400 kg/s mass flow inlet
Hot legs, outlet boundary condition	Pressure outlet
Walls, BC	No heat flux
Injection temperature [K]	293.15 (20°C)

5.8 FAVOR Analysis

To assess structural integrity of RPVs subjected to PTS transient, both deterministic and probabilistic fracture mechanics (PFM) analyses are performed. While deterministic analysis can ensure RPV integrity, it can be extremely conservative. Probabilistic analysis provides a more realistic evaluation of the vessel condition and the corresponding safety level. By setting limits on the allowable probability of failure, reactor vessel integrity is ensured. In USA, the probabilistic analyses are accepted to justify the safe operation of the RPV, whereas the deterministic analysis dominates in European countries. However, in the last few years, probabilistic methods for the assessment of RPV are widely discussed within Europe and several research projects were initiated.

From the years of 1980s, several codes have been developed in order to carry on the probabilistic analysis of reactor pressure vessels, like VISA-II, OPERA, FAVOR (Williams et al., 2004; Dickson and Malik, 2001) and PASCAL. FAVOR is one of the commonly utilized among all aforementioned codes. It was developed by Oak Ridge National Laboratory in the United States.

The reactor vessels are subjected to neutron fluence at high temperatures that leads to embrittlement in the carbon steel material of the vessel. One of the important potential risks for the structural integrity of the reactor vessel in a PWR is due to the PTS events such as LOCA. Hence, the integrity of the reactor vessel with regard to neutron fluence has to be investigated. In this thesis, the methodology and procedure for the safety analysis of the vessel exposed to pressurized thermal shock are given. FAVOR, as a widely common tool for the probabilistic analysis of reactor vessel exposed to pressurized thermal shock, is utilized.

5.8.1 Physical Model

The reactor vessel is reduced into a basic 2D physical model including only the material and dimension properties of the reactor vessel for the numerical analysis. The numerical analysis focuses on the beltline region of the reactor vessel, around which the neutron embrittlement is the greatest. The internal wall of the reactor vessel is exposed to a PTS due to the flow of ECCS. The reactor vessel is approximated by an axisymmetric 2D physical model that allows the calculation of tangential and longitudinal stresses as a function of time-dependent temperature distribution. Initially, the temperature behavior is calculated through the thickness of the vessel wall. The input deck which includes the coolant temperature, pressure, and coefficient of heat transfer between internal vessel surface and coolant is taken from the results of CFD code FLUENT. Then, the longitudinal and tangential stress histories for the transient are calculated via FAVOR.

FAVOR analysis focuses on the beltline region of the RPV, which is subjected to the maximum neutron fluence. But the inlet and outlet nozzles' region is exposed to higher stresses because of the cold water from ECCS and because of the discontinuity in the intersected geometry of hot and cold legs and RPV. The structural integrity of inlet and outlet nozzles region is not taken into account in FAVOR. The internal vessel wall is exposed to PTS due to the downward flow of

ECCS injection. This downward flow is not uniform but visually in a plume form coming from the cold legs. However, the thermal load is assumed to be axisymmetric and uniform along the longitudinal direction. In reality plastic deformation can take place at the internal vessel wall. However, the plasticity effects are eliminated in FAVOR while performing a brittle fracture mechanics analysis.

5.8.2 Generating the Input Deck for FAVOR

In this thesis, VVER-1200 reactor vessel with an internal radius of 2116 mm, vessel wall thickness of 197.5 mm with a cladding thickness of 9 mm was analyzed. The thermal-structural properties of the cladding and base metal materials at different temperatures and the stress-free temperature are tabulated in Table 5.4. The water temperature, pressure and heat transfer coefficient of water-RPV values considered in the analysis is depicted in Figure 5.19.

Table 5.4 Elastic and thermal characteristic properties of VVER–1200 RPV base metal and cladding materials (IAEA, 2006)

Material	T	E	α	α_0	ν	λ	c_p	ρ
	[°C]	[10^3 MPa]	[10^{-6} K^{-1}]	[10^{-6} K^{-1}]	[1]	[Wm^{-1}K^{-1}]	[Jkg^{-1}K^{-1}]	[kgm^{-3}]
Base material or weld	20	208		12.5	0.3	35.0	446.9	7830
	50				0.3	35.5	458.9	7822
	100	201	11.6	12.9	0.3	36.1	478.8	7809
	150				0.3	36.6	499.7	7795
	200	193	12.0	13.6	0.3	36.8	520.4	7780
	250				0.3	36.6	541.2	7765
	300	183	12.6	14.2	0.3	36.2	562.0	7750
	350	177.5			0.3	35.6	584.6	7733
Cladding	20	165		16.6	0.3	13.2	448.9	7900
	50				0.3	13.5	460.4	7889
	100	160	15.7	17.0	0.3	14.4	479.6	7870
	150				0.3	15.3	499.6	7851
	200	153	16.1	17.6	0.3	16.4	519.2	7830
	250				0.3	17.5	538.7	7809
	300	146	16.7	18.2	0.3	18.4	558.5	7788
	350	142			0.3	19.6	579.2	7766

* Stress free temperature (equal to the normal operational temperature) for recalculation of α_0 is 290°C.

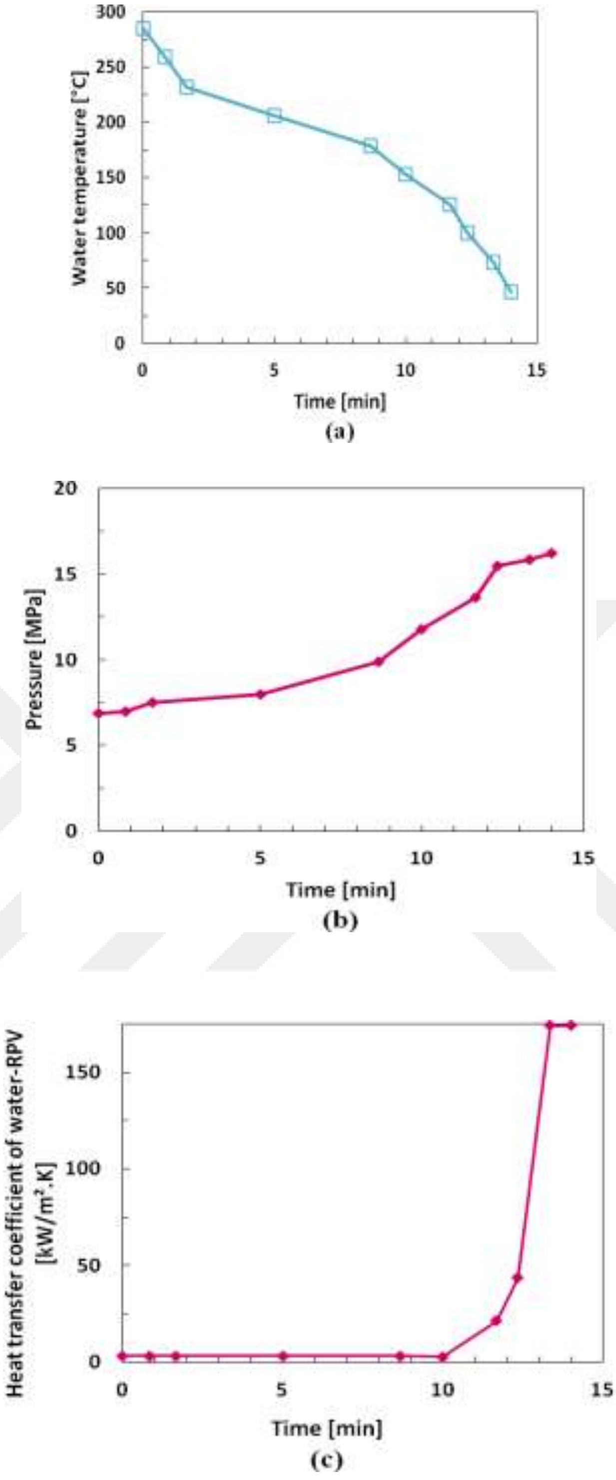

Figure 5.19 Transient histories in FAVOR (a) water temperature, (b) pressure and (c) heat transfer coefficient between water and vessel

CHAPTER VI

RESULTS AND DISCUSSION

6.1 Introduction

Prior to the transient LOCA calculations, the steady-state simulations with symmetric and asymmetric inlet boundary conditions were performed. The parallel calculation of steady-state simulation took 5 h of computation time. The temperature at the four outlets, the pressure at several points in the domain, the mass flow rate of water at the inlets, and the velocity of water at some vertical cross-sections were investigated. If those values remain approximately the same and the residuals of each quantity are less than 0.001, the solution will be assumed to reach the convergence criteria.

LBLOCA simulations provide the 3D results of the two-phase flow. The parallel calculation of transient LOCA simulation took approximately 5 days of computation time. Temperature within the inner reactor vessel wall is emphasized, however the vapor volume fraction analysis is provided to capture all mixing details in four cold legs and along the downcomer. The analyses results were investigated with CFD-Post and given below.

6.2 Results of Steady-State Symmetric and Asymmetric Inlet Cases

6.2.1 Temperature Fields

The temperature behaviors in several vertical and horizontal cross-sections for both symmetric and asymmetric boundary conditions are presented in Figure 6.1. The temperature of water is increased after it passes through the reactor core and the greatest temperature amounts 649.51 K around the top of the reactor core for symmetric inlet boundary conditions. Normally, the temperature keeps reducing gradually between the top of the core and the upper plenum as shown in Figure 6.1.

There is not much difference between the hot leg temperatures for symmetric case. However, there are remarkable differences between them for the asymmetric case as shown in Figure 6.2. For the asymmetric case, there is also some reversed flow noticed, which is not heated but directly flows into the failed loop. That is why the temperature in the hot leg of the failed loop is the lowest one. That reversed coolant leads to some confusion in the temperature distribution around the perforated walls of the core barrel. It is obvious that the temperature behavior at the closest two exits near the failed exit are also affected, particularly the closer hot leg which is the closest one in counterclockwise direction as shown in Figure 6.3. Figure 6.3 depicts the temperature contour on the horizontal plane including parts of the connecting hot and cold legs. The temperature distribution asymmetries are clear on this horizontal plane. The temperature contour depicts that the temperature variation is high in the nozzles' elevation in the RPV. The rise in the coolant temperature is nearly 35 K in the hot legs for the case of symmetric (full loop) BCs. The flowrate-averaged temperature at vessel outlet is somewhere between 576.6 K and 606.3 K for symmetric (full loop) case. The designed outlet temperature is 601.9 K for the VVER-1200 type of nuclear reactors. This is another criterion for validation of results of the analyses.

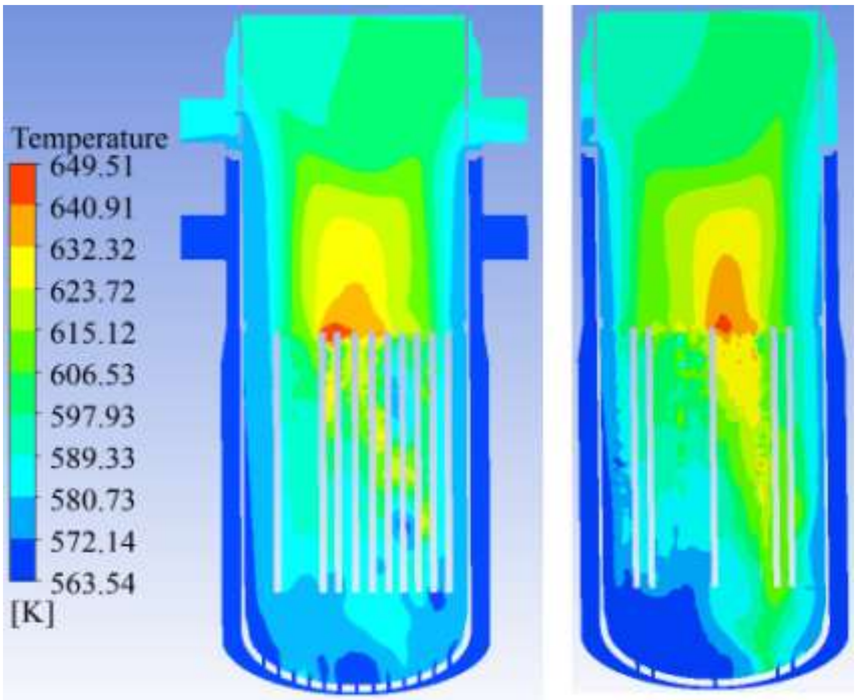

Figure 6.1 The temperature behaviors for two different vertical cross-sections 90° apart for symmetric case.

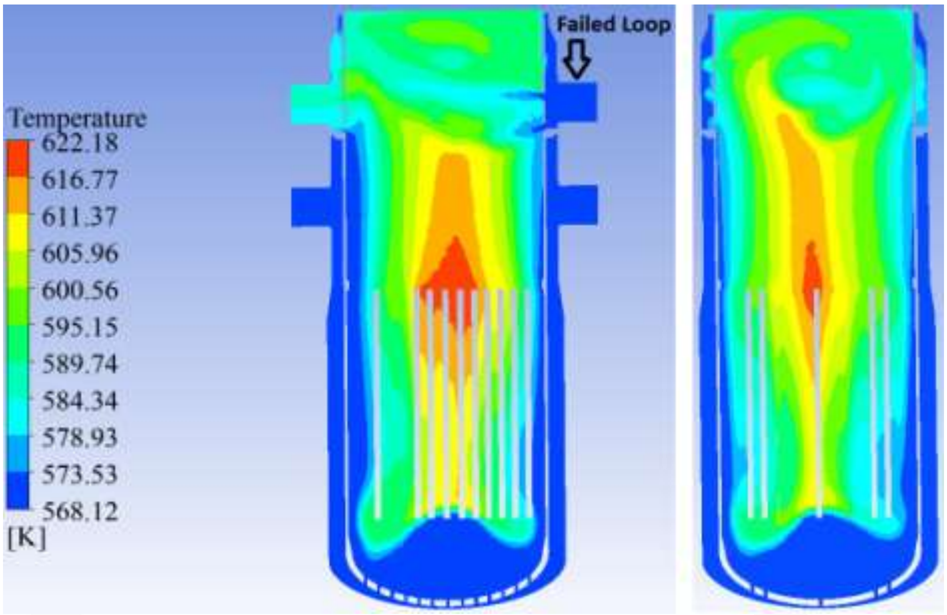

Figure 6.2 The temperature distributions for two different vertical cross-sections 90° apart for asymmetric (three-loop) case.

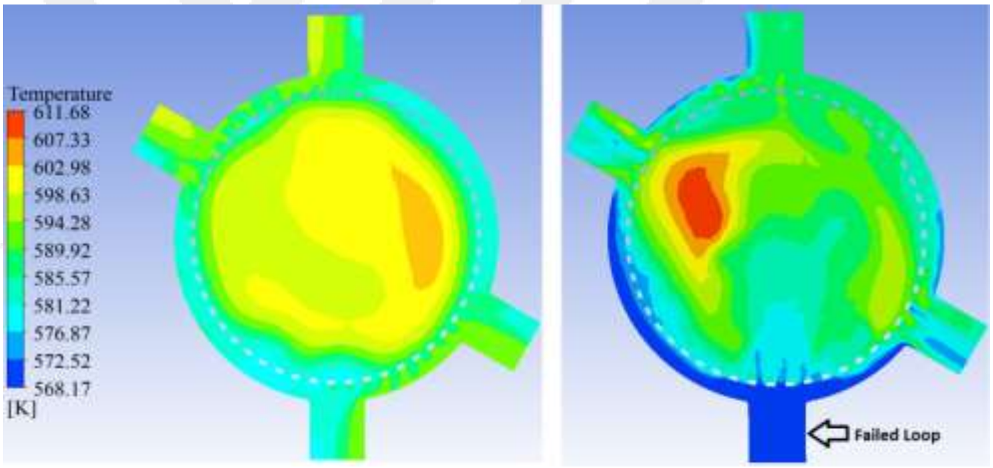

Figure 6.3 The temperature behaviors for horizontal cross-section including four hot legs.

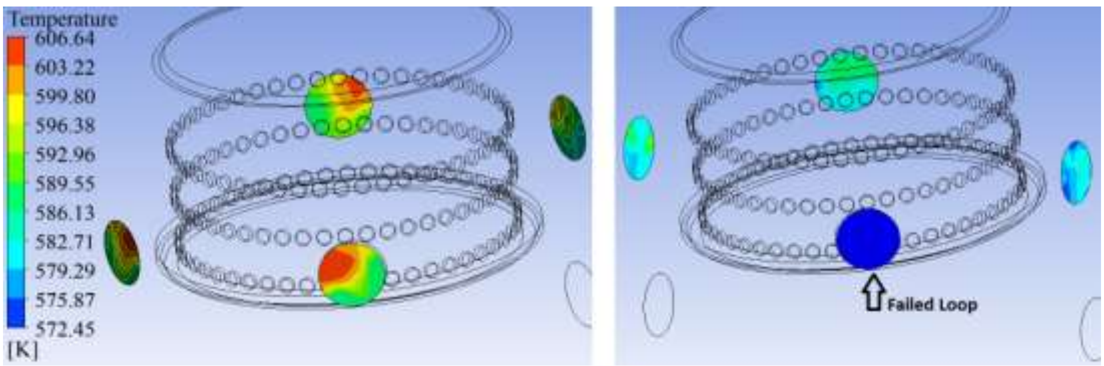

Figure 6.4 The hot leg temperatures for symmetric (left) and asymmetric (right) inlet boundary conditions.

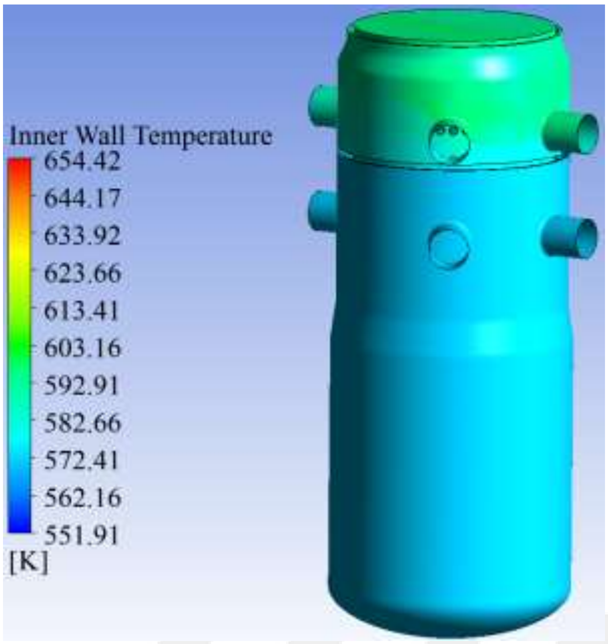

Figure 6.5 The inner wall temperature for symmetric inlet boundary conditions.

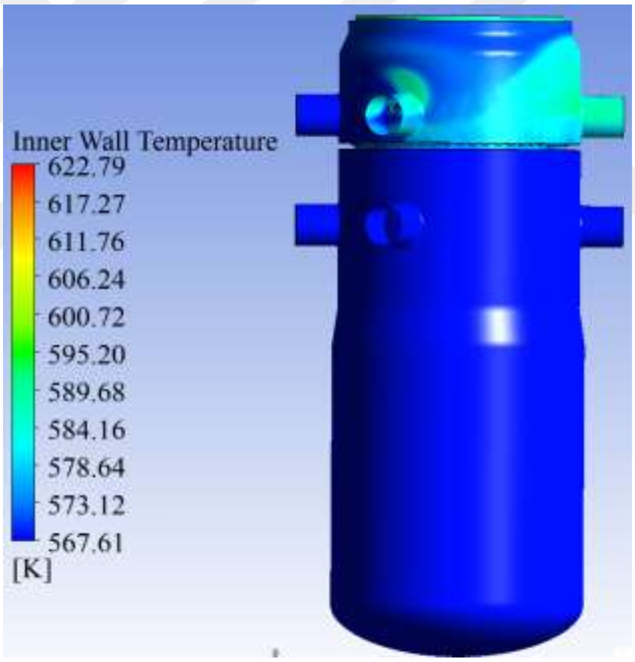

Figure 6.6 The inner wall temperature for asymmetric inlet boundary conditions.

Figure 6.7 and 6.8 illustrate the temperature streamlines inside the RPV through the VVER-1200 nuclear reactor core. Temperature reaches the maximum value before it leaves the fuel assemblies as seen in the corresponding figures.

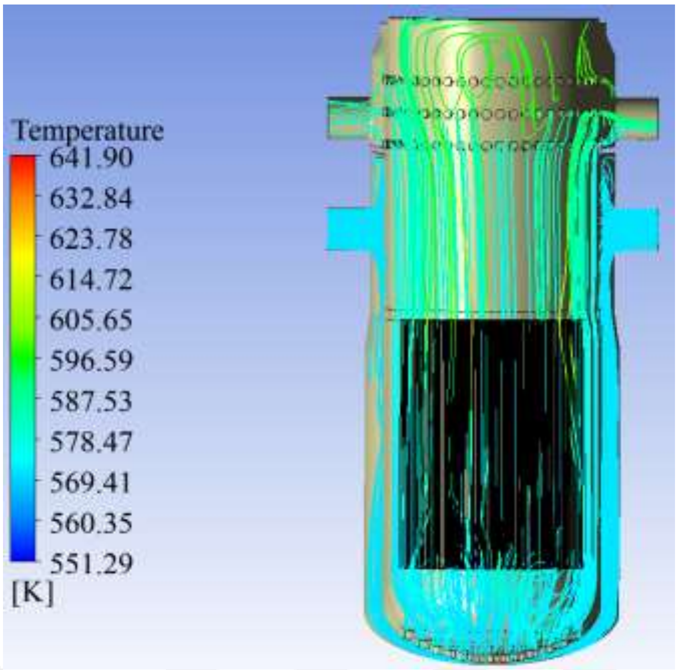

Figure 6.7 The temperature streamlines through the whole fluid domain for full-loop operational conditions.

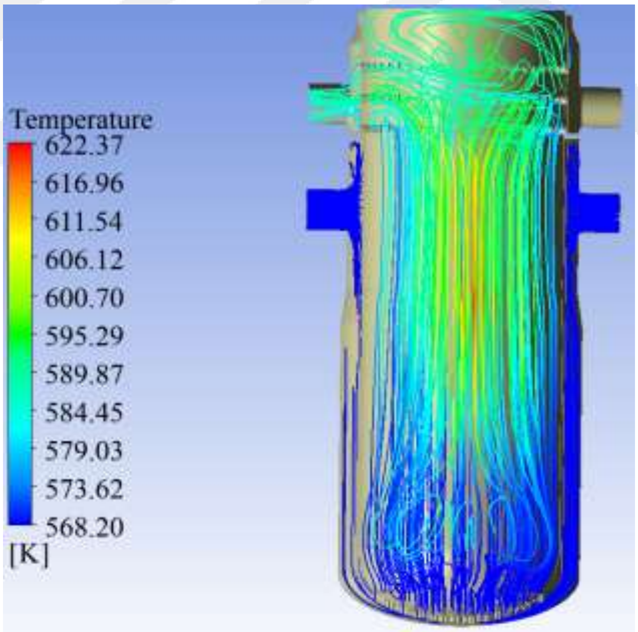

Figure 6.8 The temperature streamlines through the whole fluid domain for asymmetric operational conditions.

Figure 6.9 and 6.10 are the temperature results including both the vessel wall and the reactor core clipped on a vertical cross-section passing through the centerlines of the cold and hot legs for symmetric and asymmetric operational conditions, respectively. The maximum power density, thus, the maximum temperature is located at the geometric center of the nuclear reactor core.

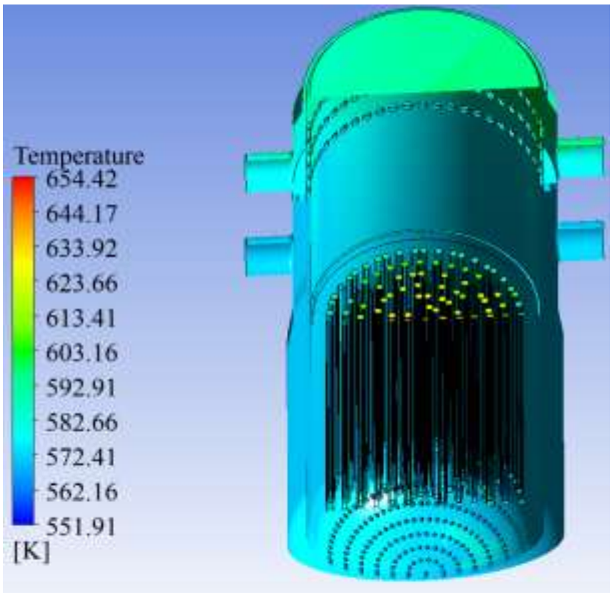

Figure 6.9 Temperature distributions in the reactor core and RPV wall for normal operational conditions.

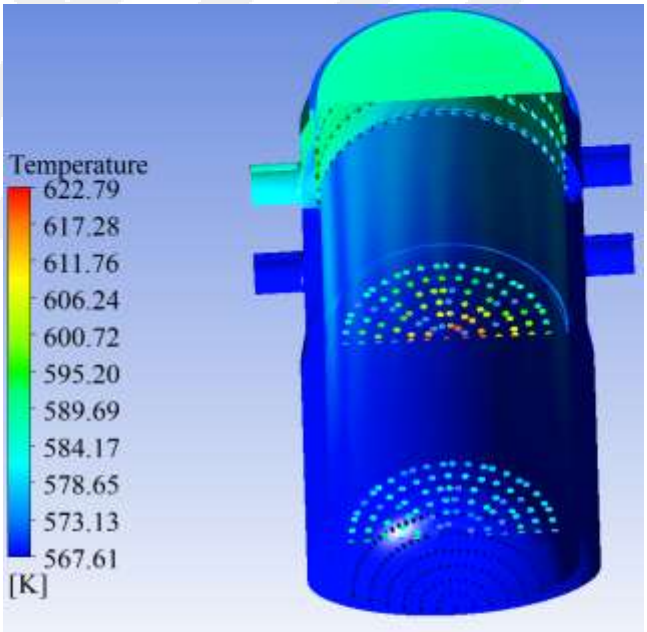

Figure 6.10 Temperature distributions in the reactor core and RPV wall for asymmetric operational conditions.

6.2.2 Velocity Fields

The velocity distributions in the domain consisting of all inlet and outlet nozzles for both the symmetric (full-loop) and asymmetric (three-loop) inlet BCs are depicted in Figure 6.11. It is clearly noticed the fluid flow from all cold legs occupies the region between the core barrel and the elliptical reactor vessel bottom. Figure 6.11

illustrates the fluid path lines in the region of the perforated core barrel bottom, where the fluid is passing through in order to decrease the effect of sector formation in the reactor core. It may be noticed the fluid flow in the downcomer is not totally uniform. In addition, there are not any recirculation vortices seen. The path lines that go directly into the downcomer region after coming from the cold legs move around the inner circumference of the RPV. There is obviously not much coolant flowing vertically down the downcomer in the region below cold legs. Figure 6.11 depicts flow path lines expressing the velocity distribution in the lower plenum and downcomer for symmetric and asymmetric BC cases calculated with FLUENT 17.2. Because of the strongly momentum-driven flow at the cold leg nozzles, the horizontal part of the flow dominates in the downcomer. The injection is distributed into two main streams forming the so-called butterfly distribution. Meanwhile, several secondary flows are obvious in various parts of the downcomer. Particularly strong vortices exist in the regions below the failed loop nozzles.

The fluid flow in the exit of the failed loop is roughly horizontal for the asymmetric (three-loop) inlet conditions applied. However, the fluid flows in the remaining three outlets are relatively homogeneous. Because the coolant flow changes direction when arriving at the lower plenum and then passing through the holes of the perforated core barrel bottom, there are some vortices noticed there and also around the fuel assemblies. In addition to these, there are some vortices around the perforated side walls of the core barrel, up in the elevation of hot legs. The vortices there, might occur because of the holes located in the core barrel wall and the hole of the hot leg are not exactly coincide to each other in location and diameter.

The coolant path lines starting from the exit of the failed loop and ending at the inlet of the failed loop are shown in Figure 6.12. The coolant streamlines in Figure 6.12 are colored by temperature magnitude. The coolant flow starting from the exit of the failed loop leaves from the other three exits directly. The coolant that leaves through the closer exit to the failed loop is much more in mass flow rate as anticipated. The same situation is available for the inlet of the failed loop. The fluid flow starting from three inlets leaves the vessel through the inlet of the failed loop, more mass flow rate of water comes from the closer inlet to the failed loop. Many vortices generate at the inlet of the failed loop.

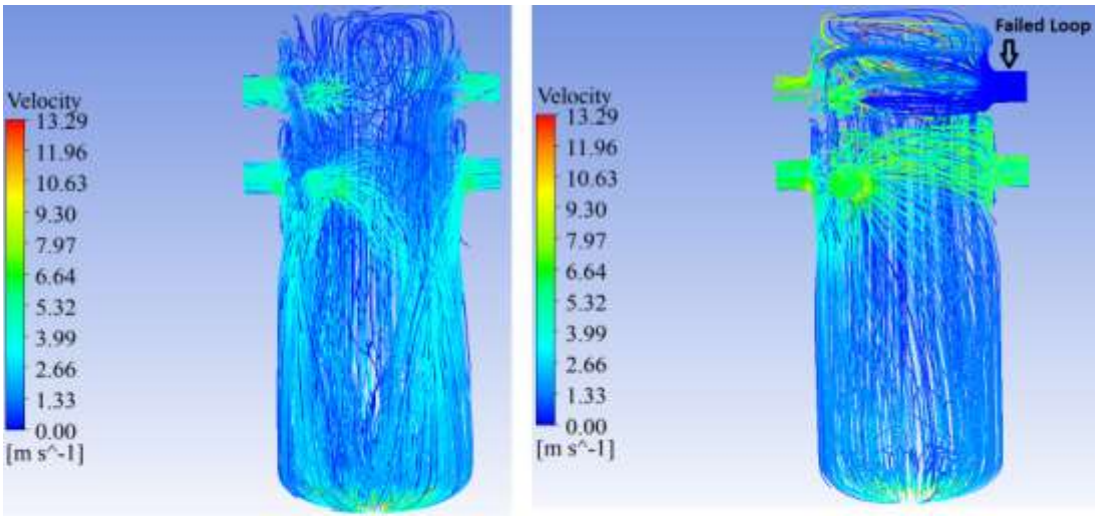

Figure 6.11 The velocity streamlines forming the butterfly distribution for both full-loop (left) and three-loop (right) cases.

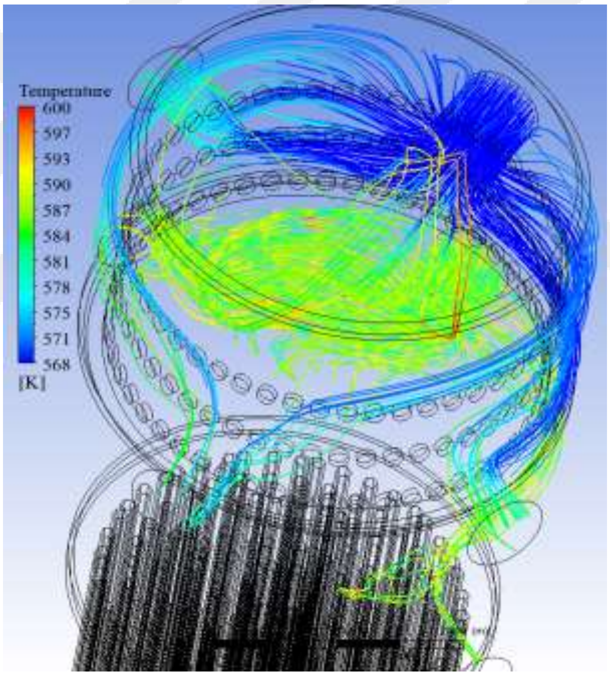

Figure 6.12 The temperature streamlines entering from outlet of the failed loop and exiting to inlet of failed loop.

The water coolant velocity behavior in the VVER-1200 lower plenum of the VVER-1200 with a great magnification is shown in Figure 6.13 for symmetric (three-loop) case and in Figure 6.14 for asymmetric (full-loop) case. The flow streamlines in these figures are colored by velocity value. Swirls can be seen in the velocity streamlines. Amount of swirling can be deduced from the color of velocity streamlines.

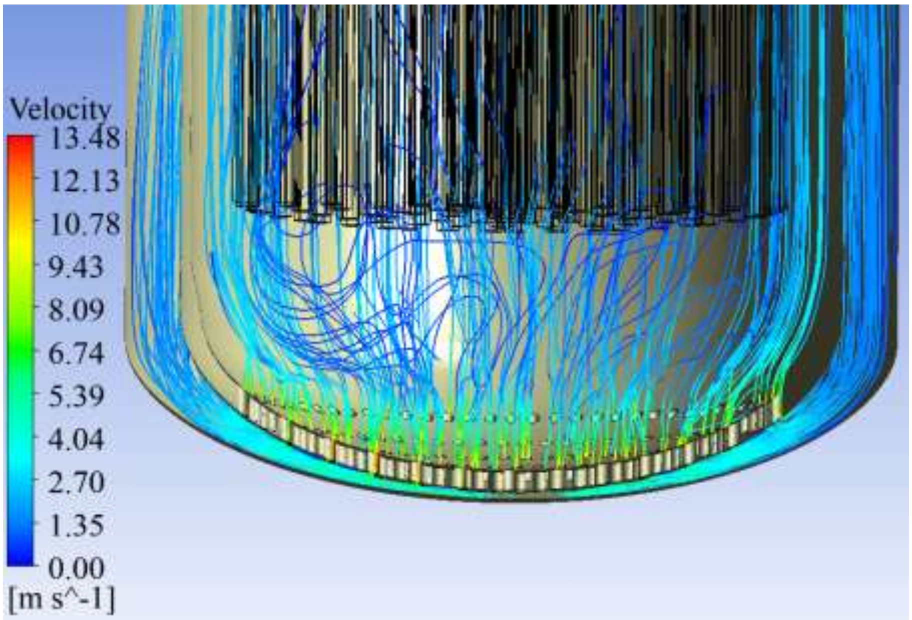

Figure 6.13 Water coolant velocity streamlines in lower plenum for symmetric (three-loop) case.

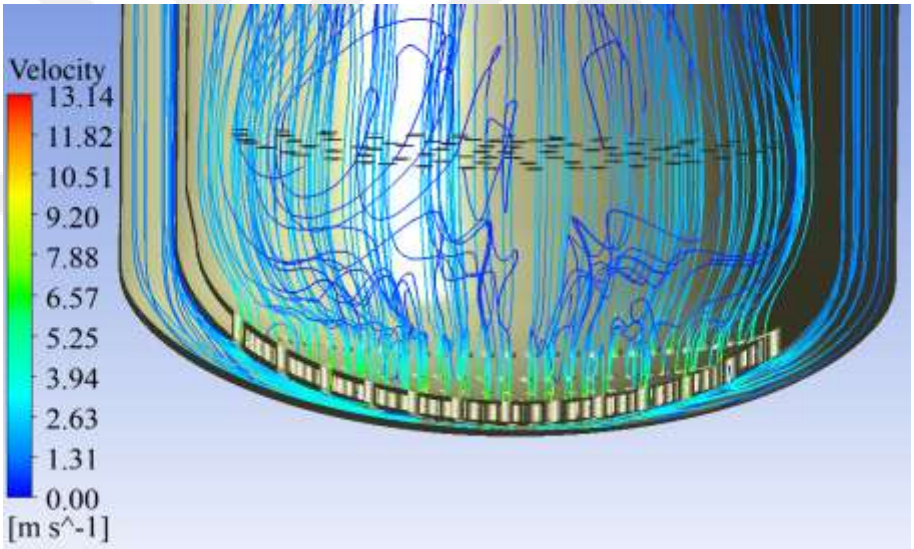

Figure 6.14 Water coolant velocity streamlines in lower plenum for asymmetric (full-loop) case.

From these figures above, one can see the difference in greatest values of the coolant velocity in both cases investigated in the lower plenum zone, which represents between the downcomer and the perforated elliptic core barrel bottom. The water coolant velocity can reach up to 13.5 m/s. The maximum velocity of the water is located near the outlet parts of the investigated zone.

6.2.3 The Pressures at Several Points in the Domain

The pressure drop in a nuclear reactor mostly comes from the frictional resistance acting on the vessel wall and the shape resistance caused by the changes of flow channels. Hence, mostly the pressure gradient when the water passes through these channels contributes to the pressure drop. The selected pressure-reading points were set at different positions to evaluate the pressure of each section as shown in Figure 6.15. Those pressure values were read at both symmetric and asymmetric operating conditions. The pressure-read points were selected at the core inlet and outlet to ensure the pressure drop validates the analytical data. As calculated in Section 5.4, the pressure drop through the VVER-1200 nuclear reactor core is nearly 52 kPa under normal operational conditions. Based on those results obtained, it states that the pressure drop gained by the analyses can be described as the reliability of the established CFD technique.

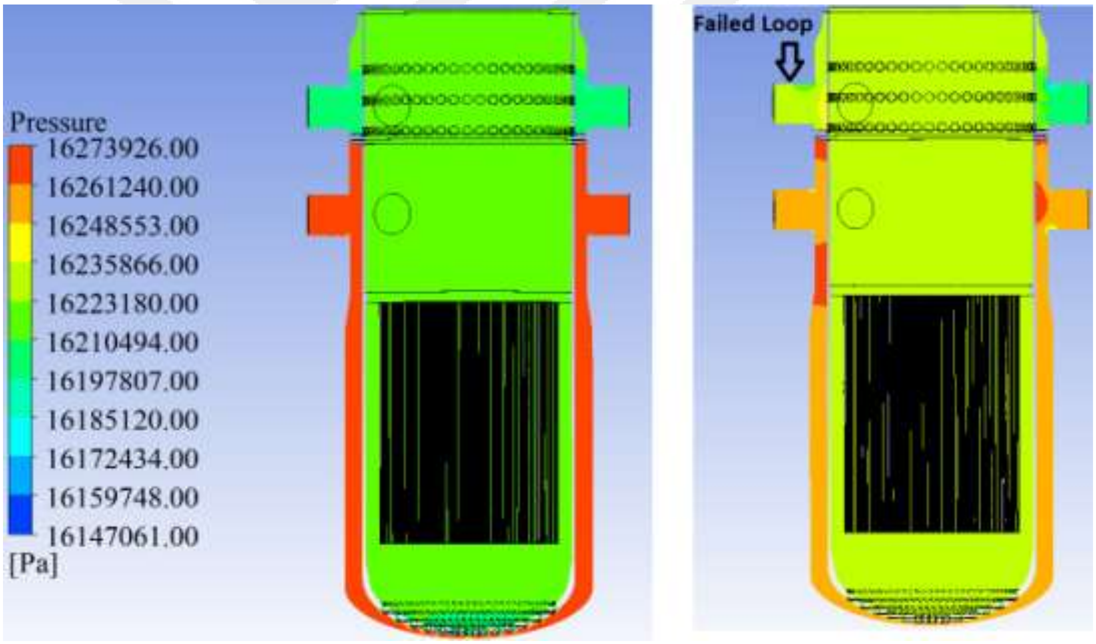

Figure 6.15 Pressure contours for the vertical cross-section including cold and hot legs

Figure 6.16 and Figure 6.17 show the pressure behaviors of RPV looking outside the fluid domain for symmetric (full-loop) and asymmetric (three-loop) inlet conditions cases.

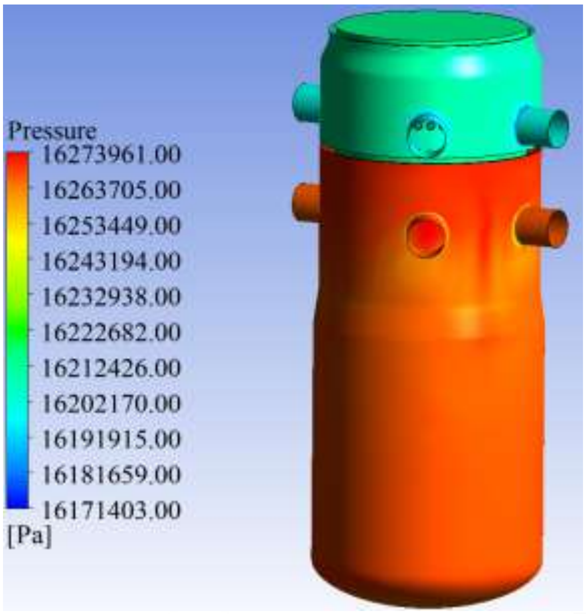

Figure 6.16 Pressure values for the VVER-1200 RPV looking outside the fluid domain for symmetric case.

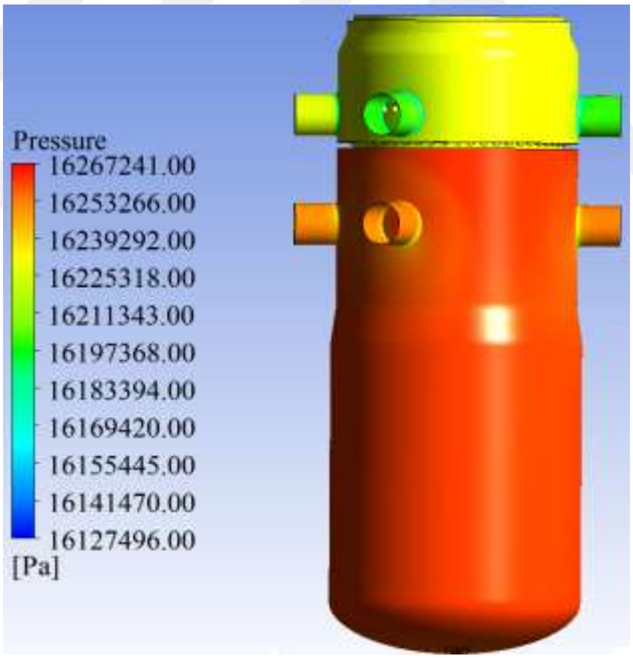

Figure 6.17 Pressure values for the VVER-1200 RPV looking outside the fluid domain for asymmetric (three-loop) case.

6.2.4 Mass Flow Rate Distribution throughout the Core

For most fuel assemblies, the entering mass flow rates possess an axisymmetrical uniform distribution in the reactor core, which is in agreement with the practical flow rate distribution for the case of symmetric boundary conditions. This consequence indicates the accuracy of the technique used in the analysis. On the other hand, for asymmetric (three-loop) inlet conditions, the mass flow rates throughout 163 fuel assemblies do not possess a uniform distribution compared with the symmetric-operating-condition case. The central region closer to the failed loop is lower than other three loops. It obviously shows that the flow rate behavior at the reactor core entrance has been significantly affected by the fail of one loop.

6.3 Results of LOCA Case

A hypothetical LBLOCA is supposed in an outlet nozzle pipe for a four-loop VVER-1200. The obtained results from the simulations are compared with the benchmark data of outlet temperature of VVER-1200 for symmetric normal operating conditions before, in Section 6.2.1.

6.3.1 Cold Leg and Downcomer Behavior

The most critical situations for LBLOCA occur once 20ºC ECCS coolant is added into the cold legs, which are initially covered by hot steam. The ECCS injection stream will continue to the downcomer and decrease the temperature of the vessel surfaces resulting in high thermal gradients.

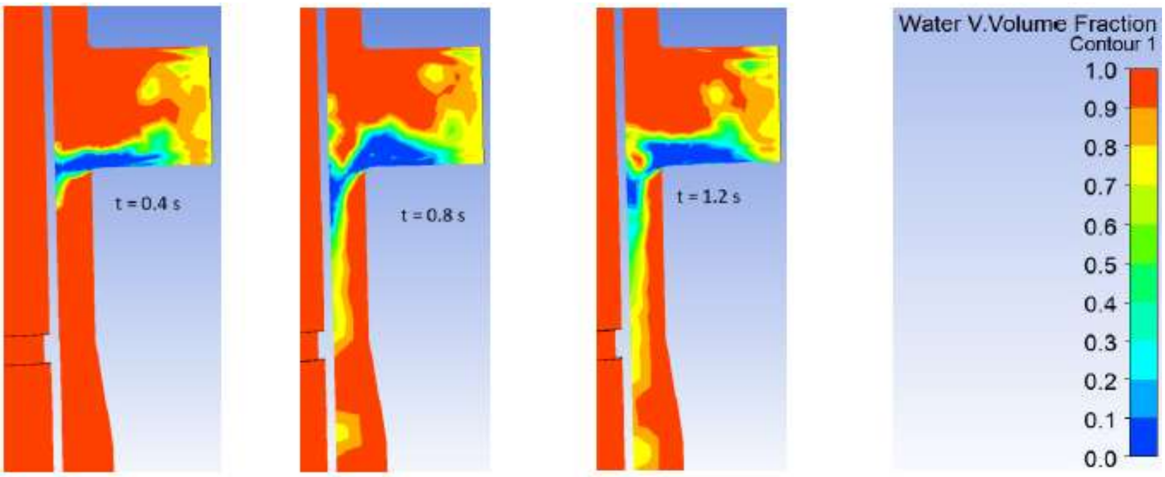

Figure 6.18 Vapor volume fractions at the beginning of the emergency core cooling system injection.

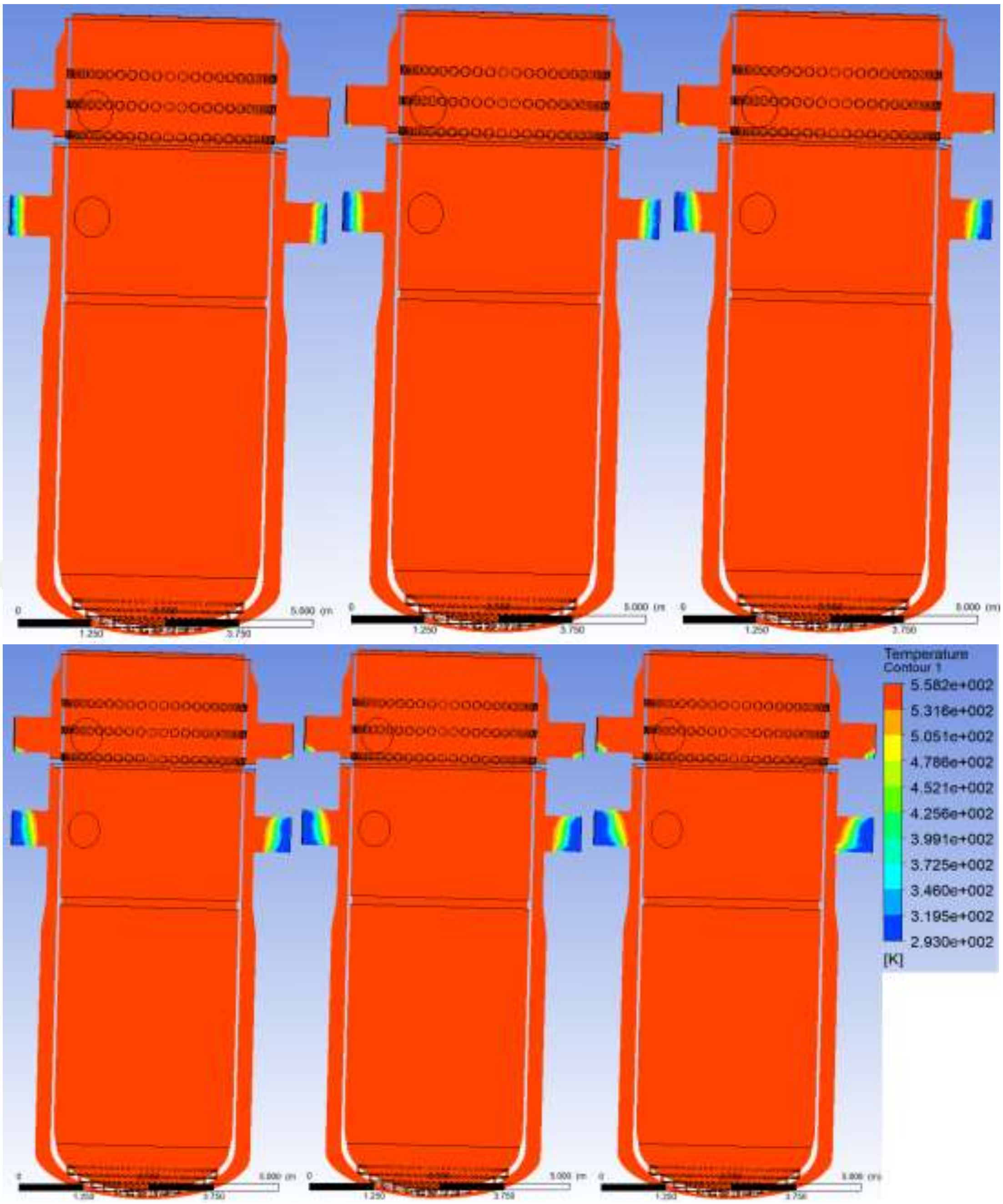

Figure 6.19 Temperature distributions at the beginning of the emergency core cooling system injection.

6.3.2 Whole Vessel Behavior

The temperature in the whole vessel wall varies between 293 K and 558 K. 293 K represents the temperature of the ECCS water injected, while 558 K represents the saturation temperature of steam at 6.9 MPa pressure at initial BCs. The grown temperature gradients become more important with time (Figure 6.19). In the first times of ECCS, when the amount of coolant in the reactor vessel is small, the added coolant flows by touching the inner reactor vessel surface. Consequently, only small temperature gradients occur in the top region of the downcomer. A few seconds later, due to the raised mass flow rate of ECCS injection, detachment from the internal RPV surface occurs. Subsequently, development of the cooling plume in the RPV wall begins as the amount of ECCS injection raises.

Initially, it affects temperatures only along the height of the downcomer. Two regions with serious temperature gradients are formed. These are below the inlet nozzles and at the bottom of the downcomer. However, a few seconds later safety injections from both loops start to interfere at the bottom of the downcomer and from that time, the flow of the cooling plume in all directions occurs. Consequently, an extra region with large temperature gradients located in the middle of the reactor vessel and below the inlet nozzle connection, forms.

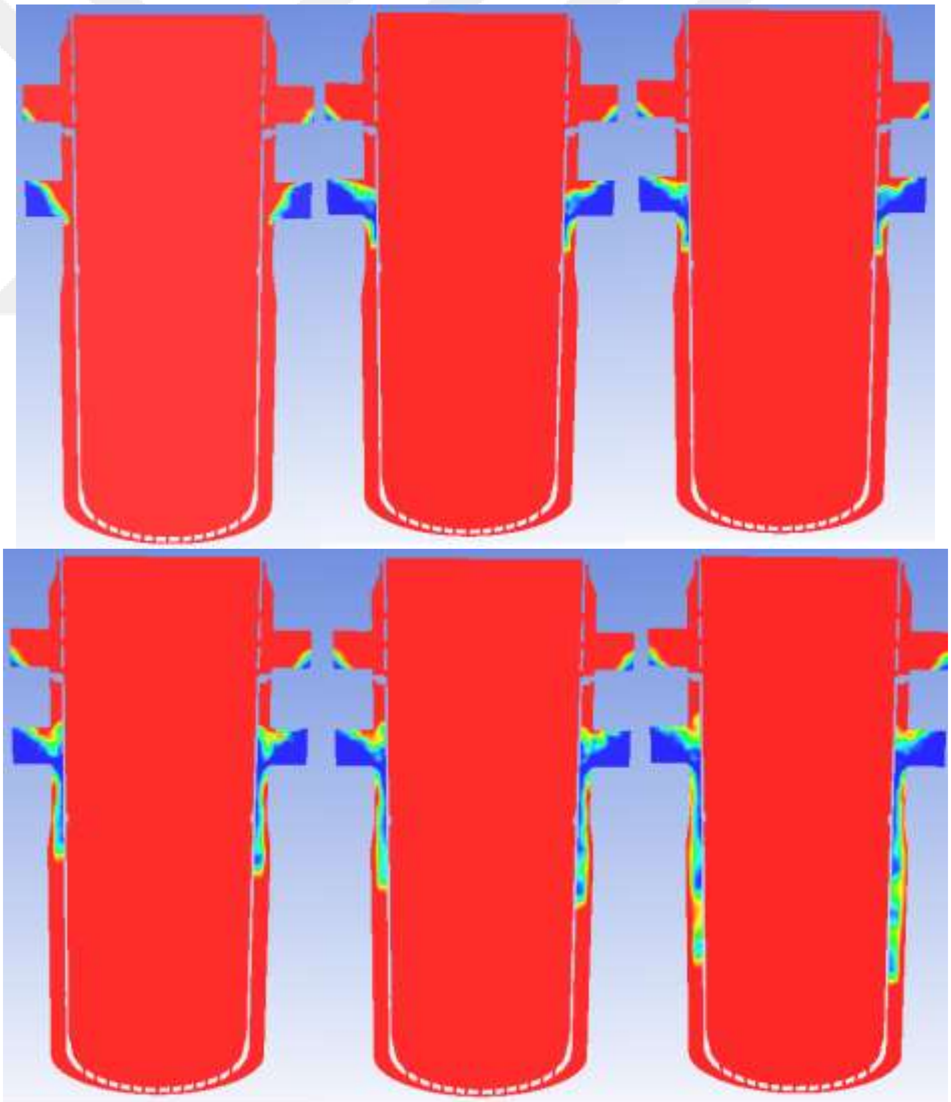

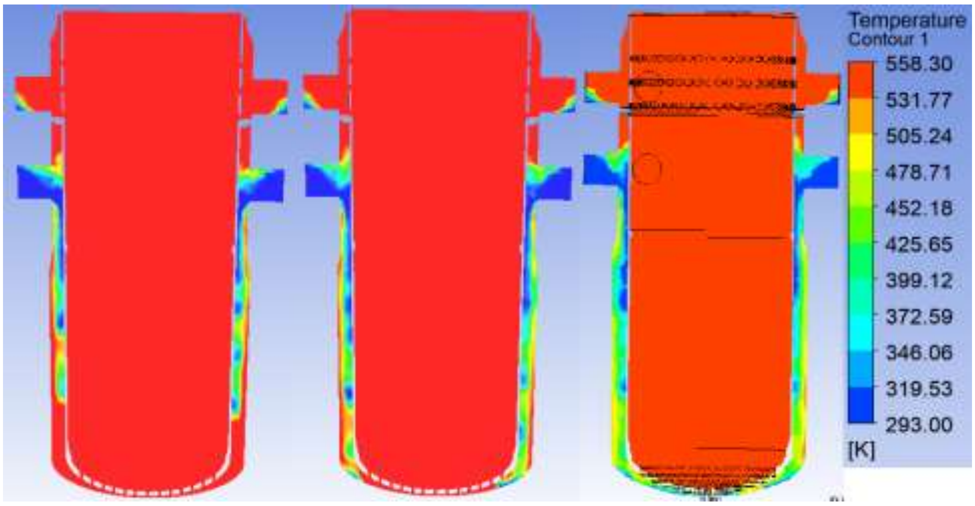

Figure 6.20 Temperature distributions while the coolant proceeds in the downcomer.

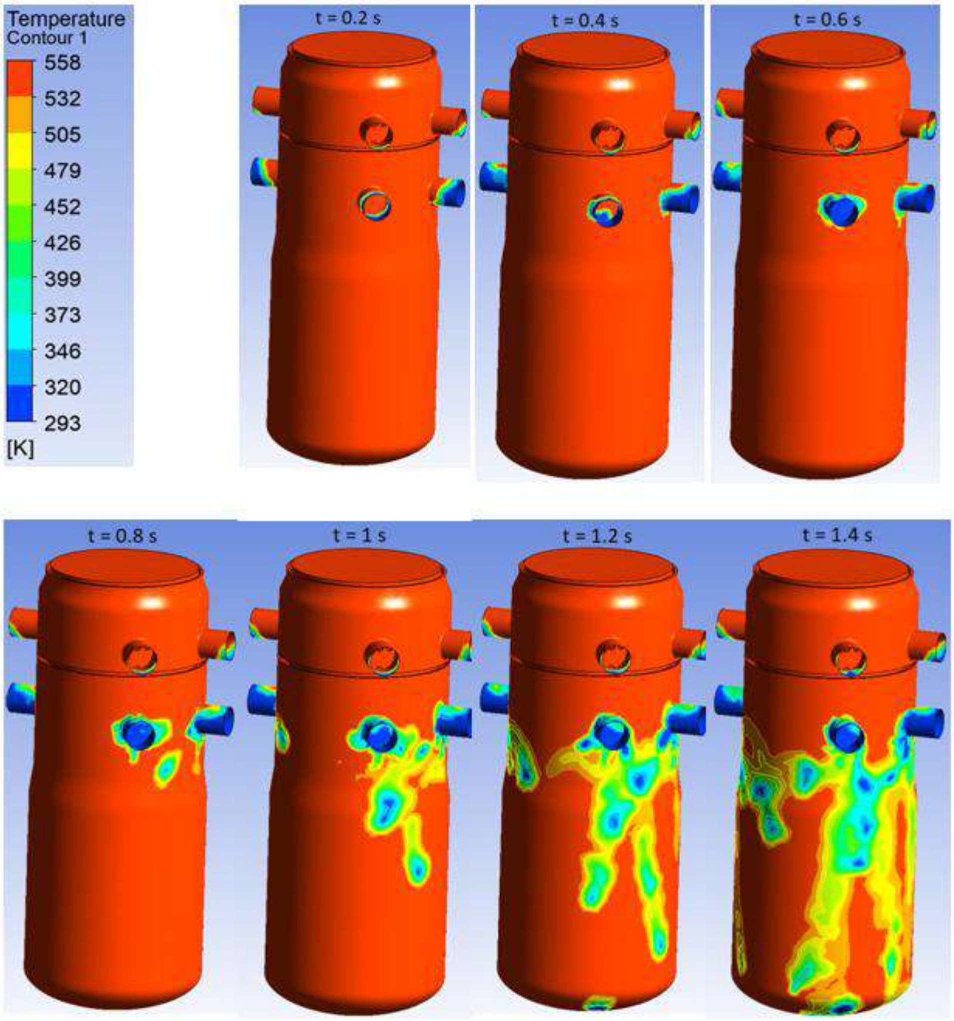

Figure 6.21 Temperature distributions at the reactor vessel wall.

6.4 Results of FAVOR

In this section, various data were obtained with the FAVLoad module for the LBLOCA accident. As a result of the simulation of this accident with FLUENT, values such as time-dependent coolant temperature, coolant pressure, coolant convection heat transfer coefficient were obtained. Then, these values were entered as input to the FAVLoad module. As a result, by operating the FAVLoad module, values such as time-dependent temperature, tangential stress, axial stress, stress intensity factor were obtained along the RPV wall for flaws of different sizes.

The vessel wall temperature, tangential stress and longitudinal stress distributions during the transient are depicted in Figures 6.22, 6.23, 6.24, respectively. The internal RPV wall temperature decreases, while the tangential and longitudinal stresses changes up to a compressive stress value on the external wall of the RPV during the whole transient. This is expected because tangential stress values generally tend to decrease as the coolant pressure is high from the inner surface of the reactor pressure vessel to the outer surface. The little discontinuity of the longitudinal and tangential stress distributions in the interface between the base metal and cladding occurs because of the different material properties of them. The greater coefficient of thermal expansion and the lower thermal conductivity causes increased thermal stress in the cladding zone of the vessel wall. In the analysis, it should be underlined that the welding residual stresses are taken into account for longitudinal welds. However, tangential weld residual stresses are not taken into account.

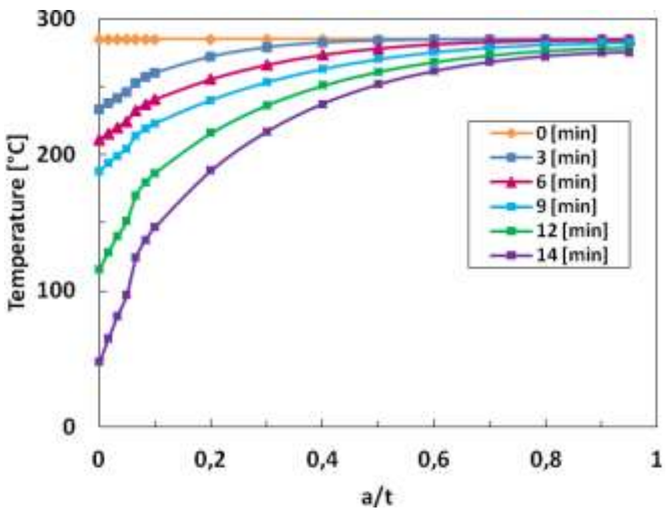

Figure 6.22 Temperature behaviors through the RPV wall thickness at 6 different instances of the transient.

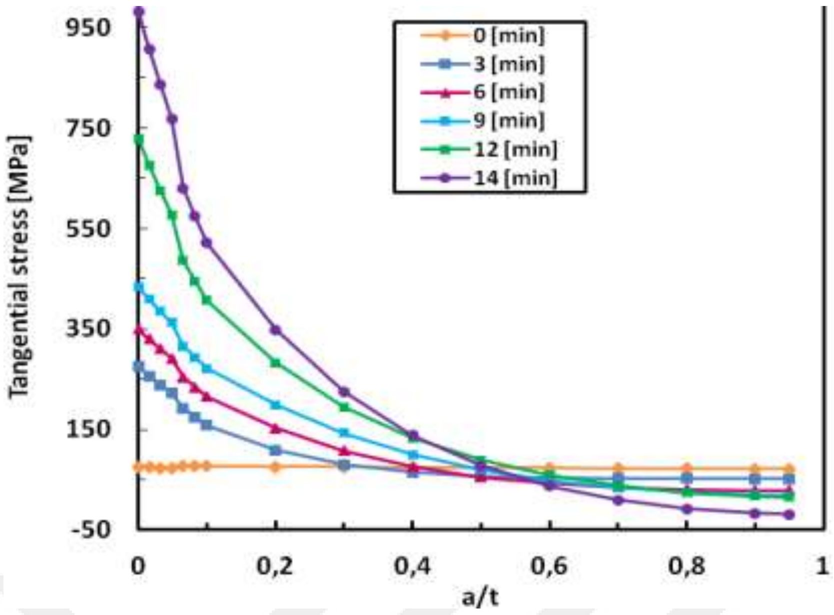

Figure 6.23 Tangential stress behaviors through the thickness at 6 different instances of the transient.

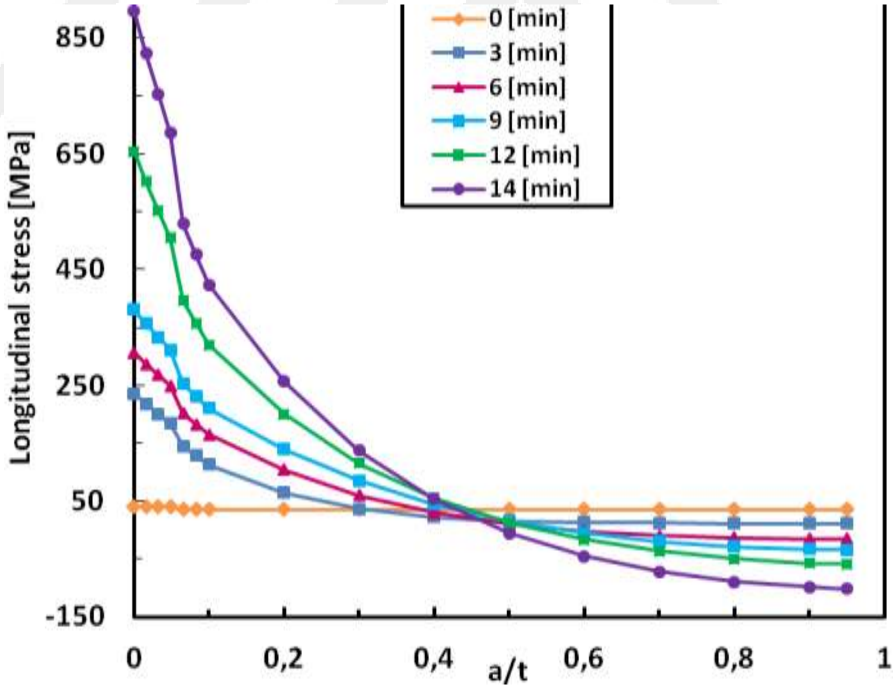

Figure 6.24 Longitudinal stress behaviors through the thickness at 6 different instances of the transient.

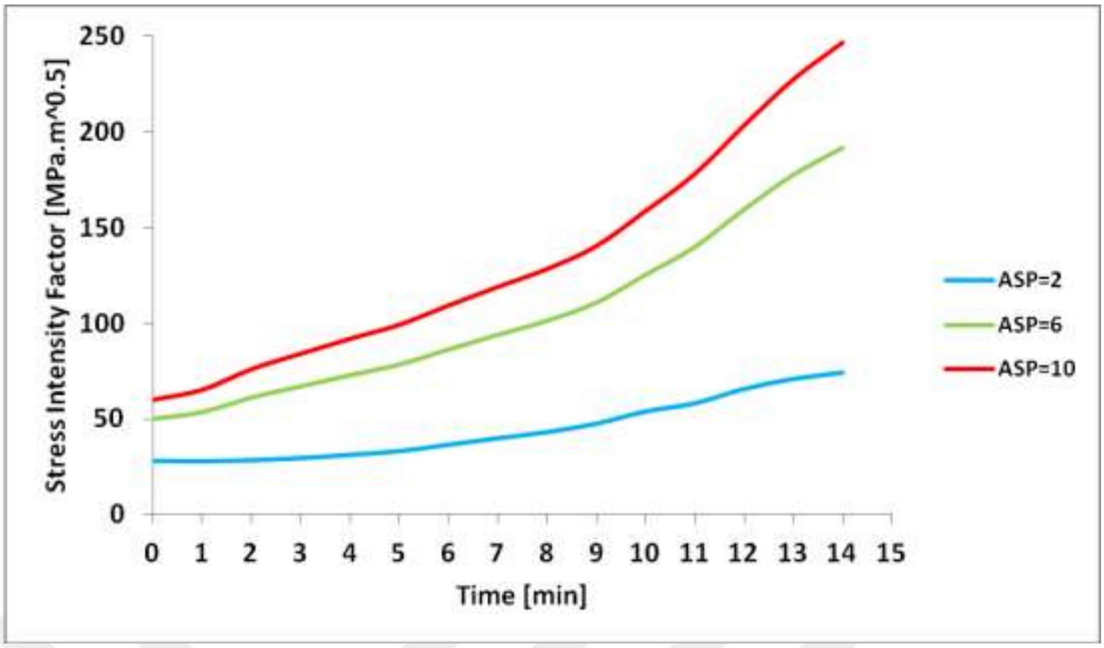

Figure 6.25 Time plot of the stress intensity factor for internal axial semielliptical flaw at different aspect ratios for the deepest point of RPV.

Figure 6.25 shows the time-dependent variation of the stress intensity factor for the deepest point of the reactor pressure vessel at different aspect ratios. The stress intensity factor is low at the low aspect ratios due to the low flaw length. In addition, it has been observed that the stress intensity factor takes high values when the pressure is high. The stress intensity factor varies as combinations of temperature, circumferential and tangential stress.

CHAPTER VII

CONCLUSION

7.1 Conclusion

In this thesis study, three comprehensive CFD simulations were performed in order to obtain the temperature, pressure, velocity and mass flow rate behaviors through a VVER-1200 RPV with both symmetric (full-loop) and asymmetric (three-loop) inlet BCs, and loss-of-coolant accident scenario using ANSYS FLUENT 17.2. Coupled CFD and FAVOR analysis of RPV in the VVER-1200 have been performed. Therefore, this thesis study includes the thermal-hydraulic analyses by simplifying with the porous media model in ANSYS FLUENT and also applying a coupled CFD-FAVOR analysis methodology in order to use the resource more effectively that is available to the general researchers or academicians. This thesis has four major components. The first one, use of ANSYS FLUENT with a single-phase flow for normal operating conditions of a VVER-1200 RPV is verified due to its design parameters. After that, the same single-phase simulation is performed for asymmetric (three-loop) inlet boundary conditions, including RCP fail in one of the four loops. Then, the multi-phase flow and the porous medium approach are implemented into FLUENT for simulating internal flows in RPV under the core reflooding in accident scenario of a LOCA, during which the coolant from the inlet nozzles are of focus interest. Fourthly, a coupling methodology in order to connect a CFD code to a nuclear engineering system-code is carried out to fulfill the mechanical part of the dissertation.

The aim of this dissertation is to investigate the complicated coolant flow in a VVER-1200 RPV for prescribed conditions. The tiny and minute details of the inner geometry of RPV were ignored. 163 fuel assemblies displayed a uniform distribution about the central point of the reactor core. The reactor core was simplified in a way by using the porous media model. Therefore, the computational time and efforts could be shortened greatly. For the Computational Fluid Dynamics simulations, total mesh numbers of nearly 1.7, 1.9, 2.6 and 4.8 million are established in order to carry out the well-required mesh independency analysis. More-refined grid system with element number of greater than 4.8 million does not have any serious effect on the outlet temperature results. Hence, the final model consists of approximately 4.8 million elements.

CFD simulations have been performed for the generated VVER-1200 RPV model operating under both symmetric (full-loop) and asymmetric (three-loop) inlet BCs, respectively. The obtained pressure drop value through the reactor core has been compared to the calculated pressure drop for any VVER-1200 in Section 5.5. Results verified that they were in acceptable match with each other. The temperature behaviors among the core are also illustrated. The analyses have been validated by the design coolant temperature value at reactor outlet, which is 601.9 K from VVER-1200 status report given in references for VVER-1200 reactor plant nominal operation. The fluid mixing phenomena for both the symmetric and asymmetric inlet condition cases have been carried out and concluded that the corresponding parameters around the failed loop are affected greatly by the variations in inlet conditions. The temperature behaviors at the nearest two exits to the failed loop's exit are also influenced, especially the closer outlet nozzle connection. The flow rate behavior at the core inlet is affected by the failed loop for asymmetric (three-loop) inlet BCs. According to the results, it can be approved that the utilized technique for analyzing coolant flow and heat transfer characteristics in the RPV of a VVER-1200 for several different inlet BCs is conceivable and adequate. The future studies are directed to the development of the reactor vessel model of VVER-1200 to improve the geometrical details and investigate the time-dependent distributions in more detail. Temperature and pressure values found from these analyses can be applied as BCs of a structural system code to obtain stress fields through the wall thickness of the RPV for an accident.

The time-step size of the LOCA analysis is limited by the Courant number that is very small for the discontinuity in the geometry of nozzle and downcomer intersection. It is set as 0.00001 not to cause a fail or error during the simulations. However, after the fluid completely passes that intersection region, the time-step size is increased a little bit for computational time concerns. Another limitation is that

FLUENT cannot give the void fraction in the RCS, but can only calculate the water vapor volume fraction in the coolant for multi-phase flows.

A coupled CFD and nuclear engineering system-code is developed by connecting a commercial computational fluid dynamics code (ANSYS FLUENT) with a system-code (FAVOR). This method allows also to obtain the mechanical results of stresses and stress intensity factors for the system as well as three-dimensional thermal and flow analyses utilizing the FLUENT. While coupling, ANSYS FLUENT is the master code, which means that its results are used as temperature, pressure and heat transfer coefficient inputs for FAVOR runs.

Valuable design-related results can be obtained by coupled CFD-system code analyses for the engineers of next generation of nuclear power plants. The results given in this dissertation can be utilized for further studies of the VVER-1200 thermal- hydraulic design. There are also numerous potential future work in addition to these. In commercial CFD programs, additional capabilities are now becoming available, such as the mechanical simulation and fluid-structure interactions, which can exist in the future.

7.2 Contributions

Several contributions to the literature are achieved by completing this dissertation and listed below:

- There are several studies which deal with the coupling of CFD codes and nuclear engineering system codes such as RELAP5 as told in the literature survey of this thesis. However, there is not any study concerning the CFD - FAVOR coupling in the open literature. Thus, by means of this thesis study, various thermoelastic cases can be investigated thoroughly as the solid models of each RPV component are available.
- Up to now, numerous researchers have performed three-dimensional computational fluid dynamics analyses for coolant flow in several different components of pressurized water reactors and VVER-1000s. However, there are not many studies concerning the new design of VVER nuclear reactors, namely VVER-1200.

- This dissertation firstly summarizes results obtained through the CFD simulation for analyzing the reactor vessel model of a VVER consisting of four loops with symmetric inlet boundary conditions for regular operation and asymmetric inlet boundary conditions in case of a sudden fail in one of the reactor coolant pumps. The results match with the ones in the open literature, thereby leading up further study including a transient LOCA scenario.
- The thesis then summarizes results obtained through the CFD simulation for analyzing an accident scenario in the reactor vessel of a VVER having four loops. The transient LOCA simulation is based on two-phase volume-of-fluid model.
- Moreover, temperature field varies significantly over time and it is not conservative to determine thermal loads for thermoelastic analysis, thereby requiring a mechanical analysis by FAVOR code.
- In the light of the knowledge obtained as a result of the analysis, more and more different accident scenarios by changing mesh types, turbulent methods, wall functions, boundary conditions, RPV components, transients and many more such characteristics can be performed for further studies.

REFERENCES

Abdi, M. R., Asgari, M., Saraee, K. R. E., Talebi, M. (2012). Numerical Simulation of Split Vane in a 60 Fuel Rod Bundle of VVER-440 Reactor and Survey the Effect of Large Length Split Vane (LLSV) and Half-Length Split Vane (HLSV) on Heat Transfer Distribution. *World Applied Sciences Journal* **18 (7)**, 909-917.

Alonzo-García, A., Gutiérrez-Torres, C. C., Jiménez-Bernal, J. A. (2016). Computational Fluid Dynamics in Turbulent Flow Applications

ANSYS FLUENT (2011). Release 17.2, Reference Guide.

Asmolov, V. G., Gusev, I. N., Kazanskiy, V. R., Povarov, V. P., Statsura, D. B. (2017). New Generation First-of-the Kind Unit –VVER-1200 Design Features, *Nuclear Energy and Technology* **3**, 260–269.

Böttcher, M. (2006). Detailed CFX-5 Study of the Coolant Mixing within the Reactor Pressure Vessel of a VVER-1000 Reactor during a Non-symmetrical Heat-up Test, *Proceeding of the Benchmarking of CFD Codes for Application to Nuclear Reactor Safety (CFD4NRS)*, 5-7 September 2006, Garching (Munich), Germany.

Böttcher, M. (2008). Detailed CFX-5 Study of the Coolant Mixing within the Reactor Pressure Vessel of a VVER-1000 Reactor during a Non-symmetrical Heat-up Test, *Nuclear Engineering and Design* **238 (3),** 445-452.

Cai, J., Watanabe, T. (2011). Numerical Simulation of Thermal Stratification in Cold Legs by Using OpenFOAM, *Progress in Nuclear Science and Technology* **2**, 107-113.

Cartland Glover, G. M., Höhne, Th., Kliem, S., Rohde, U., Weiss, F.–P., Prasser, H.-M. (2007). Hydrodynamic Phenomena in the Downcomer during Flow Rate Transients in the Primary Circuit of a PWR, *Nuclear Engineering and Design* **237**, 732–748.

Chaudhry, V., Kumar, A., Ingole, S. M., Balasubramanian, A. K, Muktibodh, U. C. (2014). Thermo-Mechanical Transient Analysis of Reactor Pressure Vessel, *Procedia Engineering* **86**, 809 – 817.

Chen, M., Lu, F., Wang, R., Yu, W., Wang, D., Zhang, G., Xue, F. (2015). The Probabilistic Structural Integrity Assessment of Reactor Pressure Vessels under Pressurized Thermal Shock Loading, *Nuclear Engineering and Design*, **294**, 93-102.

Dickson, T., Malik, S. (2001). An Updated Probabilistic Fracture Mechanics Methodology for Application to Pressurized Thermal Shock, *Int. J. Press. Vess. Piping* **78**, 155–163.

Duderstadt, J. J., Hamilton, L. J. (1976). Nuclear reactor analysis. John Wiley and Sons, New York.

Espinoza, S. (2006). Investigations of the VVER-1000 Coolant Transient Benchmark Phase 1 with the Coupled System Code RELAP5/PARCS. *Progress in Nuclear Energy*, **48**, 865-879.

Faidy, C., Chapuliot, S., Dickson, T., Pistora, V., Onazawa, K. (2010). PROSIR: Probabilistic Structural Integrity of a PWR Reactor Pressure Vessel. Final report.

Farkas, I., Hutli, E., Farkas, T., Takacs, A., Toth, I., Guba, A. (2017). The Applicability of CFD to Simulate and Study the Mixing Process and the Thermo-Hydraulic Consequences of a Main Steam Line Break (MSLB) in PWR Model, *Thermal Science* **21(6)**, 3025-3036.

Fernández-Arias, P., Vergara, D., Orosa, J. A. (2020). A Global Review of PWR Nuclear Power Plants, *Appl. Sci.***,** **10**, 4434.

Fyza, N., Hossain, A., Sarkar, R. (2019). Analysis of the Thermal-hydraulic Parameters of VVER-1200 due to Loss of Coolant Accident Concurrent with Loss of Offsite Power, *Energy Procedia* **160**, 155-161.

Gálik, G., Kutiš, V., Paulech, J., Murín, J. (2019). Modelling the Effects of Oscillating Stripe Cooling during a LOCA Event in a VVER440/213 Reactor Pressure Vessel, *VIII. International Conference on Computational Methods for*

Coupled Problems in Science and Engineering, COUPLED PROBLEMS 2019, 553-561.

Gonzalez-Albuixech, V. F., Qian, G., Sharabi, M., Niffenegger, M., Niceno, B., Lafferty, N. (2015). Comparison of PTS Analyses of RPVs based on 3D-CFD and RELAP5, *Nuclear Engineering and Design*, **291**, 168-178.

Gottlasz, V., Hutli, E., Tar, D., Ézsöl, G., Baranyai, G. (2013). Measuring of Velocity and Temperature Field in a Model of Reactor Vessel Downcomer and Cold-Legs Inlets, *10th International Symposium on Particle Image Velocimetry – PIV13*, Delft, the Netherlands, July 2-4.

Hermanský, P., Krajčovič, M. (2012). The Numerical Simulation of the WWER440/V213 Reactor Pressure Vessel Internals Response to Maximum Hypothetical Large Break Loss of Coolant Accident, *11th International Conference Energy – Ecology – Economy*, May 15-17, High Tatras, Slovak Republic.

Höhne, T., Bezrukov, Y. (2005). CFD Calculation of a Mixing Experiment in the VVER-1000 Reactor Model, *The 4-th International Conference Safety Assurance of Nuclear Power Plants with WWER*, 23-25 May, Podolsk, Moscow Region, Russian Federation.

Huang, C.-C., Chou, H.-W., Chen, B.-Y., Liu, R.-F., Lin, H.-C. (2012). Probabilistic Fracture Analysis for Boiling Water Reactor Pressure Vessels Subjected to Low Temperature Over-Pressure Event, *Annals of Nuclear Energy*, **43**, 61-67.

Huang, K.-R., Huang, C.-C., Chou, H.-W. (2016). Deterministic and Probabilistic Fracture Mechanics Analysis for Structural Integrity Assessment of Pressurized Water Reactor Pressure Vessel, *J. Pressure Vessel Technol*., **138(3)**, 031202

IAEA. (2006). Guidelines on Pressurized Thermal Shock Analysis for WWER Nuclear Power Plants, IAEA-EBP-WWER-08, Vienna.

IAEA. (2009). Integrity of Reactor Pressure Vessels in Nuclear Power Plants: Assessment of Irradiation Embrittlement Effects in Reactor Pressure Vessel Steels, IAEA Nuclear Energy Series No. NP-T-3.11, Vienna.

IAEA. (2011a). Status report 107 - VVER-1200 (V-392M) (VVER1200 (V-392M)), IAEA NPTDS, Vienna.

IAEA. (2011b). Status report 108 - VVER-1200 (V-491) (VVER-1200 (V-491)), IAEA NPTDS, Vienna.

IAEA. (2020). Power Reactor Information System (PRIS). https://www.iaea.org/PRIS/home.aspx (20.08.2020).

Jaros, M., Lafferty, N., Qian, G., Niceno, B., Niffenegger, M. (2017). Computational Fluid Dynamics Study of Pressurized Thermal Shock Transients in the Reactor Pressure Vessel, *26th International Conference Nuclear Energy for New Europe (NENE 2017)*, September 11-14, Bled-Slovenia.

Kanlıkama, B., Abuşoğlu, A., Güzelbey, İ. H. (2013). Coupled Thermoelastic Analysis of Thick-Walled Pressurized Cylinders, *International Journal of Energy and Power Engineering* **2 (2)**, 60-68.

Kutiš, V., Jakubec, J., Paulech, J., Gálik, G., Sedlár, T. (2016). CFD Analysis of Downcomer of Nuclear Reactor VVER 440, *Journal of Mechanical Engineering* **66 (2)**, 55 – 62.

Kütük, B., Güzelbey, İ. H. (2020). Computational Fluid Dynamics Analyses of a VVER-1200 Nuclear Reactor Vessel for Symmetric Inlet, Asymmetric Inlet, and LOCA Conditions, *International Journal of Pressure Vessels and Piping* **187**, 104165.

Lamarsh, J. R., Baratta, A. J. (2001). Introduction to nuclear engineering. Prentice Hall, New York.

Liu, J., Zhang, J., Shi, J., Sun, B., Ji, H. (2018). Numerical Simulation and Experimental Research on CHF Characteristics of AP1000 Nuclear Reactor, *Journal of Nuclear Science and Technology*, **55(12)**, 1412-1424.

Marie, S., Menager, Y., Chapuliot, S. (2005). Stress Intensity Factors for Underclad and Through Clad Defects in a Reactor Pressure Vessel Submitted to a Pressurized Thermal Shock. *Int. J. Press. Vess. Piping* **82**, 746–760.

Mohanty, S., Soppet, W. K., Majumdar, S., Natesan, K. (2016). Thermal–Mechanical Stress Analysis of Pressurized Water Reactor Pressure Vessel with/without a Preexisting Crack under Grid Load Following Conditions, *Nuclear Engineering and Design* **310**,112-124.

Moretti, F., Melideo, D., Del Nevo, A., D'Auria, F. (2008). CFD Analysis of a Slug Mixing Experiment Conducted on a VVER-1000 Model, *Science and Technology of Nuclear Installation*, **2009,** 436218.

Niffenegger, M., Reichlin, K. (2012). The Proper Use of Thermal Expansion Coefficients in Finite Element Calculations, *Nucl. Eng. Des.* **243**, 356–359.

Niwemuhwezi, A., Lee, S. (2018). A Comparative Study of Safety Systems from Selected Advanced Nuclear Reactors, *Transactions of the Korean Nuclear Society Autumn Meeting*, Yeosu, Korea, October 25-26.

Qian, G., González-Albuixech, V. F., Niffenegger, M. (2014). Probabilistic Assessment of a Reactor Pressure Vessel Subjected to Pressurized Thermal Shocks by using Crack Distributions, *Nuclear Engineering and Design*, **270**, 312-324.

Qian, G., Niffenegger, M. (2013). Procedures, Methods and Computer Codes for the Probabilistic Assessment of Reactor Pressure Vessels Subjected to Pressurized Thermal Shocks. *Nuclear Engineering and Design*, **258**, 35-50.

Qian, G., Niffenegger, M. (2014). Deterministic and Probabilistic Analysis of a Reactor Pressure Vessel Subjected to Pressurized Thermal Shocks, *Nuclear Engineering and Design*, **273**, 381-395.

Ragheb, M. (2016). Loss of Coolant Accident, LOCA, Lecture Notes, 11/13/2016.

Rautaheimo, P., Salminen, E., Siikonen, T., Hyvärinen, J. (1999). Turbulent Mixing Between VVER-440 Fuel Bundle Subchannels: A CFD Study. *9th International Topical Meeting on Nuclear Reactor Thermal Hydraulics (NURETH-9).* San Francisco, USA.

Rohde, U., Höhne, T., Kliem, S., Hemström, B., Scheuerer, M., Toppila, T., Aszodi, A., Boros, I., Farkas, I., Mühlbauer, P., Vyskocil, L., Klepac, J., Remis, J., Dury, T. (2007). Fluid Mixing and Flow Distribution in a Primary Circuit of a Nuclear

Pressurized Water Reactor—Validation of CFD Codes, Nuclear Engineering and Design **237 (15–17)**, 1639-1655.

Rosatom (2020). The VVER Today: Evolution, Design, Safety.

Ruan, X., Nakasuji, T., Morishita, K. (2017). 3D CFD and FEM Evaluations of RPV Stress Intensity Factor during PTS Loading, *E-Journal of Advanced Maintenance*, **9 (2)**, 84-90.

Sharabi, M., Gonzalez-Albuixech, V. F., Lafferty, N., Niceno, B., Niffenegger, M. (2016). Computational Fluid Dynamics Study of Pressurized Thermal Shock Phenomena in the Reactor Pressure Vessel, *Nuclear Engineering and Design*, **299**, 136-145.

Shrivastav, V., Sen, R. N., Yadav, R. S. (2012). Structural Integrity Assessment of VVER-1000 RPV under Accidental Cool down Transients.

Williams, P. T., Dickson, T. L., Yin, S. (2007). Fracture Analysis of Vessels-Oak Ridge FAVOR, V06.1, Computer Code: Theory and Implementation of Algorithms, Methods, and Correlations.

Yan, Y. (2011). Development of a Coupled CFD—System-Code Capability (with a Modified Porous Media Model) and its Applications to Simulate Current and Next Generation Reactors, Dissertation, Doctor of Philosophy in Nuclear Engineering in the Graduate College of the University of Illinois at Urbana-Champaign.

Yıldırım, A. (2018). Structural Analysis of PWR (Pressurized Water Reactors) Vessel with FAVOR (Fracture Analysis of Vessels Oak Ridge) Code, Dissertation, Master of Science in Nuclear Engineering in Hacettepe University.

Zhang, Q., Wang, Z. W., Tang, C. Y., Hu, D. P., Liu, P. Q., Xia, L. Z. (2012). Analytical Solution of the Thermo-mechanical Stresses in a Multilayered Composite Pressure Vessel Considering the Influence of the Closed Ends, *International Journal of Pressure Vessels and Piping* **98**, 102-110.

Zsíros, G., Tóth, S., Aszódi, A. (2012). Analysis of Coolant Flow in Central Tube of VVER-440 Fuel Assemblies, *Kerntechnik* **77 (4)**, 258-264.

CURRICULUM VITAE

PERSONAL INFO

Name Surname:	Begüm (KANLIKAMA) KÜTÜK

EDUCATION

M.Sc.	Gaziantep University, Department of Mechanical Eng.	2013
B.Sc.	Hacettepe University, Dept. of Nuclear Energy Eng.	2009

LANGUAGE

English	YÖKDİL	88.75	2020

WORK EXPERIENCE

2015-Present	Gaziantep University, Faculty of Aeronautical and Aerospace, Dept. of Aircraft and Aerospace Eng.	Res. Asst.
2011-2015	Gaziantep University, Faculty of Engineering, Dept. of Mechanical Engineering	Res. Asst.

PUBLICATIONS

Journal Papers

[1] Kütük, B., Güzelbey, İ. H. (2020). Computational Fluid Dynamics Analyses of a VVER-1200 Nuclear Reactor Vessel for Symmetric Inlet, Asymmetric Inlet, and LOCA Conditions, *International Journal of Pressure Vessels and Piping 187*, 104165.

[2] Kanlıkama, B., Abuşoğlu, A., Güzelbey, İ. H. (2013). Coupled Thermoelastic Analysis of Thick-Walled Pressurized Cylinders, *International Journal of Energy and Power Engineering*, 2(2), 60-68.

Conference Proceedings

[1] Kütük, B., Güzelbey, İ. H. (2019). VVER-1200 Nükleer Reaktörü Basınç Kabının Soğutucu Kaybı Kazası Esnasında Hesaplamalı Akışkanlar Dinamiği Analizi, *21. Ulusal Mekanik Kongresi*, 2-6 September, Niğde Ömer Halisdemir University, (National).

[2] Kütük, B., Güzelbey, İ. H. (2017). Computational Fluid Dynamics Analysis of Hot and Cold Legs Region of VVER-1200 Reactor Pressure Vessel (RPV), *4th International Conference on Computational and Experimental Science and* Engineering (ICCESEN-2017), 4-8 October, Antalya, (Abstract, International).

[3] Kütük, B., Güzelbey, İ. H. (2017). Coupled Axisymmetric Thermoelastic and Two-Dimensional Thermodynamic Potentials Analyses of VVER-1200 Nuclear Reactor Pressure Vessel (RPV), *4th International Conference on Computational and Experimental Science and Engineering (ICCESEN-2017)*, 4-8 October, Antalya, (Abstract, International).

[4] Kütük, B., Güzelbey, İ. H. (2017). VVER-1200 Nükleer Reaktörlerinin Soğuk ve Sıcak Ayak Bölgesinin Hesaplamalı Akışkanlar Dinamiği (CFD) Analizi, *XX. Ulusal Mekanik Kongresi*, 5-9 Eylül, Uludağ University, Bursa, Turkey (National).